

**Effects of pine beetle infestations and treatments
on hydrology and geomorphology:
Integrating stand-level data and knowledge
into mesoscale watershed functions**

Y. Alila, D. Bewley, P. Kuraś, P. Marren,
M. Hassan, C. Luo, and T. Blair

Mountain Pine Beetle Working Paper 2009-06

Department of Forest Resources Management,

University of British Columbia

Forest Sciences Centre

2424 Main Mall

Vancouver, BC V6T 1Z4

MPBI Project # 8.54

Natural Resources Canada
Canadian Forest Service
Pacific Forestry Centre
506 West Burnside Road
Victoria, BC V8Z 1M5
Canada

2009

© Her Majesty the Queen in Right of Canada 2009

Printed in Canada

Library and Archives Canada Cataloguing in Publication

Effects of pine beetle infestations and treatments on hydrology and geomorphology [electronic resource] : integrating stand-level data and knowledge in mesoscale watershed functions / Y. Alila ... [et al.].

(Mountain pine beetle working paper ; 2009-06)

"MPBI Project # 8.54".

Includes bibliographical references.

Type of computer file: Electronic monograph in PDF format.

Issued also in printed form.

Includes abstract in French.

ISBN 978-1-100-13143-6

Cat. no.: Fo143-3/2009-6E-PDF

1. Forest hydrology--British Columbia--Baker Creek Watershed (Cariboo)--Computer simulation. 2. Runoff--British Columbia--Baker Creek Watershed (Cariboo)--Computer simulation. 3. Streamflow--British Columbia--Baker Creek Watershed (Cariboo)--Computer simulation. 4. Geomorphology--British Columbia--Baker Creek Watershed (Cariboo). 5. River channels--British Columbia--Baker Creek Watershed (Cariboo). 6. Forest management--Environmental aspects--British Columbia--Baker Creek Watershed (Cariboo). 7. Mountain pine beetle--British Columbia--Baker Creek Watershed (Cariboo). I. Alila, Younes, 1962- II. Pacific Forestry Centre III. Series: Mountain Pine Beetle Initiative working paper (Online) 2009-06

SB945 M78 E33 2009

551.480915'20971175

C2009-980161-2

Abstract

The physically based Distributed Hydrology Soil Vegetation Model (DHSVM) is developed, calibrated, and applied in a long-term simulation experiment to quantify the effects of mountain pine beetle infestation and treatment alternatives on the streamflow characteristics of snow-dominated interior watersheds ranging in scale from tens to hundreds of square kilometres. Predicted increases in peak flow that result from pine beetle infestation and salvage logging were used to investigate potential effects on channel geomorphology. The study is being conducted on the Baker Creek drainage, located near the confluence of the Upper Fraser and Quesnel Rivers in the North Cariboo region of British Columbia. A wealth of historic long-term and newly collected more intensive short-term measurements of hydroclimatic data supports this numerical modelling study. This project integrates results from several completed and ongoing stand-level Federal Mountain Pine Beetle Program research projects into operationally critical watershed scale functions related to the hydrogeomorphic regimes.

Key words: Mountain pine beetle, hydrology, geomorphology, peak flow, water yield

Résumé

Le Distributed Hydrology Soil Vegetation Model (DHSVM), physiquement établi, est conçu, calibré et appliqué dans le cadre d'une expérience de simulation à long terme visant à quantifier les effets de l'infestation de dendroctone du pin ponderosa et des choix de traitement sur les caractéristiques de l'écoulement fluvial des bassins versants intérieurs dominés par la neige, dont l'étendue varie entre des dizaines et des centaines de kilomètres carrés. Les augmentations prédites du débit de pointe résultant de l'infestation de dendroctone du pin et de la coupe de récupération ont été utilisées pour déterminer les effets potentiels sur la géomorphologie des canaux. L'étude s'effectue sur le bassin Baker Creek, près du confluent des rivières Upper Fraser et Quesnel, dans la région de North Cariboo, en Colombie-Britannique. Un riche patrimoine de données hydroclimatiques, dont certaines ont été recueillies depuis longtemps et d'autres sont plus récentes et plus denses, appuie la présente étude de modélisation numérique. Elle intègre les résultats de plusieurs projets de recherche, achevés ou en cours, réalisés à l'échelle du peuplement dans le cadre du Programme fédéral sur le dendroctone du pin ponderosa, aux fonctions plus fondamentales sur le plan opérationnel à l'échelle des bassins versants en lien avec les régimes hydrogéomorphiques.

Mots clés : dendroctone du pin ponderosa, hydrologie, géomorphologie, débit de pointe, apport d'eau

Table of Contents

Abstract	iii
1 INTRODUCTION	1
2 STUDY AREA	2
3 HYDROLOGY	6
3.1 Methods	6
3.1.1 Fieldwork	6
3.1.2 Automatic weather stations	6
3.1.3 Snowplot measurements	9
3.1.4 Radiation measurements	13
3.1.5 Streamflow measurements	14
3.2 Modeling	16
3.2.1 Overview of model development, calibration, and scenario analysis	16
3.2.2 The Distributed Hydrology Soil Vegetation Model development	16
3.2.3 The Distributed Hydrology Soil Vegetation Model calibration	20
3.2.4 Distributed Hydrology Soil Vegetation Model scenario description	22
3.3 Results and Discussion	23
3.3.1 Automatic weather stations	23
3.3.2 Snowplot results	23
3.3.3 Snow accumulation	23
3.3.4 Snow ablation	26
3.3.5 Possible wind effects on snow	28
3.3.6 Albedo investigation	30
3.4 Simulated Effects on Peak Flow and Water Yield Regimes	33
3.4.1 Does forest removal in snow environment affects the larger peak flow events?	35
4 GEOMORPHOLOGY	39
4.1 Introduction	39
4.2 Geology and Quaternary Evolution of the Study Watershed	40
4.3 Methods	41
4.4 Results	43
4.4.1 Downstream channel changes	43
4.4.2 Channel classification using threshold methods	54
4.4.3 Sensitivity-based analysis of potential mountain pine beetle impacts	56
5 DISCUSSION	60
6 CONCLUSIONS	62
7 ACKNOWLEDGEMENTS	63
8 LITERATURE CITED	64

List of Tables

Table 1. AWS names, positions, elevations, and BEC zone.	7
Table 2. Station sensor descriptions for a typical Baker Creek AWS.	9
Table 3. Snowplot names and descriptions	11
Table 4. Vegetation categories and physical parameters required by DHSVM.	17
Table 5. Percentage, attacked, or harvested of watershed forested for each scenario.	22
Table 6. Predicted changes of peak flows, water yield and time advance in peak flow.	33
Table 7. Reach average values for valley slope, sinuosity, and meander wavelength and summary of channel characteristics for the main subreaches of the Baker Creek catchment.	45
Table 8. Measured and calculated properties for surveyed sites in the Baker Creek catchment.	50
Table 9. Simplified version of the Nanson and Croke (1992) classification of floodplain types based on specific stream power.	55
Table 10. Simplified version of the Church (2002) classification of alluvial river channels based on the Shields number.	55
Table 11. Scenarios for channel width and depth changes.	61

List of Figures

Figure 1. Baker Creek Watershed: Elevation contour lines and stream network.	3
Figure 2. Baker Creek watershed: locations of existing long-term hydrometric, climate, and snow course stations.	4
Figure 3. Representative hydrographs for the Baker Creek catchment, using data from the Water Survey of Canada gauging station in Quesnel, at the confluence of Baker Creek and the Fraser River.	5
Figure 4. Location of AWS and snowplots across Baker Creek catchment, according to elevation (left) and BEC zone (right).	7
Figure 5. Western-AWS setup.	8
Figure 6. Google Earth aerial image of three low elevation snowplots (SP-LO), and corresponding ground photos (also including site SP-LO-CC).	10
Figure 7. Sample hemispherical photos taken at each forested SP-LO snowplot in March 2008, used to derive forest density and optical parameter values.	12
Figure 8. The UBC radiometer array setup (left) and measurement of shortwave transmissivity during April 2007 (right).	13
Figure 9. Deployment of the pyranometers in suspended albedo-mode (left) and calibration of the ASD-spectroradiometer (right).	14
Figure 10. Location of 12 streamflow gauges equipped with continuously recording pressure transducers on the tributaries of Baker Creek.	15
Figure 11. Typical installations of water level recorder pressure transducer and datalogger at 12 stream gauging locations within Baker Creek.	15
Figure 12. Distribution of vegetation within Baker Creek watersheds in 1970.	18
Figure 13. Percentage of Baker Creek watershed harvested and planned for harvest 1970–2020.	18
Figure 14. Percentage of mature pine forest area in Baker Creek infested with mountain pine beetle.	19
Figure 15. Simulated forest roads in Baker Creek watershed.	19

Figure 16. Soil distribution and classification in Baker Creek watershed.....	20
Figure 17. Simulated and observed hydrographs (Qsim: with roads, Qsim_rd: without roads).	21
Figure 18. Comparison of SWE at two pixels (left elevation 1400 m; right elevation 1000 m).	22
Figure 19. Sample AWS data from Western AWS (1205 m asl) (black) and Central AWS (905 m asl) (green), between November 1, 2007, and March 10, 2008.	24
Figure 20. Snowplot (SP) data from winter 2007–2008, including plot mean values of snow depth, snow density, and snow water equivalent.	25
Figure 21. March 29 (peak) SWE data, sorted by stand type for all elevations.	27
Figure 22. March 29 (peak) SWE data, sorted by elevation for all stand types.	27
Figure 23. Plot ablation rates between March 29 and April 24, 2008.	27
Figure 24. A 350-ha clearcut on the eastern hillslope of Baker Creek, December 2007.	29
Figure 25a. Possible higher windspeed scour events at W-AWS relative to Cen-AWS, December 2007.	29
Figure 25b Daily snow albedo values measured in the clearcut, grey stand (6-m gap diameter), and red stand (3- and 6-m gap diameters), March 18 to May 3, 2008.	31
Figure 26. General site conditions (top) and downward photos (bottom) from the clearcut (left), grey stand (middle), and red-attacked stand (right) on May 3, 2008.	31
Figure 27. Litter piles used to obtain “pure” albedo values of needles and bark using the ASD- spectroradiometer.	32
Figure 28. Spectral reflectances of snow increasingly littered with red needles.	32
Figure 29. Scenario 1 post-logging peak flow regime in comparison to baseline.	34
Figure 30. Scenario 3 post-logging peak flow regime in comparison to baseline.	34
Figure 31. Percent change in peak flow versus return period (frequency-based comparison: right); percent change in peak flow versus control discharge (paired event based comparison: left).	36
Figure 32. Geological map of the Baker Creek area, modified from Riddell (compiler, 2006).	41
Figure 33. Long profile of Baker, Mount, and Merston Creeks, interpolated from contour crossing on 1:70 000 mapping of the catchment (20-m contour intervals).	44
Figure 34. Measured channel cross-sections from Baker, Mount, and Merston Creeks.	49
Figure 35. Changes in the width/depth ratio along Baker, Mount, and Merston Creeks.	52
Figure 36. (A) Changes in specific stream power along Baker, Mount, and Merston Creeks. (B) Shields number changes along Baker, Mount, and Merston Creeks. (C) Changes in the relative bed stability index along Baker, Mount, and Merston Creeks.	53
Figure 37. Downstream hydraulic geometry relationships for the Baker Creek catchment.	58
Figure 38. A sensitivity analysis of the potential impact of mountain pine beetle related hydrological changes on the Baker Creek catchment, based on possible discharge increases of 20%, 40%, 60%, 80%, and 100%.	59

1 INTRODUCTION

The mountain pine beetle (MPB) epidemic is creating disturbances with unprecedented values of equivalent cut area over larger watersheds. While the effect of these disturbances on the watershed hydrologic response could be significant, it cannot be inferred from the current literature. Our present knowledge of hydrologic changes resulting from forest disturbances is based on experiments conducted either at the stand level or on small watersheds less than few square kilometres. Concerns have often been raised about the validity of extrapolating experimental results from small to larger scales because hydrologic processes and relationships are expected to be different across scales (Hélie et al. 2005). Therefore, studies that advance the understanding and prediction of forest landscape disturbances over mesoscale watersheds in the tens to hundreds of square kilometres are of paramount practical importance.

The study of the effects of forest landscape disturbances on hydrology has traditionally been conducted using three methods. In the first method the differences in hydrologic processes such as snow accumulation, snowmelt, and soil moisture fluxes between disturbed and forested stands (Boon 2007; Teti 2008; Rex and Dubé 2009). The most challenging question related to this type of study is how this stand-level knowledge translates to an operationally useful aggregate watershed-scale function such as streamflow, particularly over larger drainages.

In the second method, the differences in the hydrologic response between disturbed and undisturbed drainages are quantified using the paired watershed technique. One of the fundamental conditions used in the selection of the paired watersheds is that the disturbed (treatment) and undisturbed (control) catchments have to be similar in climate and physiography. This condition can only be achieved over smaller catchments; therefore, a paired watershed approach is not an option for studying forest disturbances over larger catchments.

The third and perhaps only method suitable for the study of disturbances over larger watersheds is to synergistically supplement experimental results with modelling (Ziemer et al. 1991). A hydrologic model

- (1) alleviates problems associated with paired watershed studies by acting as a control to filter out effects of climate variability,
- (2) allows same watershed to act as its own control, and
- (3) is useful for integrating stand-level information into a physically reasonable description of basin response to forest disturbances.

Based on these premises, we have used hydrologic models to quantify the effects of forest management on hydrology in several experimental watersheds following an approach outlined in Alila and Beckers (2001). This approach does not require the expensive long-term data collection exercise of a paired watershed study but uses shorter, more intensively monitored hydroclimatic data to develop/calibrate watershed model applications and use them subsequently in a long-term simulation mode to generate time series of watershed hydrologic response for alternative forest disturbance scenarios. Longer-term proxy climate data (either synthetically generated or observed at nearby regional climate station) that reflect the regional and at-site climatic characteristics of the study watershed are used as input to the watershed model.

Over the last 10 years, we have applied this combined field-numerical modelling approach in the smaller Pentiction (5 km²), Carnation (10 km²), and Redfish (25 km²) experimental watersheds in British Columbia to quantify the long-term effects of different forest management scenarios on streamflow characteristics (Whitaker et al. 2002, 2003; Beckers and Alila 2004; Schnorbus and Alila 2004; Thyer et al. 2004). The work in progress that we report in this multi-year project is a logical extension of the same line of work to MPB-infested larger watersheds.

The main objective of this study is to predict the magnitude of the impact of MPB infestations and treatments by salvage logging on the water yield and peak flow regimes and the subsequent implications on channel geomorphology at multiple scales.

The detailed objectives of this study are to:

- Establish a dense network of stream gauges and weather stations to collect hydroclimatic data in several stages and in a nested fashion over a large watershed. The ultimate long-term goal is to use the collected data to test existing distributed models and develop new distributed modelling concepts over operationally relevant watershed scales;
- take advantage of ongoing and already published stand-level studies within and outside British Columbia, for coniferous and deciduous forest, to better parameterize an existing distributed physical hydrology model and further reduce its prediction uncertainties for MPB scenario analyses;
- use the same distributed physically based hydrologic model to quantify the effects of MPB infestation and salvage harvesting on streamflow characteristics using long-term simulations; and
- investigate the potential effects of MPB on channel instabilities using the predicted changes in the peak flow regime of step 3 and the various physiographic and climatic factors that control watershed response.

This report is structured in two major parts: Chapter 3 (Hydrology) and Chapter 4 (Geomorphology). Each could be considered as a stand-alone document.

2 STUDY AREA

The study area is the Baker Creek watershed, a western tributary of the Fraser River, at Quesnel (Figure 1). Baker Creek is a 1570-km² drainage located in the Interior Plateau of central British Columbia (Figure 1a), at the heart of the MPB infestation area. Infestation rates across the catchment exceed 80%, with almost all mature lodgepole pine at the red or grey stages of infestation. Clearcutting of dead trees is ongoing across the catchment. Elevations within the catchment range from 470 to 1530 m above sea level (asl). The Fraser River flows north to south to the east of the catchment, while Baker Creek and its tributaries flow south to north, before turning sharply to the east where it meets the Fraser River at the city of Quesnel. The catchment is located in the Fraser Plateau physiographic region (Lord and Mackintosh 1982), and lies primarily at an elevation of 900 to 1000 m asl, with rounded ridges and summits of 1200 to 1500 m elevation forming the boundaries of the catchment. Where Baker Creek passes from the Fraser Plateau physiographic region to the Fraser River Basin physiographic region, it is incised into the underlying bedrock, and lower Baker Creek is confined within a steep-sided valley.

Two Environment Canada climate stations are located within or close to the catchment: one in Quesnel, at an altitude of 545 m, and one at Punchesakut Lake, in the centre of the catchment, at an elevation of 915 m (Figure 2). Long-term (1971–2000) climate records indicate a mean annual precipitation at Quesnel of 540.3 mm (of which 386.9 mm or 71.6% is rainfall, the remainder occurring as snow), and 511.4 mm at Punchesakut Lake (339.8 mm or 66.4% from rainfall). Within the catchment, precipitation falls almost entirely as snow from November to March and almost entirely as rainfall from April to October, with most rain falling in June and July. Temperatures vary widely throughout the year, with minimum values in January and maximum values in July. Average temperature in January is –9.3°C and the July average is 14.4°C.

The hydrology of Baker Creek is nival and strongly reflects the high seasonality of both the temperature and precipitation. Flow is low during winter and autumn, with seasonal high flows caused by the spring freshet, and summer rainfall causing additional high flows. The Water Survey of Canada has gauged Baker Creek at its tributary with the Fraser since 1963; these data are summarized in Figure 3. The maximum flow series is the maximum discharge that has occurred in any year during the 43-year period of record (1963–2006) (Figure 3). The onset of snowmelt occurs in late March and early April, and peak flows from snowmelt and rain-on-snow events typically occur in late April and early May. Floods from storm events can cause sharp rises in peak flow throughout the summer. These floods are easily recognized in Figure 3a as the large discharge peaks in the maximum flow series.

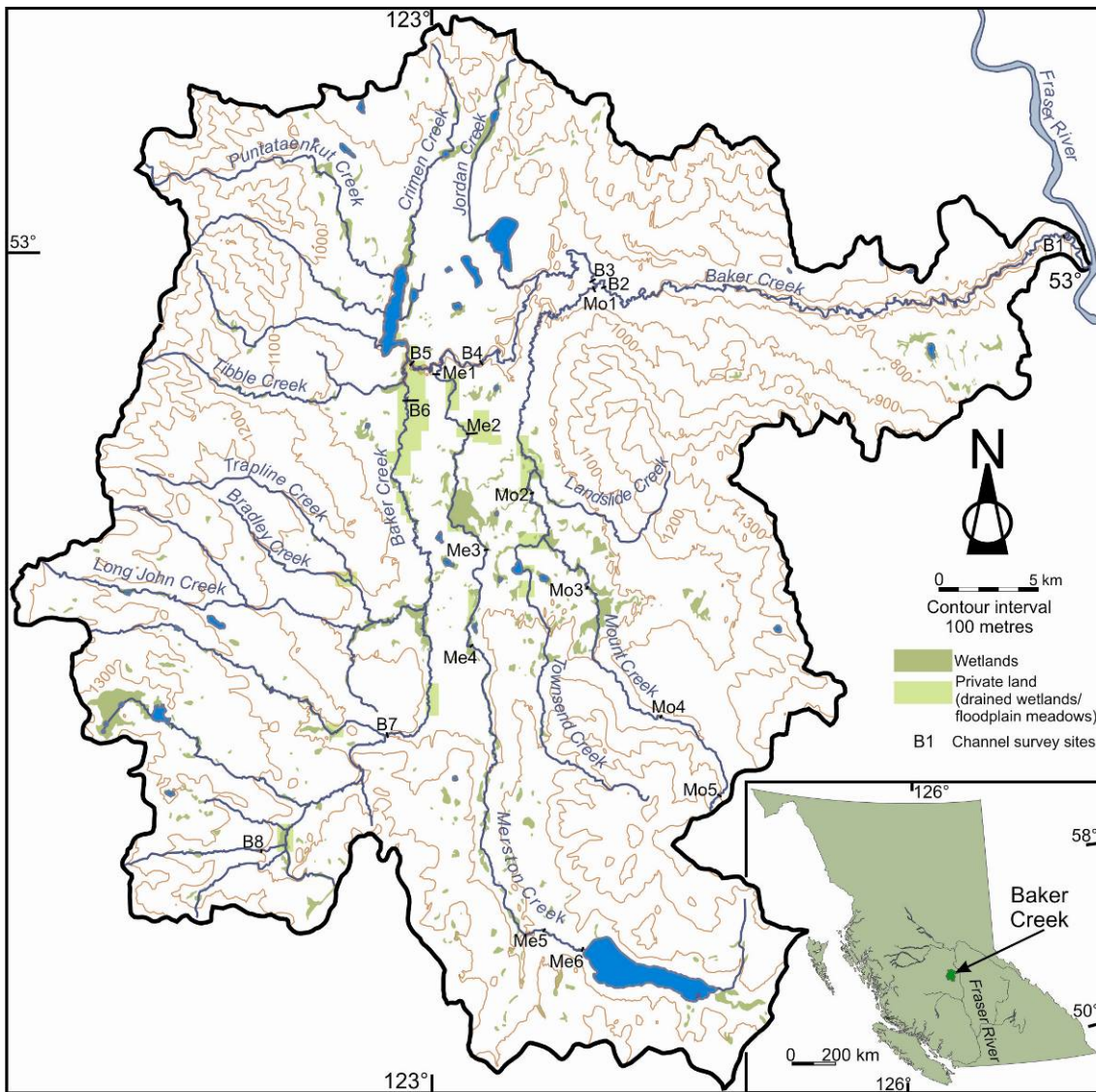


Figure 1. Baker Creek Watershed: Elevation contour lines and stream network.

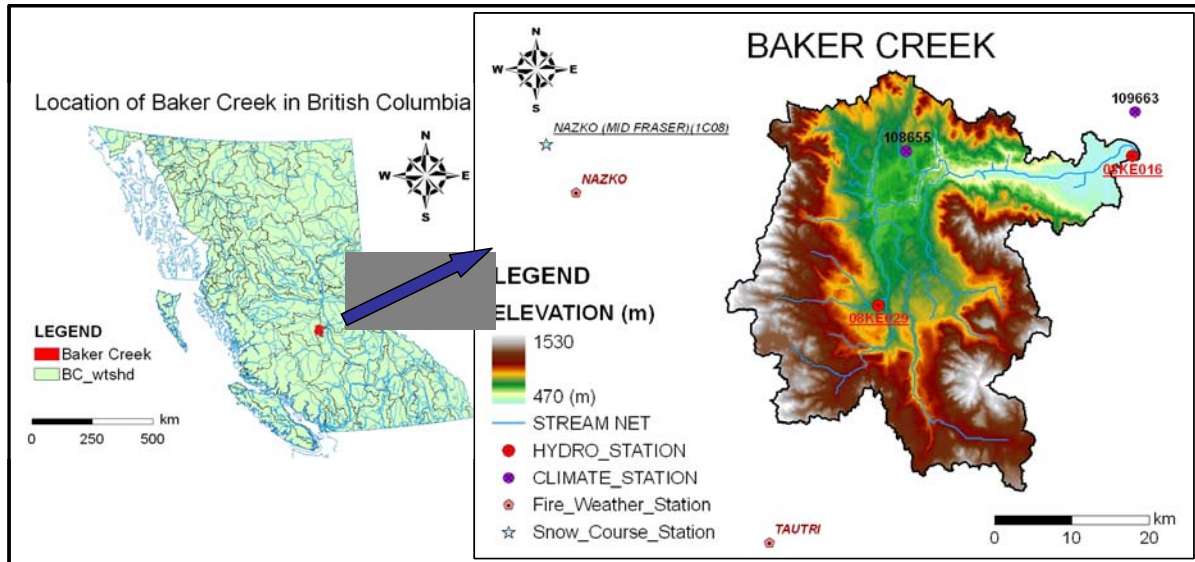


Figure 2. Baker Creek watershed: locations of existing long-term hydrometric, climate, and snow course stations.

Based on the data used to prepare Figure 3, the mean annual flood of Baker Creek is $39.5 \text{ m}^3\text{s}^{-1}$. Figure 3b shows the hydrograph for 2006, a fairly typical low baseflow, a rapid rise in discharge during the spring and a slower decline during the summer, with a return to baseflow in the autumn. Discharges in 2006 correspond fairly closely to the mean flow series in Figure 3a. The data series for 2007, although incomplete due to problems with the Water Survey of Canada gauge, shows at least two flood peaks with discharges over $80 \text{ m}^3\text{s}^{-1}$, one in late April and one in early May, separated by a period where flow reduced to $40\text{--}50 \text{ m}^3\text{s}^{-1}$. Anecdotal evidence from farmers living within the catchment suggests that floodplain meadows in the middle reaches of the catchment experienced three separate periods of overbank flooding during 2007.

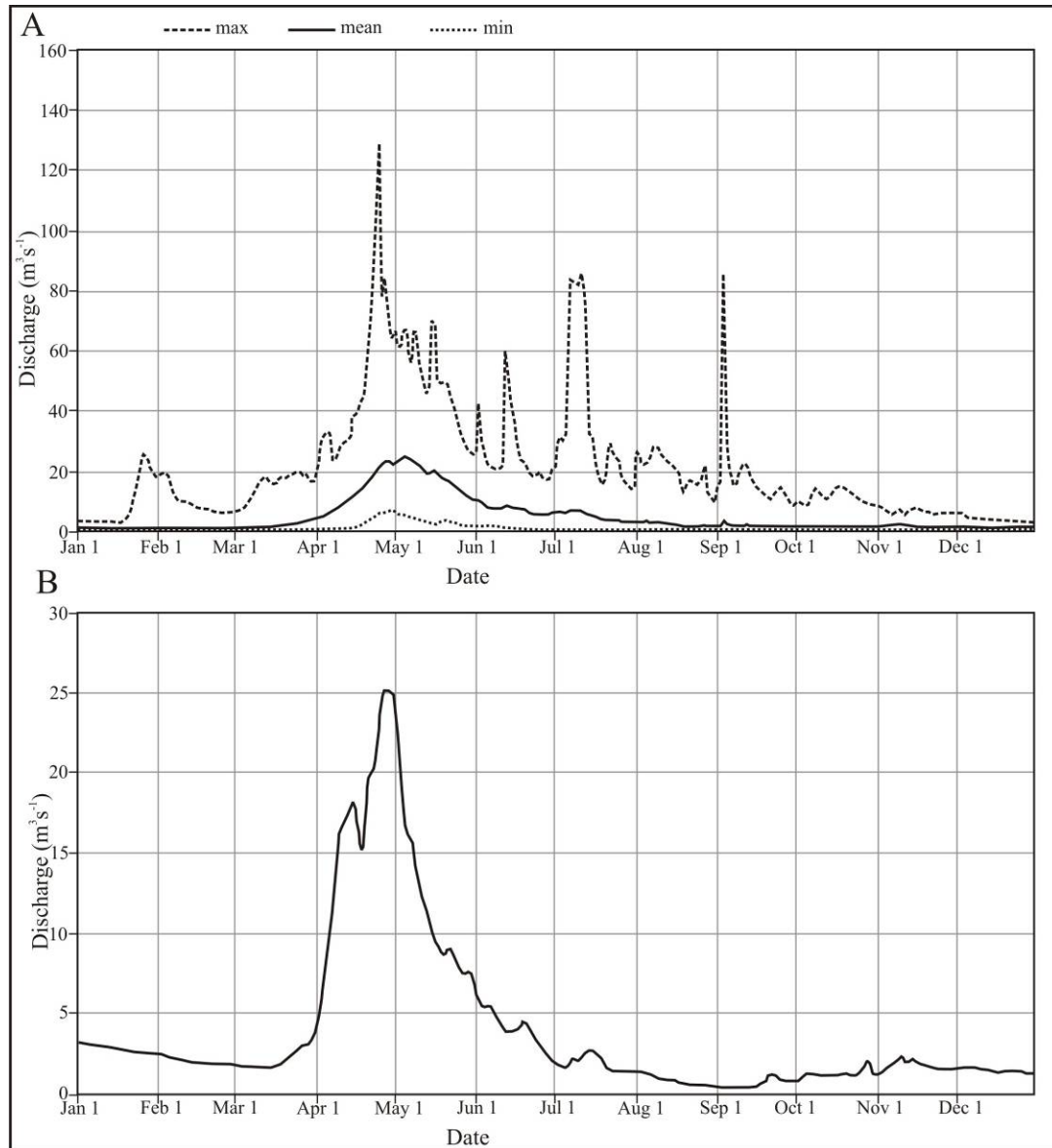


Figure 3. Representative hydrographs for the Baker Creek catchment, using data from the Water Survey of Canada gauging station in Quesnel, at the confluence of Baker Creek and the Fraser River.

Note: (A) Long-term (1963–2006) average daily flow, maximum daily flow, and minimum daily flow time series. (B) Typical annual hydrograph, using 2006 data, showing the steep rise to peak flow during the spring, with maximum flow occurring during late April, followed by a more gradual decline to low flows during the summer.

3 HYDROLOGY

3.1 Methods

3.1.1 Fieldwork

The immediate two main objectives of our fieldwork at Baker Creek are

- (1) to provide a spatially distributed dataset of the various meteorological variables required to run the Distributed Hydrology Soil Vegetation Model (Wigmosta et al. 1994), for simulating the mountain pine beetle (MPB) effects and treatment scenarios on snow and water discharge across the catchment; and
- (2) to efficiently sample the variability of snow water equivalent (SWE) across a large pine-dominated catchment affected by MPB, to examine the degree to which the MPB forest cover types control snow variability relative to other controlling factors such as elevation.

The resulting mean plot values of SWE can also be used to validate the DHSVM-predicted SWE values throughout the winter season, from which adjustments can be made to the model algorithms, which represent physically the various snow accumulations and melt processes occurring in MPB stands. A subsidiary objective, in conjunction with other project collaborators, is to improve the radiation transfer algorithms for the various MPB-affected stands; we focus on the effect of dead needle-fall on snow albedo, and the effect of dead stand enhancement of thermal irradiance. Both of these processes may significantly alter the energy and mass balances of the snowpack under various MPB stand types, but have received little explicit consideration in previous work. Each of these three objectives is now described in further detail below, and some initial datasets outlined, which incorporate measurements taken up until late March 2008.

3.1.2 Automatic weather stations

Eight automatic weather stations (AWS) were set up and completed between May and November 2007 before the winter 2007–2008 season. This complements two existing Meteorological Survey of Canada (MSC) weather stations for a network of 10 weather stations. Our weather stations were strategically placed across the catchment to capture the spatial variability in meteorological variables controlled by topographical and regional climate trends, and each station was located within a clearcut of age 0–5 years provide consistency between sites. Note that the land surface schemes present within almost all hydrological models such as DHSVM then attenuate the clearcut meteorology for forested pixels through the use of various decay coefficients (e.g., wind and solar radiation) and physical transfer algorithms. A map of AWS locations based on elevation band and biogeoclimatic ecological classification (BEC) zone is given in Figure 4. Table 1 outlines the specific names, GPS locations, and physical environment at each station.

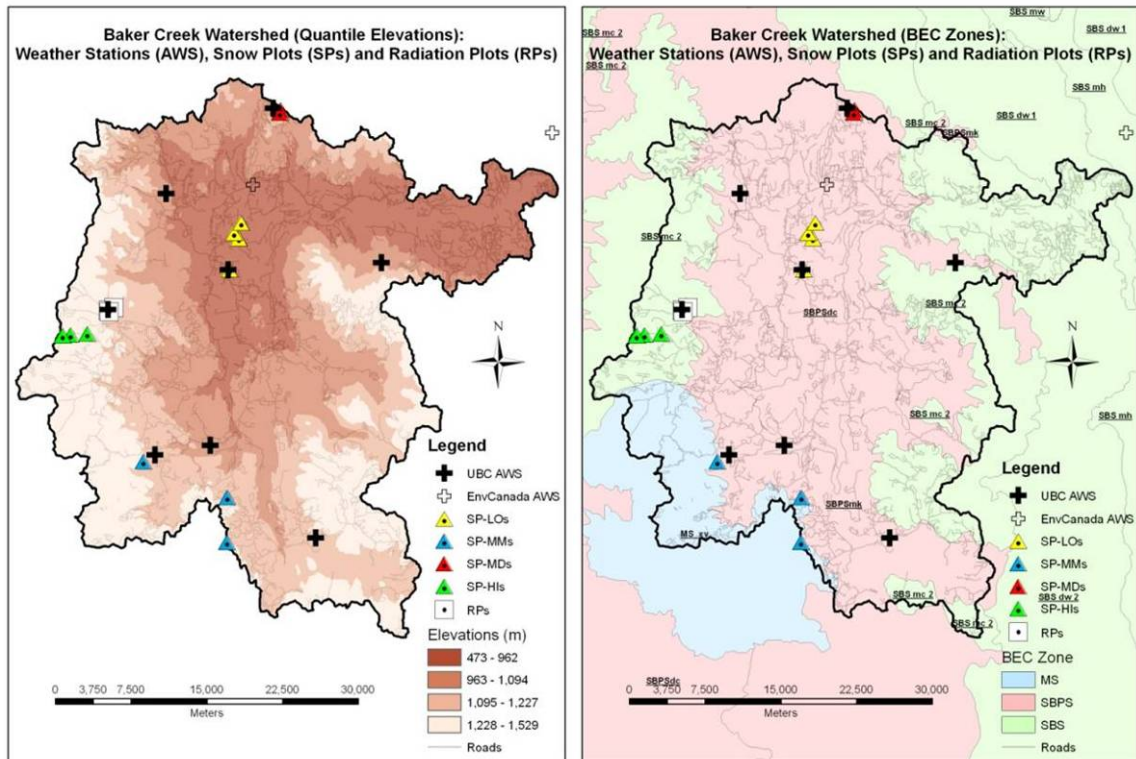


Figure 4. Location of AWS and snowplots across Baker Creek catchment, according to elevation (left) and BEC zone (right).

Table 1. AWS names, positions (in metres, UTM Zone 10N / Datum NAD 1983), elevations, and BEC zone.

Name	Alias name	Easting	Northing	Elevation (m)	BEC zone
SE-AWS	Roxanne	507755	5836233	1200	SBPSmk
N-AWS	Bud	505362	5878857	1105	SBPSmk
NE-AWS	Mickey	515423	5863117	1060	SBPSmk
NW-AWS	Nellie	494374	5870865	1050	SBPSmk
SW-AWS	Teddy	492166	5845103	1160	SBPSmk
W-AWS	Dennis	488132	5859635	1205	SBPSmk
S-AWS	Lily	497709	5845814	1020	SBPSmk
Cen-AWS	Saba	500220	5863081	910	SBPSdc

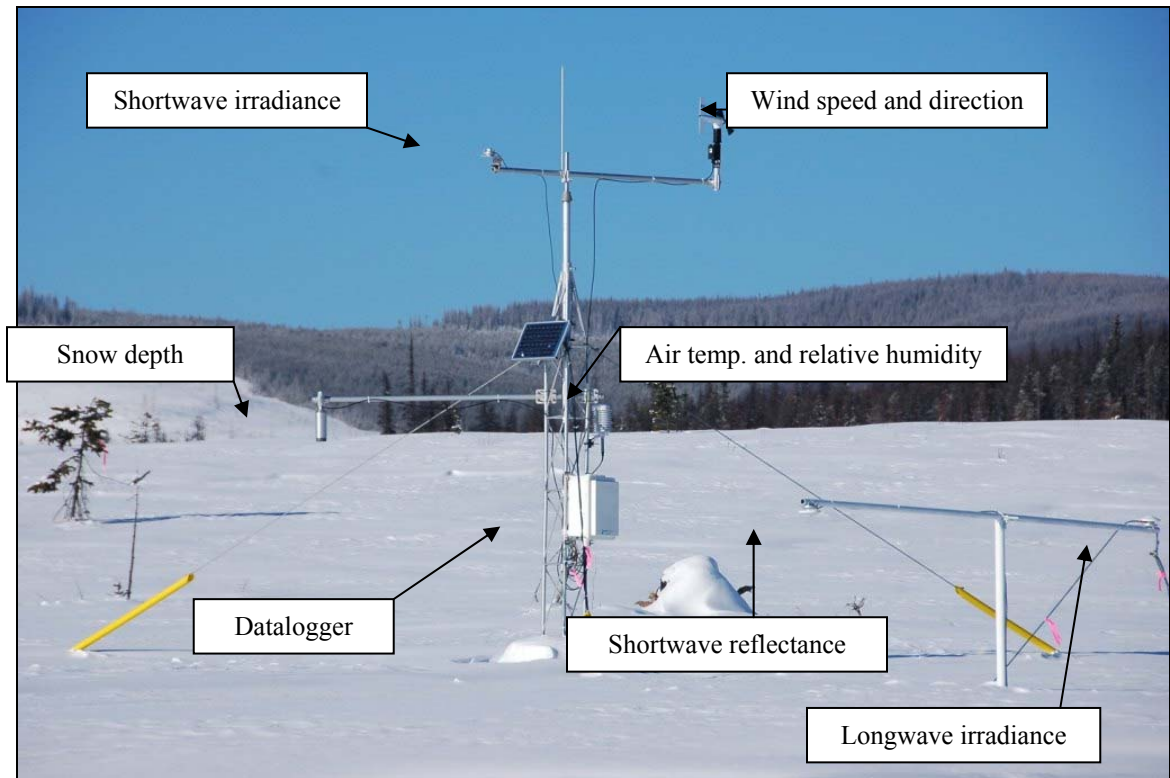


Figure 5. Western-AWS setup.

(Note: Rain gauge off to side of photo. Solar reflectance and longwave irradiance measurements are unique to this AWS.)

The meteorological variables required by DHSVM (and most other models) are air temperature, relative humidity, wind speed and direction, shortwave irradiance, and rainfall. These are being measured continuously every half-hour at each AWS, in addition to snow depth during winter and spring, which will ultimately be transformed into a continuous time series of snow water equivalent using a series of snow density measurements obtained from a Federal Snow Tube. The structure of an AWS is outlined in Figure 5. Table 2 outlines the specifications of each sensor including manufacturer, model number, stated accuracy and approximate height on AWS.

Table 2. Station sensor descriptions for a typical Baker Creek AWS.

Meteorological variable	Manufacturer	Model number	Stated accuracy	Approx. height (m)
Rainfall (tipping bucket rain gauge)	Texas Electronics	TE525M	±1%	1 m
Air temperature and relative humidity	Vaisala	HMP45C212	±0.2°C at 20°C, ±1% RH	2 m
Snow depth (sonic ranging sensor)	Campbell Scientific	SR50A	±1 cm	2 m
Solar irradiance (pyranometer)	Kipp and Zonen	SP-LITE	±10%	4 m
Wind speed and direction	RM Young	05103-10	±0.3 m/s (spd) ±3° (dir)	4 m
Datalogger for data storage	Campbell Scientific	CR1000	-	-
Power (12V battery and solar panel)	Campbell Scientific	PS100 (batt.) MSX10(sol. p)	-	-

3.1.3 Snowplot measurements

A simple stratified network of sampling plots was designed to efficiently sample the spatial and temporal snow variability across the catchment during the winter of 2007–2008, by stratifying the landscape using only forest cover and elevation. Forest cover was divided into the four main stand types covering almost all the landscape, including clearcuts harvested between 0 and 5 years ago (code CC), short regenerating pines aged 10–25 years with no MPB attack (RN), pines aged 25–60 years at various stages of MPB attack (RG), and mature pines aged beyond 60 years killed by MPB commonly referred to as “grey” or “ghost” stands (GY) (Figure 6). Elevation was divided into 4 bands, with plots located at mean values of 920 m asl (covering the lowest 12% catchment area, code H_{920}), 1100 m asl (51%, H_{1100}), 1220 m asl (75%, H_{1220}), and 1330 m asl (93%, H_{1330}). Geographically, the H_{920} plots were located in the lower catchment interior, and the H_{1100} , H_{1220} , and H_{1330} plots located towards the northern, southern, and western catchment boundaries, respectively (Figure 4).



SP-LO-CC

SP-LO-RN



SP-LO-RG



SP-LO-GY



Figure 6. Google Earth aerial image of three low elevation snowplots (SP-LO), and corresponding ground photos (also including site SP-LO-CC).

Plots were located as close together as possible within each area to minimize snowpack variability due to small changes in elevation or precipitation input with distance, which did not exceed 50 m (elevation) or 6.5 km (distance). In total, 13 plots were located across the catchment, with suitable RN and GY, and RN plots not being available within the H_{1100} and H_{1220} areas (Table 3). A further stratification of the catchment based on hillslope aspect was not made, unlike in most other studies (e.g., Watson et al. 2006; Jost et al. 2007), since slopes at Baker Creek are very gentle (mean 5.4° , standard deviation 4.2°) and insufficient to change solar irradiances beyond about 5% theoretically relative to horizontal ground. All plots were on slopes not exceeding 6° .

Table 3. Snowplot names and descriptions (positions in metres, UTM zone 10N / Datum NAD 1983).

ID	Elevation (m asl)	BEC zone	Easting	Northing	Stand type
SP-LO-CC	920	SBPSdc	500271	5863100	Clearcut
SP-LO-RN	920	SBPSdc	501613	5867671	1- to 2-m green regen.
SP-LO-RG	920	SBPSdc	500866	5866699	15- to 30-year attacked pine
SP-LO-GY	920	SBPSdc	501334	5866161	50+ year mature killed pine
SP-MD-CC	1100	SBPSmk	505999	5878713	Clearcut
SP-MD-RG	1100	SBPSmk	505934	5878384	15- to 30-year attacked pine
SP-MM-CC	1220	SBPSmk / MSxv	490931	5844517	Clearcut
SP-MM-RN	1220	SBPSmk / MSxv	499883	5838416	3- to 4-m green regen.
SP-MM-RG	1220	SBPSmk / MSxv	499084	5840654	15- to 30-year attacked pine
BOD1	1220	SBPSmk / MSxv	498885	5836218	50+ year mature killed pine
SP-HI-CC	1330	SBSmc2	484271	5857348	Clearcut
SP-HI-RG	1330	SBSmc2	485916	5857377	15- to 30-year attacked pine
SP-HI-GY	1330	SBSmc2	483457	5857274	50+ year mature killed pine

Note: Site BOD1 was set up and is monitored by Pat Teti, B.C. Ministry of Forests and Range.

For all sites except SP-MM-RN, snow measurements in each 50×50 m (0.25-ha) plot initially consisted of 36 snow depth measurements made at 10-m spacing, and 18 snow density measurements arranged in a staggered formation. Thirty-six SWE values were then obtained by multiplying individual snow depths by a mean density value. After the first two landscape surveys, the number of snow depth measurements (hence SWE data) were increased to 76 per plot by sampling every 5 m on the plot boundary and along each inside line in the x-axis, with no change to the arrangement of density measurements. This was to increase the power of detecting statistically significant differences in SWE between different forest stands of a given elevation, and between different elevation bands for a given stand type. Site SP-MM-RN was only set up just before the timing of peak snowpack in 2008, and a reduced sampling strategy was applied

using two 50-m perpendicular transects, along which snow depth measurements (and SWE estimates) were made every 5 m ($N = 21$), and density was measured at the transect intersection and end points ($N = 5$). The implications of each sampling strategy on the confidence intervals around estimated mean SWE values, and on the power to detect significant changes between plots, will be discussed as part of the *post-hoc* analysis of the data.

For either main strategy, sampling of snow depths at 5-m resolution was considered sufficient to avoid underestimating the snow depth variance (and it is assumed here SWE variance as well) due to spatial autocorrelation. This was determined from variogram analysis of 1-m measurements taken along 100-m transects in a pilot study carried out in the catchment around the time of peak snowpack in 2007. This study indicated that decorrelation lengths were approximately 1–3 m in a 5-year-old clearcut, and 3–5 m in representative red-attacked and grey stands. Other more heterogeneous stands (e.g., those on hummocky terrain, or grey stands with substantial windthrow damage) were not measured as part of this pilot study, and were therefore avoided when selecting sites for the 2007–2008 campaign.

In total, a full landscape snow survey of 13 plots using the relevant depth and density sampling designs took about 1.5–2 days to complete, usually by two teams of two people visiting one of the four main plot clusters each day. This enabled sites up to 40 km away to be sampled near instantaneously, which reduced the potential for snowfall and windstorm events or rapid melting to contribute further SWE variance between site locations in a given survey (beyond the hypothesized controls of elevation and stand type). Surveys were generally carried out monthly during the snow accumulation phase, and at weekly or bi-weekly intervals around the time of peak snowpack and major melting. Site access by a combination of truck and snowmobiles remained good up until washout of a logging road section prevented sampling of the H_{1330} sites beyond early May 2008.

To relate the SWE data to the stand characteristics at each plot, hemispherical (“fisheye”) photographs have been taken at each forested plot during March (Figure 7) to provide information such as Plant Area Index and the optical canopy parameters of shortwave transmissivity and sky-view factor. In April 2008, these photographic data were supplemented with traditional forest inventory measurements of diameter at breast height, species, MPB attack, height, and age made in each of four 100-m² circular areas. These results were subsequently used to improve the calibration of the forest structural parameters required as input to run DHSVM and other hydrological models.

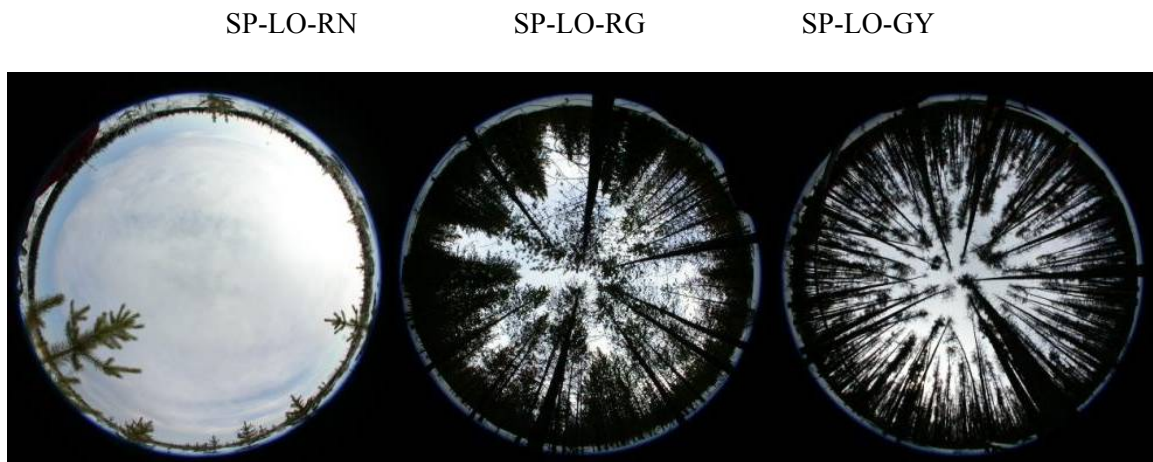


Figure 7. Sample hemispherical photos taken at each forested SP-LO snowplot in March 2008, used to derive forest density and optical parameter values.

3.1.4 Radiation measurements

A radiometer array consisting of 12 pyranometers measuring shortwave radiation flux, and 2 pyrgeometers measuring longwave radiation flux was purchased primarily to directly measure the variability of incoming radiative fluxes through the various MPB stands relative to fresh clearcut areas in which the canopy has no effect (Figure 8). Initial tests, however, determined that the difference in shortwave irradiance measured by a pyranometer and predicted by software analysis of a hemispherical photograph taken at the pyranometer location was generally less than 10% and within the range of measurement error. Shortwave transmissivity may therefore be sampled more effectively using hemispherical photography, which can be applied at any number of points within the stand and requires far less human resources than the time-consuming movement and levelling of pyranometers. Alternatively, short-term (minute to hourly) changes in cloud cover, which may affect rates of transmissivity through the stand, can only be measured by the pyranometers, although the cumulative effect of this decreases on longer timescales of days to weeks.

Instead, the pyranometers have now been used through the winter 2007–2008 season as part of an integrated shortwave albedo (reflectance) experiment designed to measure the extent to which the large amounts of dark and non-reflective dead needle litter falling onto snow affect the (typically high) reflectivity of transmitted shortwave radiation, which may then cause greater energy absorption at the snow surface and increase melt rates relative to a cleaner snow surface. The litter effects on snow reflectance are expected to decrease as surface and buried litter contents decrease, and as the snowpack becomes older and wetter through melt, during which albedo decreases and approaches that of the litter albedo. Since needle-fall from mature dead pine stands is almost complete, litter contents are expected to be much higher in more juvenile pine stands, which are in the early phase of MPB attack.



Figure 8. The UBC radiometer array setup (left) and measurement of shortwave transmissivity during April 2007 (right).

In an experiment similar to Melloh et al. (2001), who measured the differences in litter content and snow albedo between coniferous, deciduous, and clearcut areas, we are using a three-stage approach to measure litter and snow albedo effects at different spatial and temporal scales through the melt season.

Pairs of radiometers have been suspended in mid-air above the snowpack in a juvenile red-attacked and mature killed pine stand, respectively, to measure the albedo values during the snow season both in a larger gap (1 radiometer pair) and smaller gap directly under trees (1 radiometer pair). Albedo is then

calculated by dividing the shortwave reflected from the surface (downward-facing pyranometer) to that transmitted through the stand (upward-facing pyranometer). These values are then compared against corresponding clearcut albedo values measured at a nearby AWS (W-AWS; Figure 5) to isolate the effects of litter content and stage of melt.

The spatial distributions of surface litter across a given stand are being sampled across a similar grid network of 36 stakes (50×50 m), at which a 1-m^2 downward-looking photograph is taken and analyzed within a software package to derive surface litter fractions. Since shortwave radiation only penetrates the first 2–3 cm of a snowpack, Melloh et al. (2001) theorize that surface litter fractions and albedo are well correlated; this photograph survey therefore predicts 36 point-in-time estimates of combined snow and litter albedo across an MPB stand.

An ASD-Devices Spectroradiometer (Figure 9) is being used to derive the reflectance of the various pure surfaces under consideration (snow, red needles, green needles, and tree bark) from which the surface litter fractions from method (2) can be converted into albedo estimates. The device is also being used at the photograph locations with mixed snow and litter, to calibrate the results derived from these two methods. Note that reflectance results are also given at much higher resolution than is provided by the pyranometer setups (which integrate reflectance over the entire shortwave spectrum).



Figure 9. Deployment of the pyranometers in suspended albedo-mode (left) and calibration of the ASD-spectroradiometer (right).

3.1.5 Streamflow measurements

The locations of 12 stream water-level gauges were determined early in the snow accumulation period of 2006 (November–December) and were installed at the onset of the 2007 freshet season. Water-level gauge sites are strategically located at controlled reaches (under bridges) (Figure 10) and divide the watershed into 12 sub-basins. Each gauge is continuously recording water level by a Druck—PDCR 1230 pressure transducer (10 psi) (Figure 11). Flow rating curves are being developed for each gauge by a theoretical fluid mechanic method (Kean and Smith 2005) and validated through measuring a range of flows throughout the freshet season with a salt dilution technique (Wood and Dykes 2002). Continuous flow measurements on these tributaries will allow for testing of DHSVM’s internal flow routing, as well as supporting any future sub-basin studies with continuous flow data. Unfortunately, the time required for developing reliable discharge rating curves simultaneously at these 12 locations means that flow data on

these tributaries can only be used in future updates of the DHSVM model and not the version applied in this report.

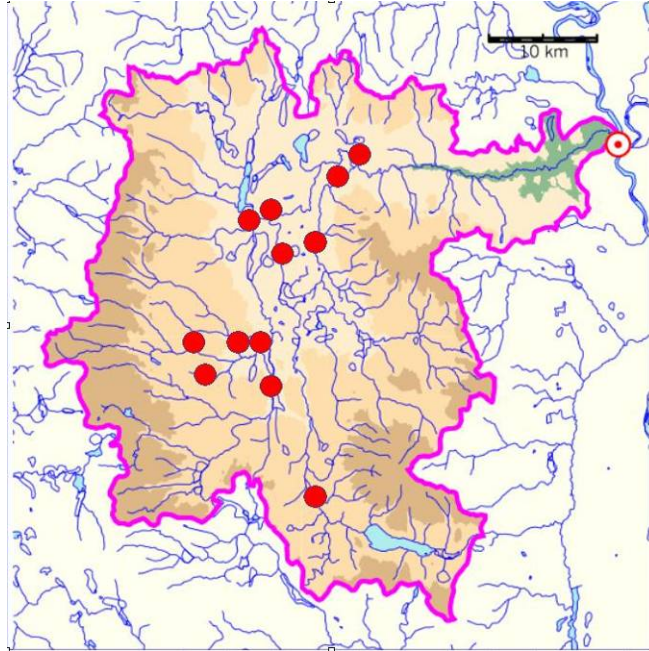


Figure 10. Location of 12 streamflow gauges equipped with continuously recording pressure transducers on the tributaries of Baker Creek.



Figure 11. Typical installations of water level recorder pressure transducer and datalogger at 12 stream gauging locations within Baker Creek.

3.2 Modeling

3.2.1 Overview of model development, calibration, and scenario analysis

The research methods adopted in this study follow an approach detailed in Alila and Beckers (2001). Model development and scenario analysis consisted of seven steps:

1. A 6400 pixel grid (500×500 m) was draped over the watershed using an available digital elevation model. Pixel size was constrained by the computing time required for running our long-term simulations in the scenario analyses.
2. Topography, stream network, soil types, forest cover types, cutblocks, and roads are input as distributed variables for each pixel.
3. Local long-term climate data from four meteorological stations were used as input to drive the model development and scenario analyses.
4. The model calculates a water and energy balance for each pixel, based on the meteorological and physical inputs for each grid-cell pixel and determines runoff over the entire watershed.
5. The model was calibrated for baseline (no harvest and no MPB attack) conditions using the 30-year record of climate and streamflow in Baker Creek and within and nearby snow course measurements.
6. The model was then used to simulate the streamflow of Baker Creek watershed to various MPB infestation and harvesting scenarios over time, using the same climate inputs.
7. The changes in streamflow for each scenario were statistically compared to the baseline condition to quantify the changes.

3.2.2 The Distributed Hydrology Soil Vegetation Model development

The model adapted for this study is the Distributed Hydrology Soil Vegetation Model (DHSVM) (Wigmosta et al. 1994). DHSVM is a physically based hydrologic model that explicitly solves the water and energy balance for each model grid-cell pixel. DHSVM consists of a two-layer canopy for evapotranspiration, a two-layer energy-balance model, for snow accumulation and melt, a one-dimensional unsaturated soil model and a two-dimensional saturated subsurface flow model. An independent one-dimensional (vertical) water balance is calculated for each pixel. Stomatal resistance is calculated for each vegetation layer based on air temperature, vapour pressure deficit, soil moisture conditions, and radiation. Evaporation of intercepted water from the surface of wet vegetation is assumed to occur at the potential rate, while transpiration from dry vegetative surfaces is calculated using a Penman-Monteith approach.

DHSVM has been applied to several catchments in the western United States and Canada (e.g., Storck et al. 1998; Whitaker et al. 2002; Beckers and Alila 2004; Thyer et al. 2004). The utility of this model in quantifying the influence of harvest type, roads, and basin physiography on water yield and peak flows (Bowling et al. 2000; La Marche and Lettenmaier 2001; VanShaar et al. 2002; Whitaker et al. 2002; Schnorbus and Alila 2004) has been demonstrated.

For Baker Creek watershed, a grid size of 500 m was adopted and the total number of grids is 6400. A sensitivity analysis showed there was little difference in results using a 200 m grid cell. However, the 200 m model application at Baker Creek is computationally more demanding, particularly for the long-term

simulations (each disturbance scenario was simulated using the 30 years of continuous climate record as input).

Topographic data were input from TRIM (20-m interval Terrain Resource Information Management) digital maps available from the BC government. Vegetation was classified into 9 categories with typical height, crown closure, and leaf area index (Table 4).

Table 4. Vegetation categories and physical parameters required by DHSVM.

Index #.	Area (%)	Class	Height (m)	Crown closure (%)	Leaf area index
1	3	Aspen	17	37.6	5.4
2	3	Douglas-fir	24	43.3	2.7
3	7	Lodgepole pine, 0–10 years	0.8	6.6	0.1
4	9	Lodgepole pine, 11–30 years	6	33.2	4.0
5	7	Lodgepole pine, 31–60 years	14	57.0	8.5
6	53	Lodgepole pine, 61+ years	21	55.0	2.8
7	5	Spruce	21	41.3	2.4
8	6	Logged	0	0	0
9	7	Rock	0	0	0

In this project, we maintained in scenarios the same operational constraints by retaining either live spruce or dead pine in these conservation areas.

The forest cover characteristics for the baseline conditions in 1970 (Figure 12) and the logging history since 1970 (Figure 13) were derived from RESULTS (B.C. Ministry of Forests and Range’s Silvicultural Database). The harvesting shows that 12% was logged in 1971 to 1980; 3% was logged in each of the following three periods, 1981–1990, 1990–2000, and 2001–2004; and 9% was estimated to be logged from 2005 to 2010. Forest cover in the future (2005–2010) was derived from the planned harvesting in the Consolidated Forest Development Plan maps. These maps show the areas, such as riparian reserves, Wildlife Habitat Areas, Old Growth Management Areas and other conservation areas, that will likely not be salvage harvested and will be retained for biodiversity objectives. In this project, we maintained in scenarios the same operational constraints by retaining either live spruce or dead pine in these conservation areas.

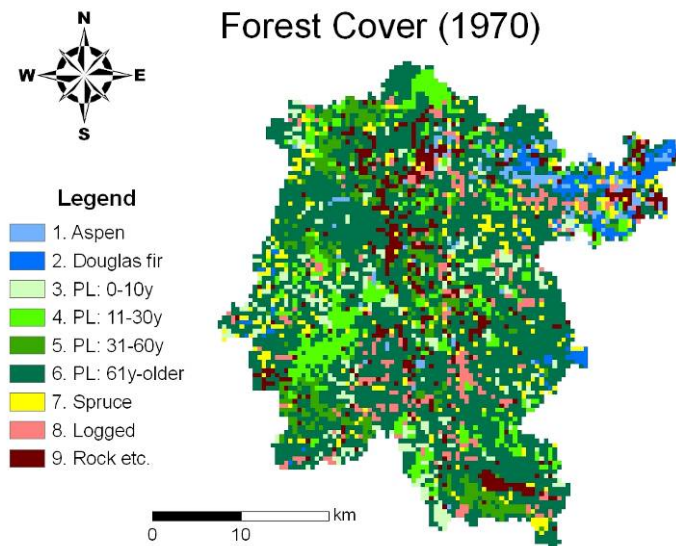


Figure 12. Distribution of vegetation within Baker Creek watersheds in 1970.

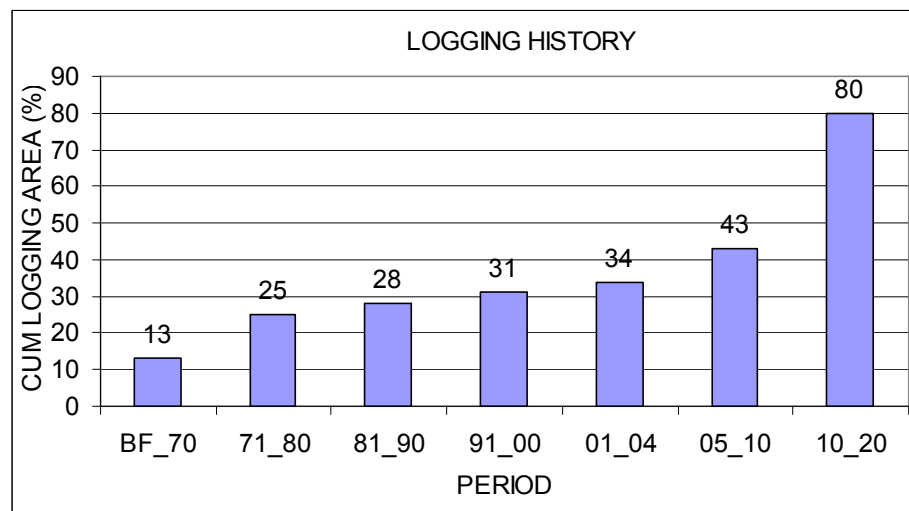


Figure 13. Percentage of Baker Creek watershed harvested and planned for harvest 1970–2020.

The areas of MPB attack in the Baker Creek watershed were obtained from the Canadian Forest Service (CFS), and more recently the B.C. Ministry of Forest and Range (MOFR), aerial detection surveys. Beetle attack began in this watershed in 1995 and grew to 85% of mature pine forest by 2005 (Figure 14).

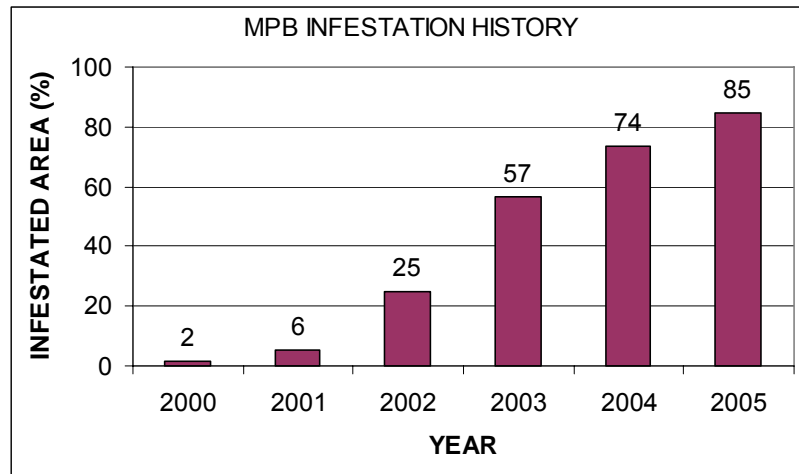


Figure 14. Percentage of mature pine forest area in Baker Creek infested with mountain pine beetle.

The road network was derived from the TRIM maps, but was filtered to only include main and secondary roads, and no spur roads (Figure 15). This was imposed by the limitations of the 500-m grid size and to reduce model processing time. Culverts were modelled at all TRIM streams and at 500-m intervals. Nine soil series are mapped in Baker Creek (Figure 16). Typical porosity, hydraulic conductivity and bulk density values were estimated from values for similar soil types.

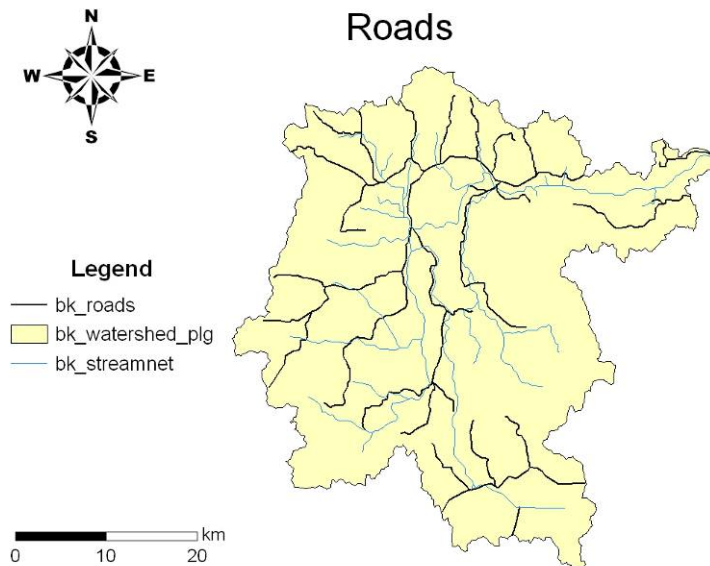


Figure 15. Simulated forest roads in Baker Creek watershed.

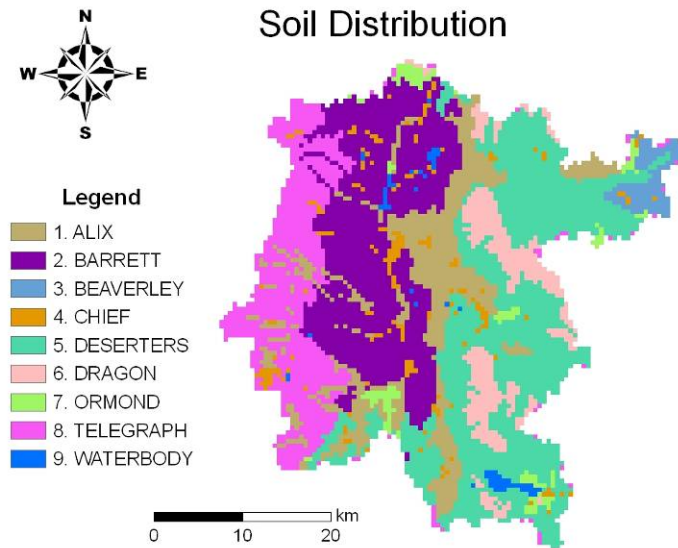


Figure 16. Soil distribution and classification in Baker Creek watershed.

Two long-term existing Water Survey of Canada (WSC) stream gauges were used in the model development and calibration. Little John Creek (169 km²) is an inactive gauge (active 1974 to 1983) on an upstream tributary. The Baker Creek gauge (continuous, active 1931–2006) is at the outlet on the main channel, above Quesnel.

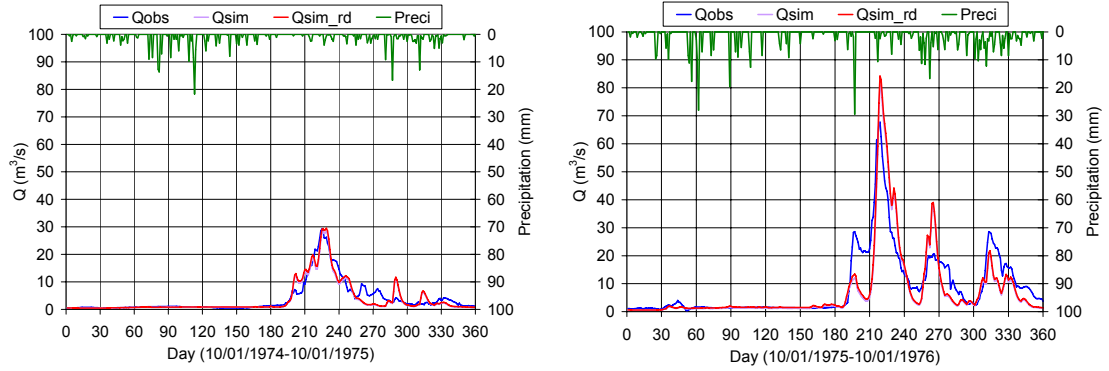
Two valley-bottom Meteorological Survey of Canada (MSC) long-term climate stations were used to drive the model during calibration and scenario analyses. One station is near the center of the watershed and a second near the outlet of Baker Creek with 30 years of record from 1975 to 2005. We also used two partial-record climate stations from the MOFR Fire Network that are representative of the upper elevation plateaus (Nazco 1995–2006 and Tautri 1990–2006), which recorded hourly precipitation, temperature, wind speed, and relative humidity from 1990 to 2006.

Precipitation, air temperature, wind speed, relative humidity, and incoming shortwave and longwave radiation must be specified as DHSVM model input for each time step. Some of these data are not available from MSC, which only provides maximum and minimum daily temperature and total daily precipitation. For this reason, we disaggregated the daily data of air temperature and precipitation into hourly data and estimated the missing parameter input, such as shortwave and longwave radiation, using well-established techniques in the literature (Waichler and Wigmosta 2003).

3.2.3 The Distributed Hydrology Soil Vegetation Model calibration

The performance of the DHSVM model, once calibrated, is evaluated visually and statistically. The visual criterion involves plotting and comparing the simulated and observed hydrographs (Figure 17). Statistically, the coefficient of model efficiency (CE) describes how well the volume and timing of the simulated hydrograph compares to the observed one, while the coefficient of model determination (CD) measures how well the shape of the simulated hydrograph reflects the observed hydrograph (Nash and Sutcliffe 1970). The closer these coefficients are to 1.00, the better the model performance. For the calibration and validation phases, CE was 0.73 and 0.80, respectively, and CD was 0.82. The calibrated model reproduces reasonably well both the timing and the flows as shown for four typical years in Figure 17.

(a) Calibration (1975 and 1976)



(b) Validation (1979 and 1982)

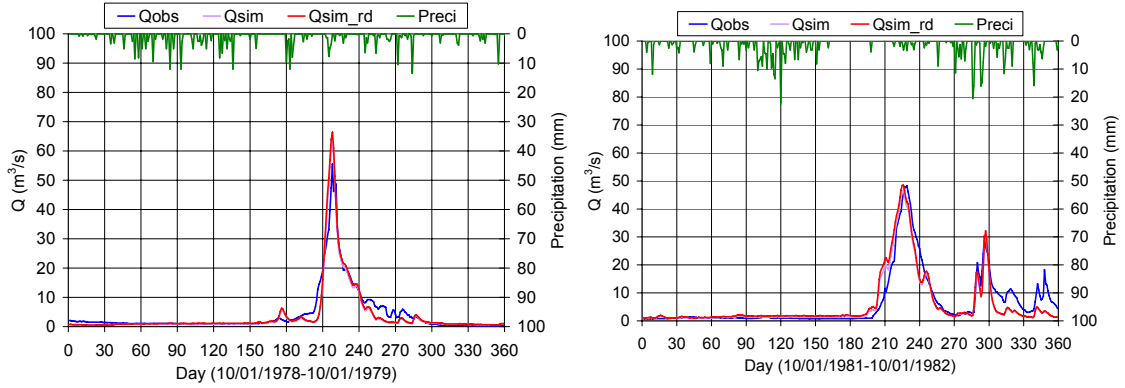


Figure 17. Simulated and observed hydrographs (Qsim: with roads, Qsim_rd: without roads).

The limitation of using two longer-term climate stations only to drive DHSVM over this large watershed makes it difficult to achieve better calibration. Spring rainfall events are likely convective in nature and their spatial variability over the watershed may not be well represented by only two climate stations.

To verify the model performance on snow estimation, the model predictions at two pixels (one at the high elevation of 1400 m, the other at the lower elevation of 1000 m) were queried and compared to a snow course station, Nazko (1C08) at elevation 1070 m. Figure 18 compares snow water equivalent (SWE) in the forest to that in open areas at both pixels for two typical years. The differences of SWE vary from 10% to 40%, and are smaller in a higher snow year (1976). The model predicted differences between randomly queried pixels of dead pine and live spruce well within published stand-level measurements in British Columbia (Winkler and Roach 2005; Winkler et al. 2005; Beaudry 2006; Teti 2008).

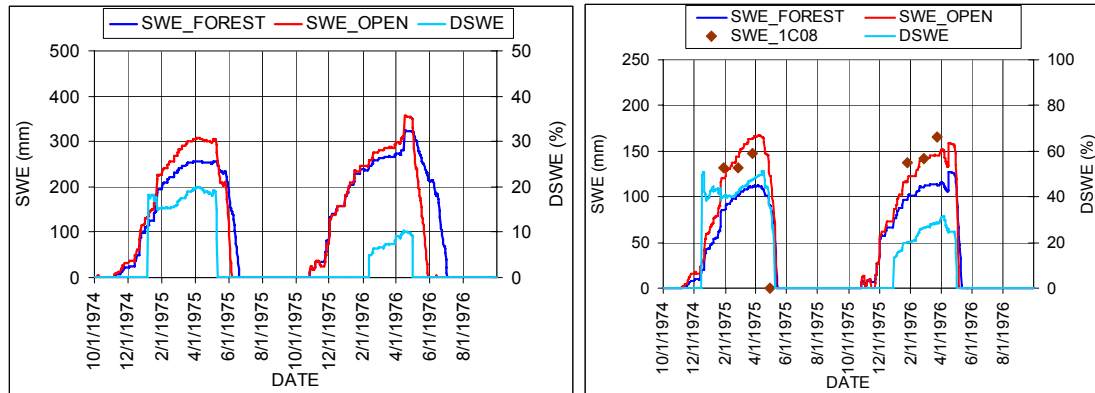


Figure 18. Comparison of SWE at two pixels (left elevation 1400 m; right elevation 1000 m).

3.2.4 Distributed Hydrology Soil Vegetation Model scenario description

We simulated with the calibrated DHSVM model one baseline and five scenarios of various combinations of historical and future salvage harvesting and MPB attack in Baker Creek watershed (Table 5).

Our baseline is based on the vegetation conditions in 1970, which included 9% bare area (rock and grasslands) and 4% harvested area, for a total bare area of 13%. Our scenario 1 represents the cumulative historic pre-infestation harvest conditions up to 1995. Before 1995, there was no significant MPB infestation in Baker Creek watershed. Total area of harvest to 1995 was 15% above baseline for a total harvested area of 28%. Our scenarios 2 through 5 represent different salvage logging strategies with 60%, 40%, 20%, and 0% retention, respectively. In these salvage logging scenarios, live spruce was retained but the substantial part of retained forest was dead pine trees of various ages. Note that dominant pine stands as young as 20 years have been infested in Baker Creek watershed.

Table 5. Percentage harvested, forested, and attacked of watershed for each scenario.

Scenario	Description	Harvested area (%)	Harvested area over baseline (%)	Forested area (%)	MPB - attacked area (%)*
0	Baseline	13	0	87	0
1	Pre-beetle 1995 conditions	28	15	72	0
2	60% retention	40	27	60	49
3	40% retention	60	47	40	38
4	20% retention	80	67	20	18
5	0% retention	100	87	0	0

Table 5 summarizes the forested area, harvested area, and watershed area infested by MPB for each scenario. Our scenario analysis does not include the simulation of forest regrowth after beetle attack or

salvage logging. Therefore, model-predicted effects on water yield and peak flow regime are representative of the time period immediately after infestation and salvage logging before any substantial recovery. The hydrologic recovery of the flow regime in interior snow-dominated environment is expected to be very slow. A study of post-treatment flow data at a similar environment in Colorado found no signs of any hydrologic recovery 30 years after logging and estimated the full hydrologic recovery of the flow regime to take 60–80 years (Troendle and King 1985; Elder et al. 2006). The study of recovery is planned for a subsequent phase of our project pending availability of funding.

3.3 Results and Discussion

3.3.1 Automatic weather stations

The construction of all eight AWS was completed by October 2007, and the first winter dataset has now been completed. A sample dataset compares the data from W-AWS at higher elevations, and Cen-AWS at lower elevations from November 1, 2007, to March 10, 2008 (Figure 19).

3.3.2 Snowplot results

The snowplot mean values of snow depth, snow density, and snow water equivalent (SWE) are presented in Figure 20 for the period between November 2007 and early May 2008. The half-hourly nearby automated measurements of snow depth at W-AWS and Cen-AWS are also shown for comparison. The following sections consider analysis of the snow data for individual phases.

3.3.3 Snow accumulation

The accumulation phase of 2007–2008 was characterized by frequent small snowfalls of up to 0.2-m depth between early November and early March. Plot mean values of snow depth all peaked on February 22 at 920 m elevation, March 29 at 1330 m elevation, and between these dates at the 1100 and 1220 m elevations, although the continuous SR50 measurements indicate actual peaks of snow depth occurred after the snowfalls of February 14 at 900 m and March 4 at 1200 m. March was uncharacteristically cool across Baker Creek and British Columbia in general, and values of SWE between February 22 and March 29 closely followed values of snow density, which generally were constant or increased slightly between February 22 and March 12, and accelerated thereafter until March 29 when peak SWE values were recorded in most plots.

While the proximity of the March 29 date to the assumed peak SWE occurrence date (April 1) across much of the Interior and Columbia-Kootenay region does not indicate the 2008 accumulation period to be extraordinary temporally, snow depth and SWE in this particular region typically peak on March 1, according to the 33-year record of monthly snow data from the nearest B.C. Ministry of Environment manual snow course (1C08-Nazko, 1030 m elevation, 25 km west of Baker Creek). SWE values measured here on March 1 and April 1, 2008, were 11% and 24% higher, respectively, than the long-term values, although corresponding values across much of the Fraser Basin were near-normal (B.C. Ministry of Environment 2008).

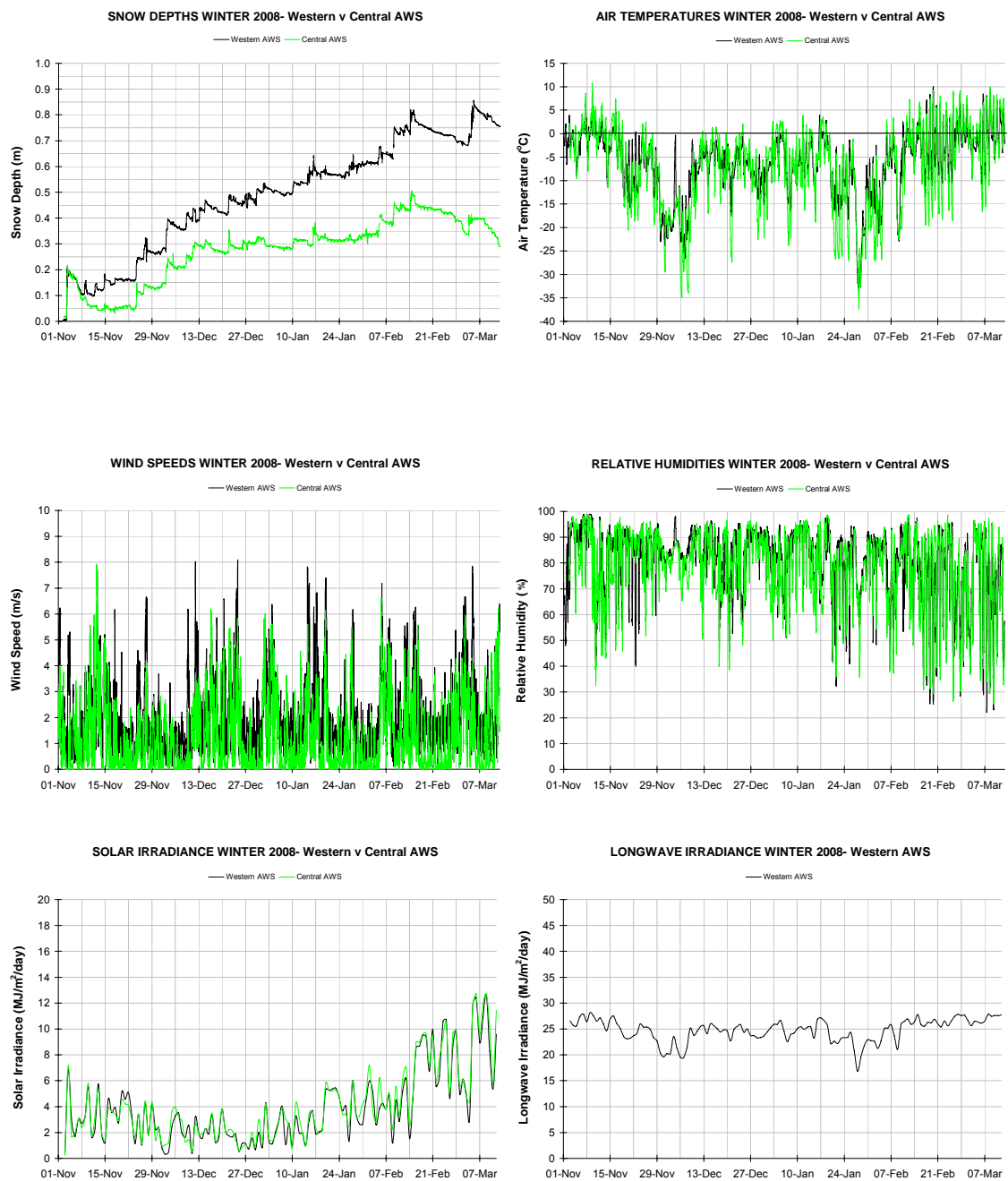


Figure 19. Sample AWS data from Western AWS (1205 m asl) (black) and Central AWS (905 m asl) (green), between November 1, 2007, and March 10, 2008.

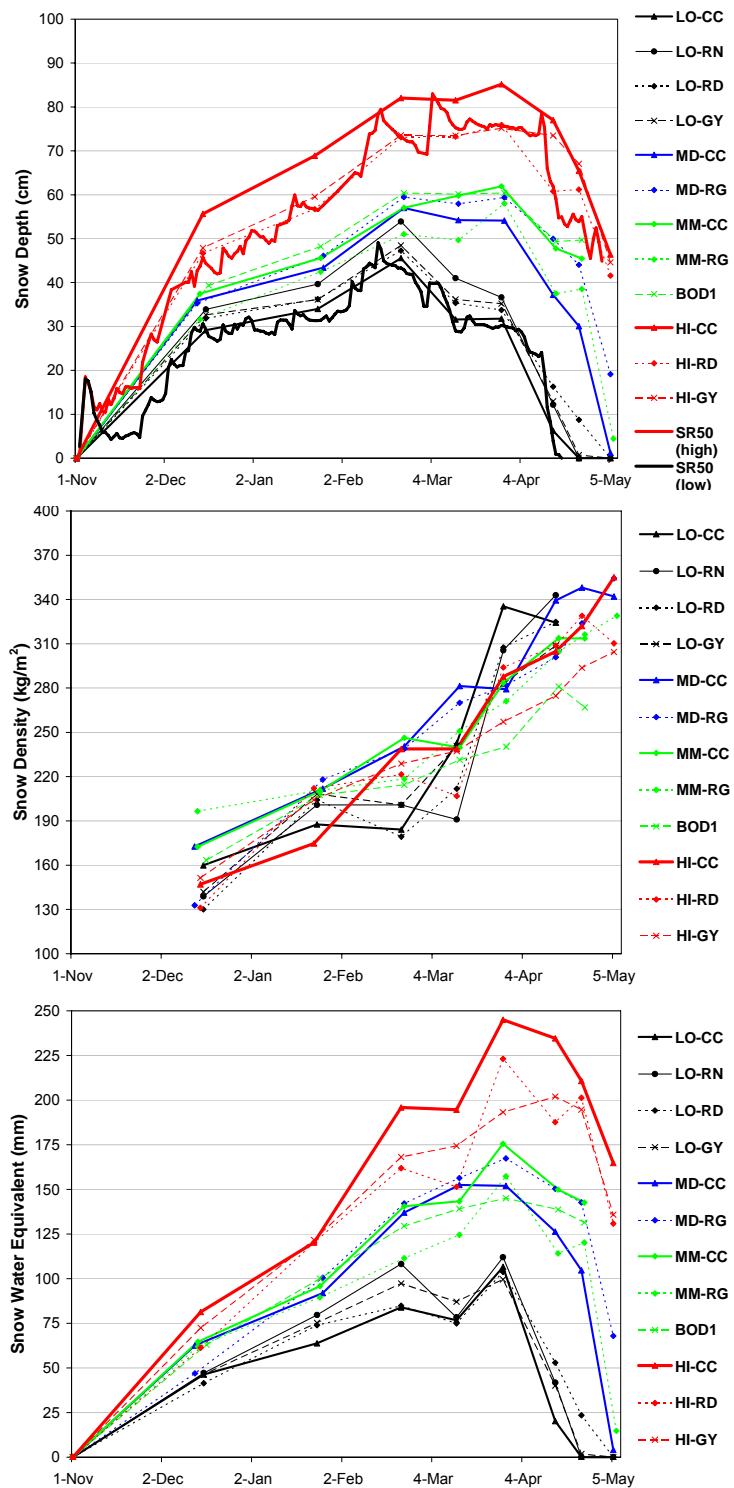


Figure 20. Snowplot (SP) data from winter 2007–2008, including plot mean values of snow depth, snow density, and snow water equivalent.

The means and variability of the (peak) March 29 SWE data are also provided when sorted by stand type (Figure 21) and elevation (Figure 22). Preliminary statistical analyses of these data indicate a near linear increase of SWE with elevation irrespective of the stand type under consideration. Significant differences were noted at the 0.05 level between the lowest and mid elevation, and between the mid- to upper-elevations. Alternatively, for a given elevation, SWE is very poorly correlated with stand type, with clearcut (CC) SWE within 10% of other stand types at the 920-m and 1100-m elevations. This may be due to the effects of reduced interception in the MPB-attacked stands, and the increase of scour and sublimation processes in the clearcuts due to higher wind speeds. The latter issue is dealt with in more detail as part of the next subsection of this report; the former is currently being investigated within related MPBI projects (e.g., Teti, MPBI 8.39). At the 1220-m elevation, CC SWE is 17% higher than the corresponding mature grey stand, but the only suitable clearcut was located 40 m higher than the other sites. At upper elevations, grey stands have higher proportions of live spruce trees resulting in a stand-level increase of interception efficiency. This was also the case at the 1330-m elevation, and the CC was also located below a slight ridge feature from which drifting snow would have originated and deposited in the clearcut. A preliminary two-way ANOVA analysis of all 12 plots indicates that elevation was sufficient to explain 84% of the SWE variance across the landscape, with almost no further variance being attributable to stand type. Note that elevation explains 93% of snow depth variance, which is higher than for SWE due to the absence of complicating spatial and temporal patterns of snow density variability.

3.3.4 Snow ablation

Figure 23 shows the ablation rates for each plot, which are again sorted by plot and elevation. These cover the period between March 29 (peak SWE) and April 24, 2008, in which snow was still present at all sites; the low sites melted out soon after this, whereas ablation progressed much more slowly at 1330 m with May 5 SWE values still around two-thirds of peak values, and at an intermediate rate at 1100 and 1220 m with melt-out probably occurring shortly after the last survey on May 5, 2008.

At most elevations, this preliminary analysis indicates slightly higher ablation rates in the open stands (CC and RN) than the subcanopy stands (RG and GY). Large reductions in melt rates of up to 60% have been observed under mature, healthy canopies in southern British Columbia relative to clearcuts (Spittlehouse and Winkler 2002) due to the canopy absorption of shortwave radiation. However, these differences may be expected to decrease in MPB forests with the loss of foliage and substantial windthrow, which increase shortwave transmittance. The collection of litter on the snow surface may also offset decreased subcanopy melt rates, and is the focus of the next subsection.

Wind redistribution of snow, particularly from the clearcuts, is likely to diminish as the snow becomes wet and increasingly cohesive (Pomeroy and Li 1997). Future ANOVA of the ablation rate data, incorporating the post-April 24, 2008, data, at higher elevations, will determine the relative effects of elevation and stand type on ablation across the catchment.

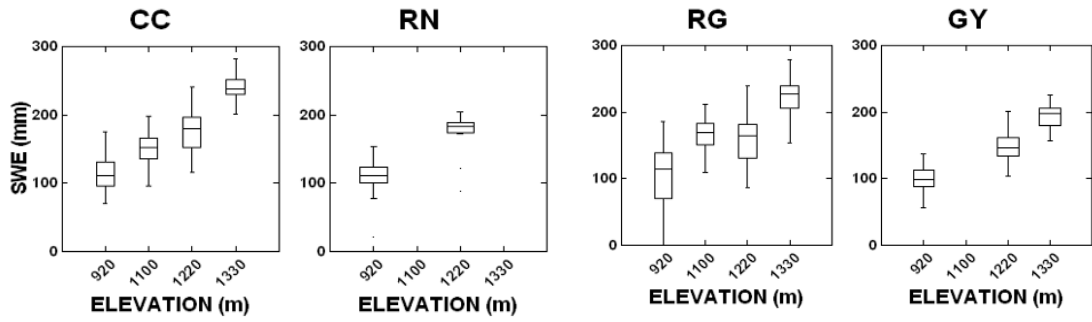


Figure 21. March 29 (peak) SWE data, sorted by stand type for all elevations.

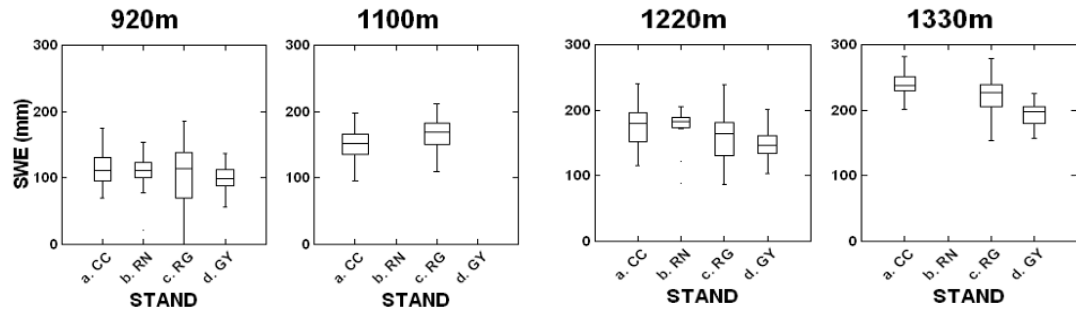


Figure 22. March 29 (peak) SWE data, sorted by elevation for all stand types.

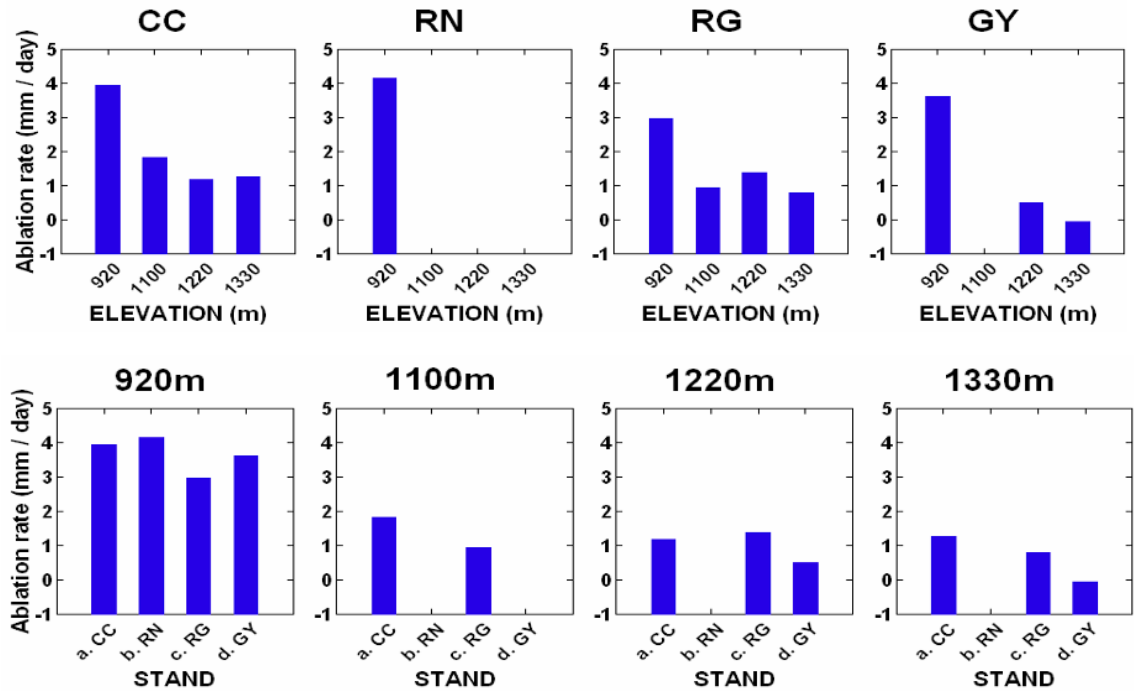


Figure 23. Plot ablation rates between March 29 and April 24, 2008.

3.3.5 Possible wind effects on snow

Unprecedented rates of salvage logging are producing clearcuts far larger than occur in areas unaffected by MPB. Although the Forest Stewardship Program (FSP) restricts the size of individual clearcutting to a maximum of 80 ha, the thin buffer zones of standing trees commonly dividing individual clearcuts are easily felled in windstorms, leading to rapid growth in the effective size of clearcuts. Some of these at Baker Creek are as large as 350 ha (Figure 24), representing significant proportions of the hillslope area. Traditional clearcut snow surveys are conducted in small clearcut areas of diameter no larger than several surrounding tree heights (e.g., Boon 2007), which effectively traps snow due to their sheltered nature from higher wind speeds which may scour the snow and enhance sublimation losses to the atmosphere (e.g., Bernier and Swanson 1993).

Initial analysis of data from all weather stations, such as those at W-AWS (Figure 5), indicate several sharp drops of snow depth each on the order of a few centimetres (or 5%–10% of total snow depth) (Figure 25a). Preliminary analysis indicates that these reductions cannot be attributed to melting events (air temperatures are below freezing), compaction and metamorphism (these occur slowly), or sublimation (wind speeds and vapour pressures are insufficient). Also, the necessary air temperature corrections were used to correct for the speed of sound signal emitted by the SR50 sensor in measuring snow depth. It may therefore be possible that erosion of snow is occurring in clearcuts as small as 25 ha, which may partially account for the apparent near-equality in peak ratio values of clearcut to subcanopy SWE outlined in previous sections. Hydrologically, the implications of this process are uncertain, since the destination of this scoured snow is unknown. Redistribution to adjacent stands would lead to differential melting rates than would be experienced in the clearcut, whereas sublimation of this snow in transit would reduce the overall water balance. The probability of blowing snow occurrence is reduced during the snowmelt phase, since the snow becomes wet and more cohesive (Pomeroy and Li 1997).

To explore this concept further, investigations are ongoing to apply the physically based Cold Regions Hydrological Model (CRHM) to the Baker Creek clearcuts using the AWS data of wind speed, air temperature, and humidity as input, and the SR50 snow depth data to validate the results. The model predicts areal rates of snow erosion, transport, and sublimation from source and destination areas. However, such models have only been developed for prairie and arctic landscapes in which wind-driven losses represent a significant proportion of annual precipitation (Pomeroy and Li 1997), so the algorithms developed for these environments may not necessarily be applicable in clearcut environments. For instance, “steady state” wind conditions are assumed in models such as CRHM since uniform fetch and constant wind speeds are common across prairie landscapes, whereas in clearcut environments both complex topography and adjacent stands make the air much more turbulent. Discussions are underway with CRHM’s primary designer, Professor John Pomeroy, regarding changes to the model algorithms and parameter values that may more realistically represent conditions at Baker Creek.



Figure 24. A 350-ha clearcut on the eastern hillslope of Baker Creek, December 2007.

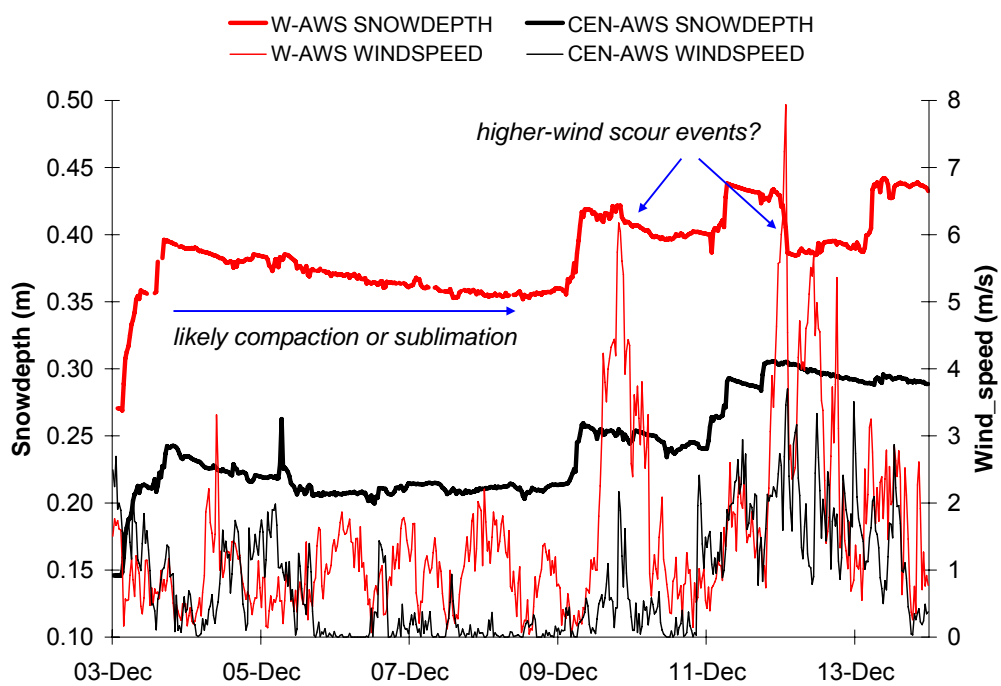


Figure 25a. Possible higher windspeed scour events at W-AWS relative to Cen-AWS, December 2007.

3.3.6 Albedo investigation

Initial results from the albedo experiment (suspended pyranometers, downward-looking photos, spectroradiometer) are as follows.

Reliable pyranometer data were obtained from mid-March 2008 onwards (Figure 25b), when fresh snowfalls with which to cover the upward-facing pyranometers and invalidate albedo calculations became increasingly uncommon. Clearcut albedo averages rose 0.88 until peak SWE (assumed March 29), and then dropped to 0.76 by the end of April due to increasing size of snow grains and wetness in between more fresh snowfalls, which melted rapidly. The snow here was still continuous (35-cm depth) at the start of May, and a further visit is required to download the mid-May data representing the transition to patchy snow cover and bareground conditions. In the adjacent red-attacked stand, March 18 values averaged 0.76 in the 6 m diameter gap, and 0.63 in the 3-m gap, although these still require slight upward corrections (about 0.05–0.10) to account for the reduction in albedo due to nearby tree trunks.

Heavily littered non-melting snow in smaller gaps may therefore be reduced in albedo by as much as 0.1 or more relative to clearcut (clean) snow; this difference only increased during melt as litter buried by previous snowfalls became progressively exposed at the snow surface. By April 26, the smaller gap only had patchy snow remaining with albedo 0.35, whereas the larger gap was snow covered with some litter, with mean albedo of 0.60 (clearcut albedo 0.78 on this date). The mature grey stand albedo values closely approximated those from the 6 m diameter gap in the red stand, since the size of gaps was the same but the presence of fallen bark pieces contributed to albedo reduction compared to purely red needles in the red stand. Downward-looking photos taken on the final survey of May 3 reveal these compositional differences between the stands (Figure 26), but stand-average calculations of litter fractions (and the effect of this on snow albedo) not reported here await analysis of all photos taken.

The ASD-spectroradiometer was used to gain not only spectral reflectance of the different litter compositions (red and green needles, and bark pieces; Figure 27), but also the change in reflectance as red needles were progressively added to an area of clean, clearcut, and non-melting snow in a repeat of the Melloh et al. (2001) experiment outlined previously. These results clearly show the decrease in reflectance, particularly within the visible spectrum (<750 nm) as more litter was added (Figure 28). The reflectance of near-infrared wavelengths (>750 nm) was less strongly affected since this depends more on the snow grain properties than on surface litter contents. Again, photo analysis is required to correlate each incremental litter fraction with the resulting drop in individual wavelength reflectance. Administrative deadline for delivery imposed by funding agencies meant that the results of such photo analysis are not included in this report.

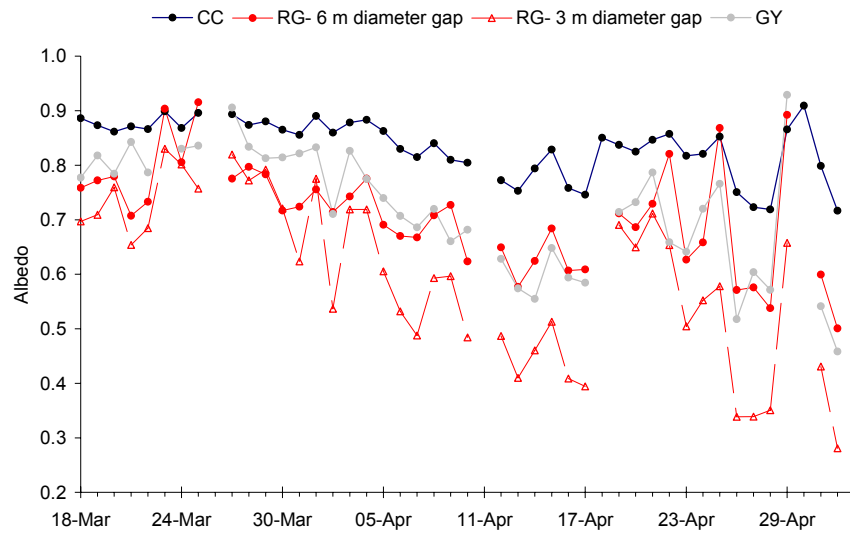


Figure 25b Daily snow albedo values measured in the clearcut, grey stand (6-m gap diameter), and red stand (3- and 6-m gap diameters), March 18 to May 3, 2008.



Figure 26. General site conditions (top) and downward photos (bottom) from the clearcut (left), grey stand (middle), and red-attached stand (right) on May 3, 2008.



Figure 27. Litter piles used to obtain “pure” albedo values of needles and bark using the ASD-spectroradiometer.

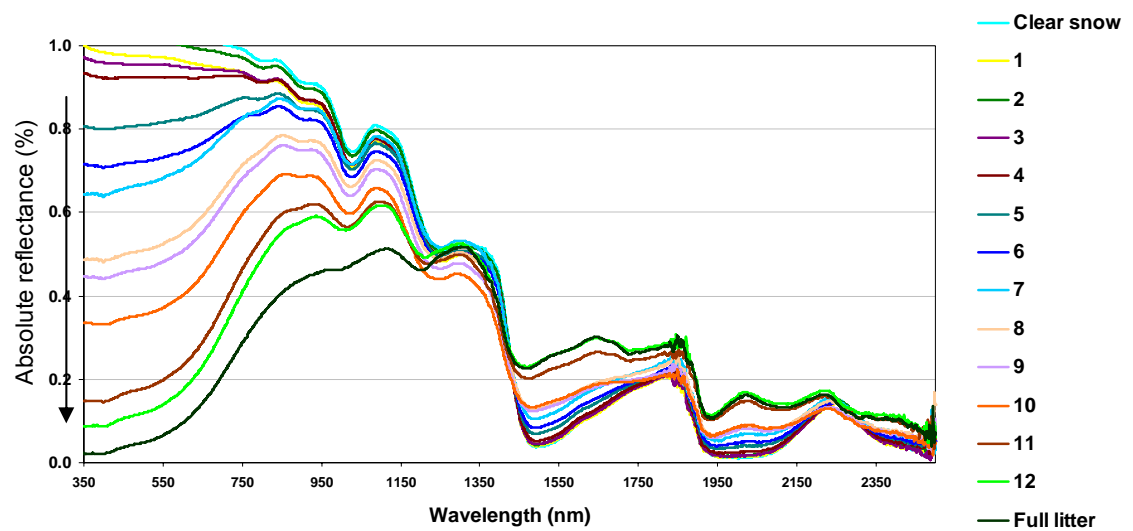


Figure 28. Spectral reflectances of snow increasingly littered with red needles.

3.4 Simulated Effects on Peak Flow and Water Yield Regimes

Newly published results in any study are normally considered reasonable if they are consistent with past observations and current understanding. However, information in the present literature is based largely on paired watershed studies over small drainages not exceeding a few square kilometres. There is limited empirical evidence about the extent to which the results from studies in small catchments can be applied at larger scales in snow-dominated watersheds. The extrapolation of results from small paired watershed studies to our larger watersheds is even more uncertain for peak flows due to the influence of, among other factors, elevation gradients and topography on the snow processes during the freshet (Troendle et al. 2001; Whitaker et al. 2002). The few paired watershed studies over larger basins had a level of cut or disturbance not large enough to be used as a reference in a comparison with our own results. Therefore, direct comparisons of results from historic paired watershed studies and the predicted effects of clearcut salvage logging in this study are not possible.

Changes to the peak flow, water yield, and timing of the peak flows are summarized in Table 6 and typical pre- and post-flood frequency curves are provided in Figures 29 and 30. In this study, measurements within Baker Creek and available stand-level knowledge on water and energy balance from recent MPB related literature (e.g., Teti 2008) were used in the parameterization and calibration to improve on the internal accuracy of DHSVM. This has helped build some confidence in model predictions but further testing and new developments in the model are planned in the next phase of this project once more of the streamflow measurements on the 12 currently monitored tributaries within Baker become available.

Table 6. Predicted changes of peak flows, water yield and time advance in peak flow.

Scenario	$\square Q_2$		ΔQ_{10}		ΔQ_{20}		ΔQ_{50}		ΔQ_{Av}		ΔWY (%)	ΔTp (days)
	m ³ /s	%	m ³ /s	%	m ³ /s	%	m ³ /s	%	m ³ /s	%	Seas	
1: Pre-MPB-1996	6	14	11	13	13	13	15	12	9	13	7	2
2: 60% retention	30	66	55	65	65	65	77	64	44	65	34	15
3: 40% retention	39	88	72	84	84	84	100	83	57	85	46	17
4: 20% retention	43	95	78	92	91	91	108	90	62	93	52	18
5: 0% retention	47	104	84	99	99	99	117	98	67	101	55	19

Statistically significant at the 95% confidence level (Sample size of annual flood maxima time series is 30 years; Confidence bands in Figures 28 and 29 were estimated based on 1000 replications using a Gumbel frequency distribution)

Note: Column 1 is scenario index in the same sequence as Table 5; columns 2 to 5 are changes in peak flow either in cubic metre per second or in percent for return periods 2, 10, 20, and 50 years, respectively; column 6 is the average of columns 2 to 5; column 7 is the change in water yield for freshet season (April to July); the last column is the time advance in peak flow averaged over 30 years, the full simulated record.

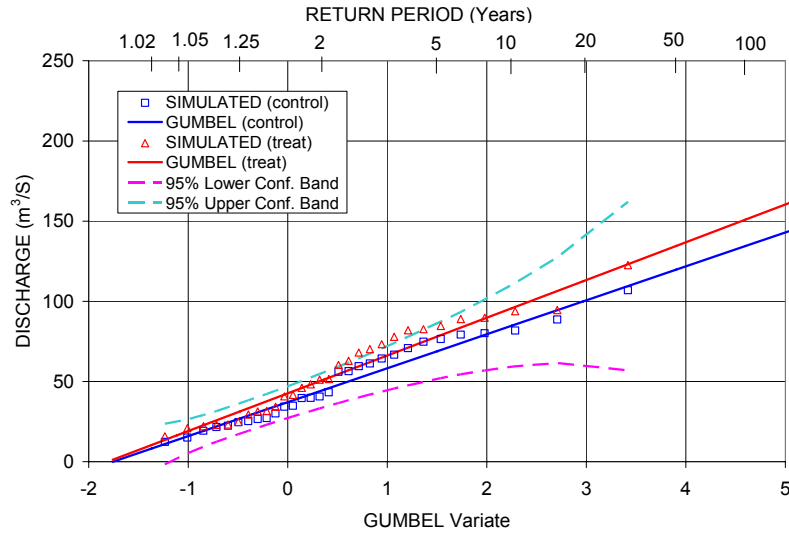


Figure 29. Scenario 1 post-logging peak flow regime in comparison to baseline.

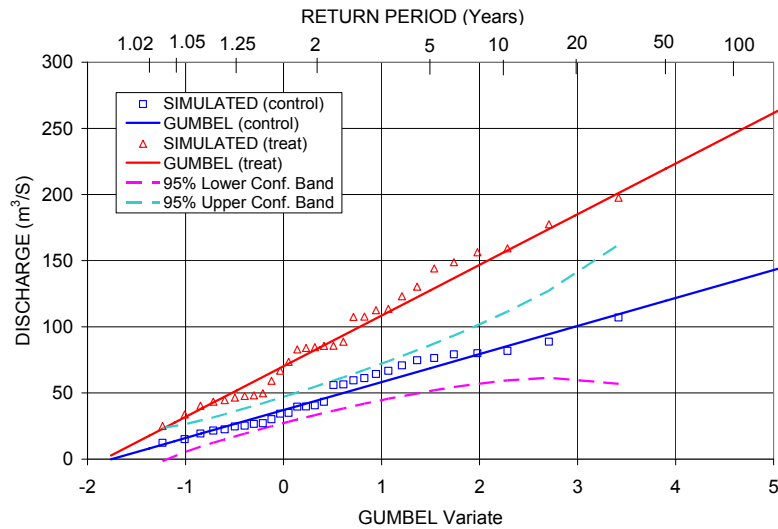


Figure 30. Scenario 3 post-logging peak flow regime in comparison to baseline.

The following conclusions were drawn from the long-term simulation experiment in this study:

1. Change in peak flow varied from 66%–104% for the 2-year event, 65%–99% for the 10-year event, 65%–99% for the 20-year event, and 77%–117% for the 50-year event (statistically significant at the 95% confidence level). They are attributed to the unprecedented large-scale disturbance from the relatively subdued topography that synchronizes both melt and runoff reaching the stream network. According to the hypsometric curve, the middle 50% section of Baker Creek watershed lies within 200-m elevation range. Baker is also dominated by north, northeast, and northwest aspects, which contribute to the late, more synchronized melt compared to watersheds dominated by southerly aspects.

2. Increases in peak flows are consistent across a wide range of return periods and appear to remain significantly large beyond the 50-year return period event. These patterns were attributed to the fact that the magnitude of the peak flow is not as significantly a function of winter snowpack accumulation as it is a function of the evolving meteorology that controls the dominantly radiation and advection melt of the snowpack in similar ways across a wide range of return period events.
3. Scenarios 2 to 5 resulted in changes in the freshet water yield ranging from 34%–55% averaged over the full simulation period of 30 years (statistically significant at the 95% confidence level). This increase in water yield caused by salvage logging and pine infestation can be attributed to the lack of forest canopy snow interception and to the absence of tree transpiration during the freshet season when soil moisture is still abundant.
4. In the snow-dominated watersheds of the drier Interior of British Columbia, the loss of tree cover alters substantially the snowmelt energy, particularly shortwave radiation. This causes an earlier melt and an advance in the time-to-peak of the freshet hydrograph. Scenarios 2 to 5 caused a 2- to 3-week advance in the time-to-peak of the snowmelt hydrograph, which is consistent with several reported paired watershed studies (e.g., Troendle and King 1985).

3.4.1 Does forest removal in snow environment affects the larger peak flow events?

It is well documented that forest harvesting, in both rain- and snow-dominated watersheds, increases peak stream discharge for small and medium events or storms. Paired watershed studies have demonstrated, however, that progressively the percentage increase in peak discharge decreases rapidly with increasing event or storm magnitude (Thomas and Megahan 1998; Beschta et al. 2000; Troendle et al. 2001; Moore and Wondzell 2005). This may be misleading, as data from paired basin studies are often collected over a short time and do not represent the peak flow regime over a wide range of return periods. Also, forest regrowth creates a degree of hydrologic recovery which confounds the single harvesting treatment in the treated watershed. It is therefore difficult to relate forest harvesting impacts to peak flow discharge return period for all but the most frequent events (Thomas and Megahan 1998; Beschta et al. 2000; Jones et al. 2000).

Analytical methods used in paired watershed studies for evaluating the effects of forest harvesting on peak flows may be another problem (Alila et al. 2009). Conventionally, the impact of logging on peak discharge is examined by comparing the change in magnitude of two chronologically paired events (control and treatment peak flows). For snow environments, a pair of events occurs in the same freshet year as annual maximum peak flows. In rain or rain-on-snow environments, each pair corresponds to the same individual storm event. This analysis, however, fails to avoid the pitfall that paired peak flow events do not necessarily occur with the same frequency or return period, either during the pre- or, most importantly, post-treatment periods.

Forest harvesting alters the hydrological processes that generate peak flows in rain, snow, or rain-on-snow dominated watersheds. This not only changes the magnitude of the peak flow event but also the rank-order of the event within the post-treatment time series and, therefore, its return period. In effect, “control” and “treatment” or pre- and post-treatment peak discharge events that define a certain return period may derive from completely dissimilar antecedent conditions. This is critical for snow-dominated watersheds, which may have completely different antecedent snowpack conditions and most importantly different snow surface energy budgets. A chronology paired event based comparison, as traditionally conducted in paired-basin studies, does not account for this fact. Under chronological pairing, two peak flow events can differ in frequency even if they do not differ in magnitude. In our view, therefore, the *only* relevant comparison of peak discharge as affected by treatment must be based on that of equal frequency. It should

not be a comparison of the same storm (in case of rain or rain-on-snow regimes) or that of the same freshet year (in case of snow regime). The distinction may appear subtle, but the results can be substantially different, if not diametrically opposite (Alila et al. 2009).

Figure 31 illustrates how the change in peak flow varies with return period using the frequency and chronology paired event analyses. These numbers were derived by running a numerical model on the same watershed in a long-term simulation exercise with the same climate input twice, once with and once without forest cover (a controlled experiment). This allows an evaluation of peak flows using a frequency-based method over a wide range of return periods. What is telling from Figure 30 is that the relation between event magnitude and relative change in peak flow shows substantially less scatter in the frequency-based comparison. When switching to a paired frequency analysis, differences in event frequency, which are inherent in the chronology paired-event analysis, are eliminated as a source of variability when relating peak flow change to event return period. Consequently, the frequency-based comparison exhibits a much stronger correlation between event return period and peak flow change than the traditional chronology paired-event approach. This leads one to conclude that a frequency-based comparison can be statistically more powerful in detecting a change in the peak flow regime than a chronology paired-event analysis (Alila et al. 2009).

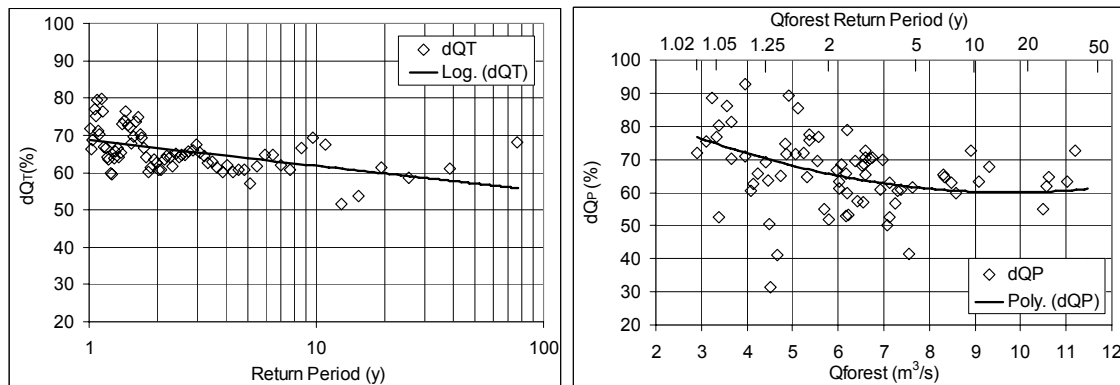


Figure 31. Percent change in peak flow versus return period (frequency-based comparison: right); percent change in peak flow versus control discharge (paired event based comparison: left).

In our study, the effects of logging on peak flow remained significantly large beyond the 2, 5, 10, and 20-year return period events. This trend has major implications on changes in frequency caused by logging, particularly for larger events. As was first reported by the Forest Practice Board of British Columbia, a 20-year event under baseline conditions is expected to become a 3-year event under MPB salvage logging Scenario 4%–20% retention (Forest Practices Branch 2007). This is equivalent to experiencing on average 7 times the pre-logging 20-year event in the two decades following treatment, assuming the slow hydrologic recovery of the flow regime as documented in the literature from similar cold and dry snow environment (Troendle and King 1985; Elder et al. 2006). What is even more intriguing is that a frequency paired peak flow analysis reveals that the larger the event, the more frequent it may become, a direct consequence of the highly non-linear and inverse relation between the magnitude and the frequency of a flood (Alila et al. 2009).

Paired watershed studies in snow-dominated environments showed increases in peak flow events that decrease rapidly with return periods (MacDonald and Stednick 2003; Moore and Wondzell 2005;

Troendle et al. 2006). Traditionally, two arguments are used to explain a rapid decrease of the magnitude of the peak flow change in paired watershed studies:

Canopy interception as a proportion of total precipitation is much larger for smaller than for bigger storm events (Zinke 1967; Spittlehouse 1998). Since every canopy has a maximum interception capacity, the effects of tree removal are greater for smaller storm events than for larger events.

The difference in soil moisture deficit between the forested and logged watersheds is more substantial for the small summer and early fall storms as trees are more actively transpiring during this growing season (Lewis et al. 2001). However, the largest peak flow events are often bigger winter storms that occur while the forest is dormant. Under dormant conditions, forested and logged watersheds can be equally wet with minimal difference in soil moisture deficit.

This above reasoning, however, may not necessarily apply to snow and rain-on-snow dominated environments. It may apply to rain-dominated watersheds, and with a well-defined flood season, where the complexity of processes that modify peak flows for smaller events can eventually be overwhelmed by the dominance of the rainfall process as the return interval increases.

The change in the magnitude of peak flow as a result of tree removal in snowmelt-dominated environment is due to multiple processes, including changes in snow accumulation and in the energy responsible for melting the snowpack. The complexity of these processes and their interactions may be maintained as the return interval increases because no one process is dominant over the others, as in the case of some rain-dominated environments. The factors involved in the change of the energy after forest removal include an increase in the amount of shortwave radiation that reaches the snowpack surface, an increase in the turbulent heat transfer due to higher wind speeds at the snowpack surface, an increase in latent heat transfer due to condensation and freezing at the surface of the snowpack, and possibly an increased persistence of the snowpack as a result of the increased peak SWE (MacDonald and Stednick 2003). The changes in snow accumulation and energy caused by forest removal tend to operate independently and, therefore, the occurrence of a large peak flow event depends on the random coincidence of conditions that favours rapid melt of a deep snowpack over a large area.

Our modelling study indicates that the relative increase in peak flow in snow-dominated watersheds persists across a wider range of return periods (definitely larger than 10- to 20-year return periods). The argument used to support the conclusion that larger peak flows may not be affected by forest removal is that peak snowmelt is limited by the amount of energy that can be delivered to the snowpack (MacDonald and Stednick 2003, p. 14). We contend that an upper limit of energy is rarely reached before the total disappearance of snow. Hence, there is always sufficient excess energy available to raise snowmelt rates, and therefore peak flows, across a wide range of return periods (Schnorbus and Alila 2004).

More critically, the lack of evidence for an increase in large peak flow events is also related to the way a large event is defined in paired watershed studies. The size of an event as defined by the return period of the peak flow of the control watershed in paired watershed studies (Jones and Grant 1996; Thomas and Megahan 1998; Jones 2000; Beschta et al. 2000; Moore and Scott 2005; Moore and Wondzell 2005) can be misleading and can potentially mask the true relationship between the relative increase in peak flow and the size of the event. For every melt season there will be two measured peak flows: one at the outlet of the control and the second at the outlet of the treatment watersheds. The two peak flow events will have two different return periods because of the difference in the ranks in their respective population of peak flow events. Also, often different energy budget and antecedent snowpack conditions due to forest cover removal generated the two events.

The inconclusive results of paired watershed studies on the effects of forest removal on large events are often blamed on the short record length in the pre- and post-treatment periods (Jones and Grant 1996;

Thomas and Megahan 1998). We contend that, irrespective of record length, a paired-event analysis will not reveal the true nature of the relation between the relative increase in peak flow and event size when the return period is decided by the ranking of the peak flow events in the control watershed. The true relationship between forest removal and peak flow change is only elucidated through a frequency-based comparison that focuses on the difference in the magnitude of peak flow for a pair of treatment and control events of the same frequency or return period and not of the same storm in rain and snow transient regimes, or of the same freshet season in snow regimes.

The effect of forest management on extreme peak flow events is controversial. It continues to be investigated almost exclusively using the paired watershed approach (Jones and Grant 1996; Thomas and Megahan 1998; Jones 2000). What fuelled this debate even further is that there are always physical reasons why the few measured larger events in the control watershed either do not change or can even decrease in absolute and relative terms in the treatment watershed.

For instance, a large peak flow might be a late melt season event when the temperature did not create an early season peak but rather contributed to the ripening of the snowpack. A deep, ripe snowpack generates synchronized melt and, as a result, a large late season peak flow event. After forest removal, the increase in energy will advance the melt and increase the flow on the rising limb of the hydrograph. At the time of peak flow of the control watershed, there may not be enough snow left on the ground to increase the magnitude of treatment peak flow above that of the control. In this case, and in the context of a chronology paired-event comparison, the forest cover removal may actually reduce the peak flow.

Does this mean that forest removal does not affect larger flows? The answer is a misleadingly “yes”, if a flow event (and by association the difference in magnitude between the treatment and control peak flows) is classified as “large” based on the record of the control watershed, as always assumed in paired watershed studies. One of the most fundamental flaws in evaluating the relation between forest harvesting and peak flows using chronological pairing is that two paired peak flow events can differ in frequency even if they do not differ in magnitude. This is because the frequency of an event depends not only on its own magnitude but also on the magnitude of all events that make up the peak flow regime. Chronological pairing therefore has the potential of concealing the true relation between forest harvesting and floods (Alila et al. 2009). In this study, we have used a frequency-based analytical approach and this explains, at least in part, why the outcomes of our project are inconsistent with main stream forest hydrology literature on the effects of forest harvesting on larger peak flows.

4 GEOMORPHOLOGY

4.1 Introduction

In fluvial geomorphology, the concept of geomorphic thresholds is used to define significant changes in processes and morphology delimiting distinctive riverine landscapes (Church 2002). The concept can be applied to channel stability (e.g., Olsen et al. 1997), and sediment transport (e.g., Carling 1988), as well as delimiting larger landscape features such as the transition between meandering and braided rivers (van den Berg 1995) and different types of floodplain or channel (Nanson and Croke 1992; Church 2002). Thresholds are usually expressed in terms of the energy available to the river (i.e., the total or unit stream power) at some specified discharge (usually bankfull or the mean annual flow) (Nanson and Croke 1992; van den Berg 1995), or the Shields number (Dade and Friend 1998; Dade 2000; Church 2002). This part of the project uses the changes in peak flows caused by the MPB epidemic predicted in Chapter 3 and geomorphic threshold theory to assess the potential for channel change in Baker Creek watershed.

The scale of the ongoing MPB epidemic is unprecedented in terms of the infested area and none of the existing studies of MPB hydrological or geomorphological impacts deal with infestation on this scale. In addition, most of the existing studies on conventional forest harvesting investigated impacts in high relief areas, such as the British Columbia Coast Mountains, or the American Rockies. None of the existing studies focused on the relatively low-relief, low precipitation Central Interior region of British Columbia, which is at the heart of the current infestation. Runoff generation relative to drainage area is relatively low in the Central Interior compared to other parts of British Columbia (Eaton et al. 2002), making it difficult to apply results from the better-studied Coast Mountains and Pacific Northwest regions to this area. It is also likely that the relatively low relief of the Central Interior will result in near-synchronous melting across the catchment, and a more rapid rise to annual peak flow than in high relief catchments, where snow will linger at high elevations longer into the melt season (Hendrick et al. 1971; Jost et al. 2007).

In addition to increased flows, the main effects of forest harvesting are related to increased sediment availability. This is primarily due to bank erosion associated with channel enlargement (Hassan et al. 2005a). Other sources include the construction of forest roads (Tang et al. 1997; Jones et al. 2000), and an increase in shallow landsliding (Tang et al. 1997; Montgomery et al. 2000), although the relative importance of landsliding in the low-relief Central Interior is as yet unknown. Forest harvesting also changes the timing and release of large woody debris (LWD) to the channel (Hassan et al. 2005b). In the short term, logging can increase the supply of wood to the channel, but will ultimately lead to in-channel wood stores being depleted, releasing sediment from wood-jam traps and changing channel morphology (Ralph et al. 1994; Abbe and Montgomery 2003; Hassan et al. 2005b). Floodplain vegetation is intimately linked to channel character and hydrology (Gurnell 1997). Floodplain inundation frequency and rates of channel change control the rate at which vegetation successions develop on floodplains (Gurnell 1997); inversely, changes in floodplain vegetation can lead to changes in sediment accumulation and accretion both in the channel and on the floodplain. In general, the presence of riparian forests increases bank instability, resulting in wider channels, while deforestation results in stream narrowing, increasing sediment storage within the riparian corridor, but reducing the availability of habitat space for aquatic species (Davis-Colley 1997; Trimble 1997; Sweeney et al. 2004).

To date, no studies have considered how the hydrological changes induced by the MPB will affect fluvial geomorphology in impacted catchments. Although the links between forest practices and fluvial geomorphology understood in broad terms (Slaymaker 2000; Gomi et al. 2005; Hassan et al. 2005a, b), most studies of channel and sediment response to land-use change have focused on long-term historical trends (e.g., Knox 1977; Magilligan and Stamp 1997; Gomez et al. 1998, 2001; Liébault et al. 2005;

Phillips and Gomez 2007). Fewer studies have investigated how the effects of relatively rapid (<5 years) changes in forest coverage, due to insect kill or clearcutting might lead to changes that induce fluvial channels to cross geomorphic thresholds (cf. Church 2002), leading to relatively rapid changes in channel character. Heede (1991) compared adjacent harvested and unharvested catchments, and found that during a period when flows were increasing in both catchments, channel cross-sections enlarged by 10% in the harvested catchment and 2.5% in the unharvested catchments. Many studies have focused on headwater streams, or streams in steep terrain prone to landsliding (e.g., Jackson et al. 2001). Hartman and Scrivener (1990) and Hartman et al. (2006) discuss the impact of forestry on Carnation Creek, located in mountainous terrain on Vancouver Island, British Columbia. In addition to an increase in landsliding in the steeper parts of the catchment, clearcutting of floodplains up to the stream margin caused destabilization of LWD, streambank erosion and channel widening, and sediment mobilization and re-sedimentation.

The aim of Chapter 4 of this project is to assess the potential for channel geomorphological changes in a MPB-infested catchment in the Central Interior of British Columbia. This region is at the heart of the MPB- infested area, and up to 80% of the vulnerable tree species of some catchments have been infested. The Baker Creek catchment was chosen because it is a major tributary of the Fraser River, and because relatively long (>30 years) records of climate and discharge are available.

4.2 Geology and Quaternary Evolution of the Study Watershed

The bedrock geology of the region (Figure 31) is dominated by volcanic material, although it is covered everywhere by a layer of unconsolidated material of Quaternary age, primarily till, alluvium, lacustrine and colluvial deposits (Lord and Mackintosh 1982) catchment. In contrast, the low relief middle-elevation areas have a thick covering of unconsolidated Quaternary sediment that limits the surface exposure of the underlying bedrock. Neogene age Chilcotin Group volcanic material is exposed along the valley of central Baker Creek, while in lower Baker Creek Cache Creek Group inter-bedded volcanic and sedimentary rocks are exposed.

Quaternary ice sheets overrode the catchment completely (Tipper 1971), creating a landscape that is both completely covered by Quaternary sediment and also strongly imprinted with a glacial signature. The whole region is strongly drumlinized, with a regional glacial palaeoflow direction to the north. This glacial history strongly influences the drainage network within the catchment. Headwater streams and minor drainage channels show a strong preferred alignment corresponding to the regional glacial palaeoflow direction, although this has been modified by post-glacial processes in some areas of the catchment. The pre-Quaternary regional drainage pattern of this area was to the north, with the palaeo-Fraser River draining to the Arctic Ocean (Lay 1940, 1941). Baker Creek reflects this regional drainage pattern.

The present-day Baker Creek flows northwards until its junction with Tibble Creek, where it turns sharply east and steepens before joining the Fraser (Figure 1). The Baker Creek palaeodrainage continues northwards from its current course, and exits the catchment between the course of the present-day Puntataenkut and Crimen Creeks (Figure 1), continuing into the catchment of the Blackwater River. The west- to east-flowing lower Baker Creek is the product of stream capture by upstream migration of a tributary of the Fraser River. Incision of the Fraser River and the formation of the Fraser River Basin physiographic region following the capture of Baker Creek have led to the steepening of lower Baker Creek (Figure 32), and the formation of a knick-point indicating the progression of the upstream migration. The knick-point is currently indicated by the presence of Baker Falls, a 2-m high waterfall flowing over a basalt cliff (Figure 32). Channel incision upstream of Baker Falls is indicated by channel cross-sections, which reveal that the river is incised into the Quaternary floodplain by up to 1.5 m as far upstream as the

confluence of Baker and Tibble Creeks. Upstream of the Baker Creek / Tibble Creek confluence, a wide floodplain forms along the full length of Baker Creek and Merston Creek, until the rivers steepen in the headwater reaches.

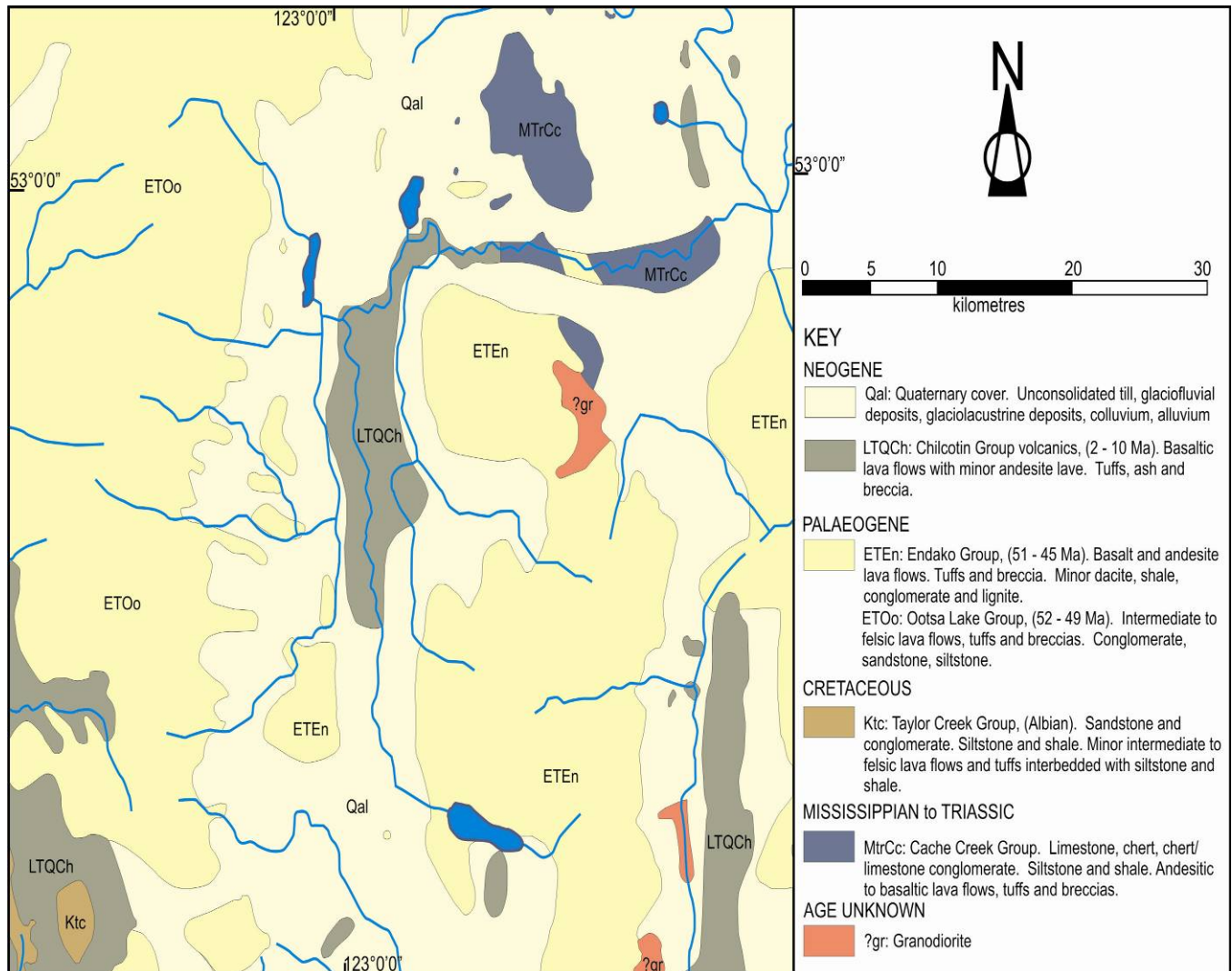


Figure 32. Geological map of the Baker Creek area, modified from Riddell (compiler, 2006).

4.3 Methods

This study tests the relative bed stability method for assessing stream channel stability proposed by Olsen et al. (1997). There is some debate about the applicability of the relative bed stability method, particularly whether bed stability can be equated to channel stability (Dalby 1999; Olsen et al. 1999). However, the assumption that there is a relationship between sediment transport, bankfull discharge, geomorphological effectiveness and alluvial pattern is long standing (Wolman and Miller 1960; Emmett and Wolman 2001; Church 2006) and is reasonable in the absence of data indicating otherwise. The relative bed stability approach is extended by using a scenario-based approach to test the sensitivity of the channel to a range of potential discharge increases derived from our long-term hydrological simulation in Part A of this project.

This approach is based on the geomorphic threshold concept (Church 2002) in that it considers downstream changes in bankfull flow regime, channel geometry and sediment supply to define channel reaches that are close to thresholds for geomorphic change, defined using the Shields number and downstream changes in unit stream power.

Olsen et al. (1997) define relative bed stability in terms of either critical shear stress or critical discharge. They suggest that critical shear stress is less suitable for channels with a slope greater than 0.02, while critical discharge is inappropriate for channels with a slope less than 0.025. Given the relatively low relief of the Baker Creek catchment, slopes in excess of 0.025 are rare, and confined only to the very uppermost headwater reaches. Relative bed stability is defined by the ratio of the critical shear stress for sediment entrainment and the shear stress at bankfull discharge:

$$\text{Relative Bed Stability (RBS)} = \tau_{\text{critical}} / \tau_{\text{bankfull}}$$

Critical shear stress is defined by the Shields (1936) criterion:

$$\tau_{ci} = \tau_{ci*}(\rho_s - \rho)gD_i$$

where τ_{ci} and τ_{ci*} are, respectively, the critical dimensional and dimensionless streambed shear stresses to entrain a particle of diameter D_i , ρ_s and ρ are the densities of sediment and water respectively, and g is the acceleration due to gravity.

Critical dimensionless shear stress, τ_{ci*} , varies as a function of both absolute particle size D_i and relative particle size D_i/D_{50} due to particle hiding and exposure (Andrews 1983). Olsen et al. (1997) use the relationship suggested by Andrews (1983) for critical dimensionless shear stress:

$$\tau_{ci*} = \theta(D_i/D_{50})^{-x}$$

where D_{50} is the median particle size of the bed material, θ represents the Shields dimensionless coefficient in homogeneous sediment when $D_i/D_{50} = 1$, and the exponent x indicates the slope of the power relationship. Olsen et al. (1997) suggest using values of 0.045 for θ and 0.7 for x , derived from Komar (1989) and Petit (1994). Using this approach, values for the critical shear stress were calculated for the D_{84} at each study site. Mean cross-sectional shear stress at bankfull discharge was calculated using the DuBoys equation:

$$\tau = \rho g R S$$

where ρ is the density of the flow, g is acceleration due to gravity, R is the hydraulic radius, and S is channel slope.

Channel cross-sections and long profiles were measured with an auto-level at 19 sites within Baker Creek catchment, located on the main stem of Baker Creek, and the two main tributaries (Mount Creek and

Merston Creek). Sites were chosen to represent the downstream changes in channel geometry, although difficulties of access limited site selection, particularly in lower Baker Creek. Bankfull depth was estimated in the field using breaks of slope as indicators (Williams 1978). Long profiles were at least 10 times the bankfull width. Grain-size data were collected using Wolman (1954) pebble counts of 100 clasts, with measurements made using a gravelometer. At some sites, bed surface material and shallow (0.2-0.4 m) subsurface material were sampled and sieved in the laboratory, to confirm the Wolman counts, and identify any differences between the armoured surface layer and the subsurface sediments. Bankfull discharges were calculated from the cross-section data using the Manning equation ($Q = (1/n)A.R^{2/3}S^{1/2}$). Values for Manning's n were estimated from the characteristics of the channel and tables in Chow (1959), and for lower Baker Creek from values calculated by Northwest Hydraulic Consultants (1992). The characteristic Shields number for each study reach is calculated from:

$$\theta = \tau / g(\rho_s - \rho)D_{50}$$

where the terms are defined as before, although D_{50} is substituted for the D_{84} required in the relative bed stability calculations. Values of θ are compared against the thresholds for alluvial channels presented in Church (2002). Power per unit channel width is diagnostic of the power available to erode and construct landforms in a fluvial system (Nanson and Croke 1992), and is defined as:

$$\omega = \gamma QS/w$$

where γ is the specific weight of water, Q is bankfull discharge, S is channel slope and w is channel width. Values of ω are compared to the thresholds for floodplain character described in Nanson and Croke (1992).

4.4 Results

4.4.1 Downstream channel changes

4.4.1.1 Long profile

The long profile of Baker Creek and its two main tributaries show three distinct zones (Figure 33; Table 7), which correspond to changes in gradient as the river traverses the physiographic regions outlined above, and passes from the fully alluvial reaches of the central catchment to the steeper headwater reaches. The changes also correspond closely to the changes in geology (Figure 32). The headwater reaches of Baker Creek and Merston Creek are medium to high gradient (0.025–0.169; Table 7), and contain many lower-gradient sections. Upper Mount Creek is consistently steeper, with a maximum slope of 0.1, and an average of 0.0143. Upstream of the confluence of Mount Creek and Baker Creek, the three main water courses all flow across the low-relief central plateau of the catchment and have low gradients with slopes in the range 0.004 to 0.005. Local steepenings occur in the reach of Baker Creek between the Mount and Merston Creek confluences, particularly the 2 m high rock step of Baker Falls, and the cascade reach immediately below, which has a slope of 0.0121. The low-gradient sections form the greatest proportion of all three major streams within the catchment. Lower Baker Creek, downstream of the confluence with Mount Creek is over-steepened due to the incision of the Fraser River and upstream knick-point migration outlined above; its slope averaged 0.0113.

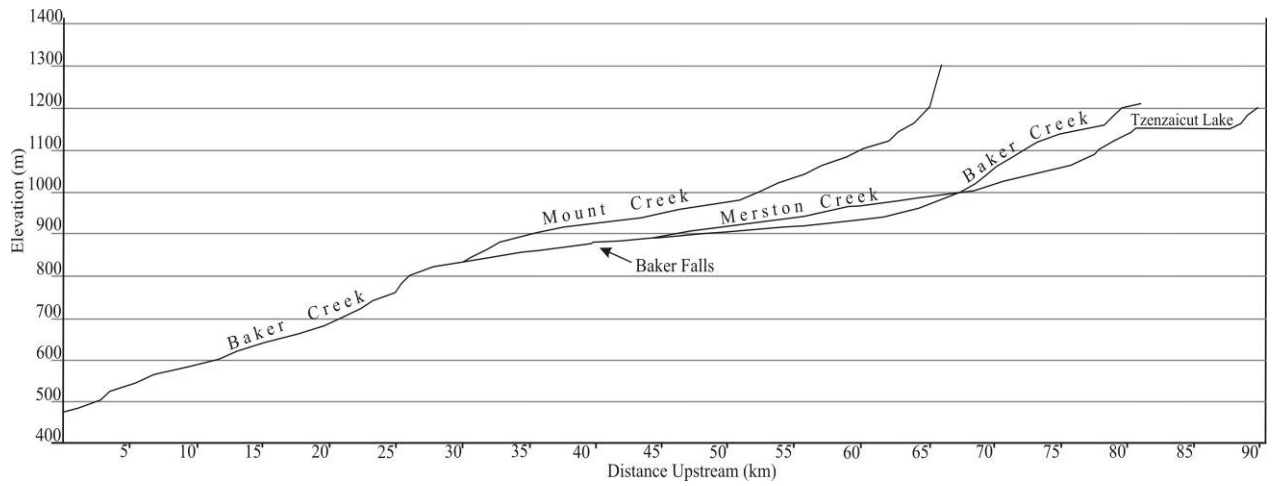


Figure 33. Long profile of Baker, Mount, and Merston Creeks, interpolated from contour crossing on 1:70 000 mapping of the catchment (20-m contour intervals). The locations of the study sites are also shown.

Table 7. Reach average values for valley slope, sinuosity, and meander wavelength and summary of channel characteristics for the main subreaches of the Baker Creek catchment.

Reach	Slope	Sinuosity	Meander wavelength	Channel type
Lower Baker Creek (0–31.7 km)	0.0113	1.38	257 m	Meandering gravel-bed river, partly confined by steep slopes and bedrock outcrops. Meander development limited in some places by confining slopes. Riffle–pool and cascade morphology present in confined reaches. Limited floodplain development.
Middle Baker Creek (31.7–47.7 km)	0.00406 (locally up to 0.0121)	1.32	132 m	Meandering gravel-bed river, partly confined by low, steep slopes. Some floodplain development. Meandering limited in some places by confining slopes. Riffle–pool morphology dominant in confined reaches. 2 m high rock step (Baker Falls), and cascade reach cause some local steepening.
Upper Baker Creek (47.7–71.6 km)	0.00439	1.8	65 m	Meandering river with well developed alluvial floodplain up to 1.3 km wide. Sand and gravel present on bed of channel. Floodplain wetlands are present, but have been largely drained to form meadows. Numerous oxbows and chute cutoffs. Some evidence of minor anabranching and avulsions.
Baker Creek Headwaters (71.6–84.6 km)	0.0169	1.2	32 m (based on one 1.3 km reach)	Low sinuosity gravel-bed riffle–pool and cascade–pool channel, with localized floodplain development and meandering on the upper plateau. Woody debris is present in forested reaches.
Lower Mount Creek (31.7–37.3 km)	0.00843	1.48	89 m	Gravel-bed riffle–pool stream confined in relatively straight reaches, alternating with highly sinuous meandering reaches in narrow (<150 m) floodplain. Woody debris is common.
Middle Mount Creek (37.3–56.2 km)	0.00449	1.62	52 m	Meandering river with well-developed floodplain, approximately 100 m wide along most of the reach, but up to 700 m wide locally. Well-developed gravel point bars and riffle–pool sequence at the downstream end of the reach with a transition to a steep-sided channel with fine-grained alluvial banks and sandy bed farther upstream. Floodplain wetlands are common, with some anabranching and localized channel disappearance.
Upper Mount Creek (56.2–68.3 km)	0.0143 (0.1 for 1 km in the headwaters)	1.16	24 m	Low sinuosity gravel-bed riffle–pool channel, largely confined with limited floodplain development except for one 1 km long reach. Steeper, step–pool morphology in the upper headwater. Woody debris common.
Lower Merston Creek (47.7–82.7 km)	0.00485 (varies between 0.00401 and	1.41	52 m	Meandering channel with sand and gravel bed and alluvial banks. Many minor anabranches and chute cutoffs. Floodplain wetlands are well-developed along the reach, but in some locations have been drained and had the channel straightened to form floodplain meadows. Beaver dams are common along the lowermost reaches (above

	0.00582)			Baker Creek), acting as localized sediment traps.
Middle Merston Creek (82.7–85.1 km)	0.0291	1.16	42 m	Low sinuosity gravel-bed riffle–pool channel, confined by glacial terraces. Limited floodplain development and meandering in short, less-confined reaches.
Upper Merston Creek above Tzenzaicut Lake (92.1–98.3 km)	0.0258	1.08	20 m	Gravel-bed low sinuosity step–pool and riffle–pool channel, mostly a steep, confined channel, with occasional wider reaches.

Notes: Meander wavelength is for fully alluvial, regular meandering reaches only. Channel types are characterized using the Montgomery and Buffington (1997) classification for mountain streams, augmented by terms from Miall (1996) for low-gradient reaches.

4.4.1.2 Sinuosity, meander wavelength, and channel pattern

The headwater reaches of all three streams are generally low sinuosity gravel bed riffle–pool channels, with high volumes of woody debris which completely spans the channel. Step–pool channels are largely confined to upper Mount Creek, although cascade–pool reaches occur in Baker and Merston Creek. Step height (at Site Mo5; refer to Figure 1 for all site indices) is about 0.3 m. The upper reaches of Baker and Merston Creeks are also characterized by many lower-gradient reaches, either on the upper plateau of the catchment, or in in-filled glacial lake basins on the headwater slopes. These lower-gradient reaches usually contain a more sinuous channel with incipient meanders developing in some locations. Typically these upstream low-gradient reaches have steep-sided alluvial banks and riffle–pool morphologies but no, or only limited, evidence for meander migration and bar formation.

The central mid-elevation plateau is characterized by well-developed floodplains and floodplain wetlands. Floodplains are highly variable in width, but can be up to 1.3 km wide on Baker Creek, 700 m wide on Mount Creek, and 400 m wide on Merston Creek. Typically though, floodplains are 100 to 200 m wide on all three creeks. Meanders are well developed, and have a high sinuosity (1.8 in Baker Creek, 1.62 in Mount Creek, and 1.41 in Merston Creek). Meander wavelengths are consistent with the widths of each channel, being longer in Baker Creek (average 132 in the middle reach and 65 m in the upper reach) than Mount or Merston Creek (52 m average in both creeks). There is a general trend of average meander wavelength decreasing upstream. All three creeks are fully alluvial throughout this section, typically with a fine to medium gravel bed, and fine-grained alluvial banks and floodplain. Typically, both banks are steep-sided, and there is no bar development. Channel banks are more degraded and less stable in reaches that have been drained, as is typical of many grazed riparian zones (Trimble and Mendel 1995). Two floodplain meadow reaches on Merston Creek have been subjected to channel diversion and straightening. Minor anabranches occur on all three rivers and the numerous oxbows and cutoffs indicate that the channel is relatively active. Most cutoffs are chute cutoffs. The increased width of the streams compared to the headwaters, and the fact that much of the floodplain has been cleared of trees means that woody debris is of only minor importance in this part of the catchment. However, the lowermost reaches of Merston Creek (and some of the tributaries of Baker Creek not described in this report) are heavily affected by beaver (*Castor canadensis*) activity. These dams increase and prolong flooding on lower Merston Creek, and act as sediment traps (Butler and Malanson 1994, 2005; Gurnell 1998).

The reach of Baker Creek between the confluences of Mount and Merston Creeks, and lower Baker Creek below the Mount Creek confluence becomes increasingly confined downstream; consequently, floodplain development becomes more limited. Highly confined, low sinuosity reaches alternate with more open reaches, where meanders develop. Near the confluence with the Fraser River, where Baker Creek passes from the Fraser Plateau physiographic region, to the Fraser River Basin physiographic region, the meanders are deeply incised. The low sinuosity reaches have a boulder cascade or riffle–pool morphology. The more open reaches are never more than 150 m wide, and the channel is frequently confined within a terraced, high-level floodplain, with the bankfull level occurring as a bench inset into the terrace.

Lower Baker Creek is gravel dominated, with a coarse gravel bed, and a gravel floodplain. Meander bends have well-developed gravel point bars. The increasingly confined nature of the channel means that there is a readily available sediment supply, both from older, higher glaciofluvial terraces, and from the steep-sided colluvial slopes composed of volcanic material that occur where the river is incised deeply, close to the Fraser River. Close to the confluence with the Fraser, glaciolacustrine sediment, deposited when the Fraser Valley has been glacially dammed, is a further important additional source of sediment (Tipper 1971). This reach of Baker Creek is well forested, and consequently, woody debris is more common. However, the increased width of the channel means that none of the woody debris spans the channel, and frequently it is transported down channel until it is deposited on a point bar.

4.4.1.3 Channel cross-section and width/depth ratio

Channel cross-sections were measured at 19 sites on the three major creeks within the Baker Creek catchment. The plotted cross-sections are shown in Figure 34, downstream changes in width/depth ratio in Figure 35 and channel dimensions are listed in Table 8. Generally, both width and width/depth ratios increase downstream, although exceptions exist. For example, site B5 is unusually wide, possibly due to anthropogenic modification, and site Me1 is narrower than the upstream sites, most probably due to beaver activity in this area. Width/depth ratios are lowest in the low-gradient central plateau, although this is likely to be largely due to the floodplains having been largely cleared of forest in this region (Davis-Colley 1997; Trimble 1997). Except for site B5, the largest width/depth ratios occur at the downstream end of the catchment, where the channel is wide, valley slopes are higher, and the channel bed and banks are composed of unconsolidated cobble-gravel sized sediment within a forested floodplain setting. Width/depth ratio changes in the catchment therefore appear to be a function of channel size, slope, riparian vegetation patterns, and channel modification history.

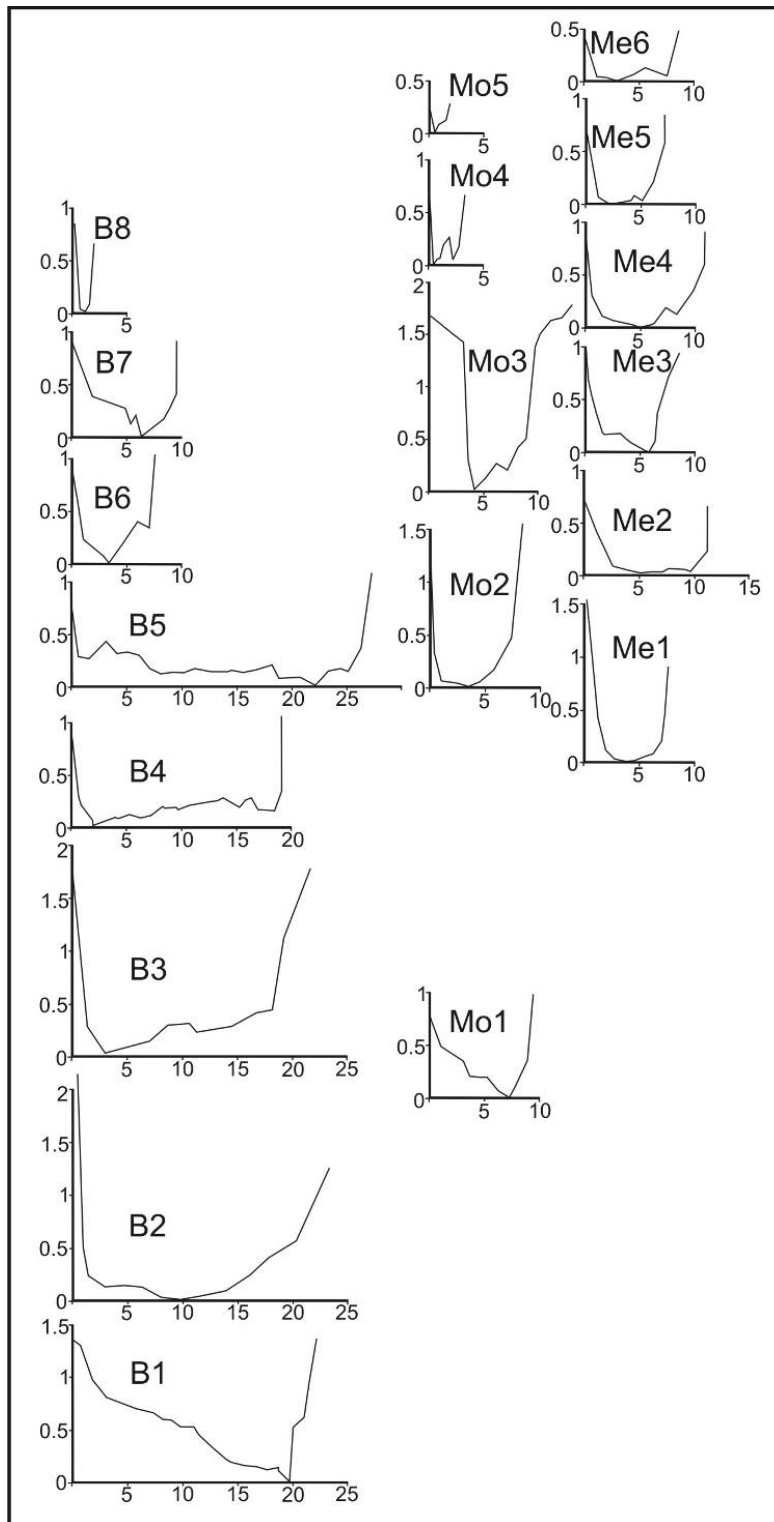


Figure 34. Measured channel cross-sections from Baker, Mount, and Merston Creeks. See Figure 1 for their locations.

Table 8. Measured and calculated properties for surveyed sites in the Baker Creek catchment.

Site	A	P	R	S	n	v	Q	w	d	Ω	ω	w/d	D ₅₀	D ₈₄	T	T _{ci} *	T _{ci}	RBS _{ss}	θ
B1	17.82	22.76	0.78	0.0053	0.03 5	1.76	31.50	22.14	0.81	1638.06	73.98	27.49	0.045 5	0.078	40.67	0.0308	38.918 7	0.9569	0.057 0
B2	22.01	23.38	0.94	0.003	0.04	1.31	28.94	22.65	0.97	851.77	37.60	23.3	0.038	0.072	27.66	0.0287	33.494 2	1.2106	0.046 4
B3	15.59	20.09	0.77	0.0025	0.03 5	1.20	18.80	18.73	0.83	461.15	24.62	22.5	0.042	0.074	19.00	0.0302	36.221 5	1.9056	0.028 8
B4	11.97	20.78	0.57	0.0121	0.06	1.26	15.20	19.02	0.62	1804.53	94.87	30.2	0.078	0.158	68.31	0.0274	70.143 2	1.0267	0.055 8
B5	14.3	27.81	0.51	0.0015	0.03	0.82	11.84	26.69	0.53	174.34	6.53	49.81	0.019	0.044	7.55	0.0249	17.786 3	2.3534	0.025 3
B6	6.06	10.39	0.58	0.0025	0.02 5	1.39	8.47	9.18	0.66	207.88	22.64	13.88			14.30		0		
B7	5.6	10.15	0.55	0.009	0.04 5	1.41	7.90	9.48	0.59	701.09	73.95	16.04	0.043	0.122	48.64	0.0216	42.781 7	0.8795	0.072 1
B8	0.72	2.35	0.30	0.027	0.03 5	2.14	1.56	1.46	0.49	413.79	283.4 1	2.93			81.85		0		
Mo1	7.18	9.97	0.71	0.0081	0.05	1.44	10.37	10.36	0.69	824.69	79.60	14.94	0.05	0.091	57.11	0.0295	43.542 5	0.7623	0.072 8
Mo2	7.36	9.32	0.79	0.0027	0.04	1.11	8.17	7.76	0.94	216.62	27.91	8.17	0.065	0.0105	20.91	0.1612	27.372 7	1.3090	0.020 5
Mo3	6.69	7.80	0.85	0.002	0.03 5	1.15	7.72	6.56	1.02	151.62	23.11	6.42	0.003	0.0055	16.82	0.0294	2.6182 8	0.1556	0.357 5
Mo4	1.82	3.97	0.45	0.0172	0.04	1.94	3.54	3.21	0.56	598.20	186.3 5	5.66	0.037	0.067	77.19	0.0296	32.172 6	0.4167	0.133 0
Mo5	0.19	1.8	0.11	0.1099	0.04	1.90	0.38	1.72	0.11	410.84	238.8 6	14.81			119.01		0		
Me1	5.32	8.3	0.64	0.0095	0.05	1.45	7.72	6.87	0.77	720.05	104.8 1	8.86	0.021	0.029	59.75	0.0358	16.834 3	0.2817	0.181 4
Me2	5.75	11.61	0.49	0.0027	0.02 5	1.30	7.48	10.61	0.54	198.30	18.69	19.56	0.025 5	0.038	13.10	0.0340	20.913 9	1.5959	0.032 7

Me3	5.85	14.21	0.41	0.0025	0.02 5	1.10	6.48	9.09	0.64	158.97	17.48	14.11	0.022	0.041	10.09	0.0291	19.295 3	1.9121	0.029 2
Me4	7.13	11.79	0.6	0.0025	0.04	0.89	6.37	10.74	0.66	156.43	14.56	16.16	0.023	0.0415	14.82	0.0297	19.977 7	1.3477	0.041 1
Me5	3.85	7.45	0.51	0.008	0.04	1.43	5.54	7.08	0.54	435.09	61.45	13.01	0.041 5	0.066	40.51	0.0325	34.707 1	0.8566	0.062 2
Me6	2.58	8.53	0.3	0.0072	0.04	0.95	2.47	8.45	0.31	174.70	20.67	27.62	0.027	0.043	21.37	0.0324	22.590 0	1.0567	0.050 4

A is bankfull cross-sectional area; P is wetted perimeter; R is hydraulic radius calculated from A/P ; S is channel bed slope, measured in the field; n is Manning's n, with values estimated either from Northwest Hydraulic Consultants (1992), or Chow (1959); v is average water velocity, calculated from the Manning equation; Q is bankfull discharge calculated from $v \times A$; w is bankfull channel width, measured in the field; d is mean bankfull depth, calculated from A/w ; Ω is total stream power, in Wm^{-2} ; ω is unit stream power in Wm^{-2} , calculated from Ω/w ; D_{50} and D_{84} are the grain size at the 50th and 84th percentile, respectively, measured using Wolman pebble counts; τ , τ_{ci} , and τ_{cl} are the mean cross-sectional shear stress and critical dimensional and dimensional shear stresses, respectively, as used in the various equations described in the methods section; RBS_{ss} is the relative bed stability based on shear stress calculated from τ_{cl}/τ ; θ is the Shields number.

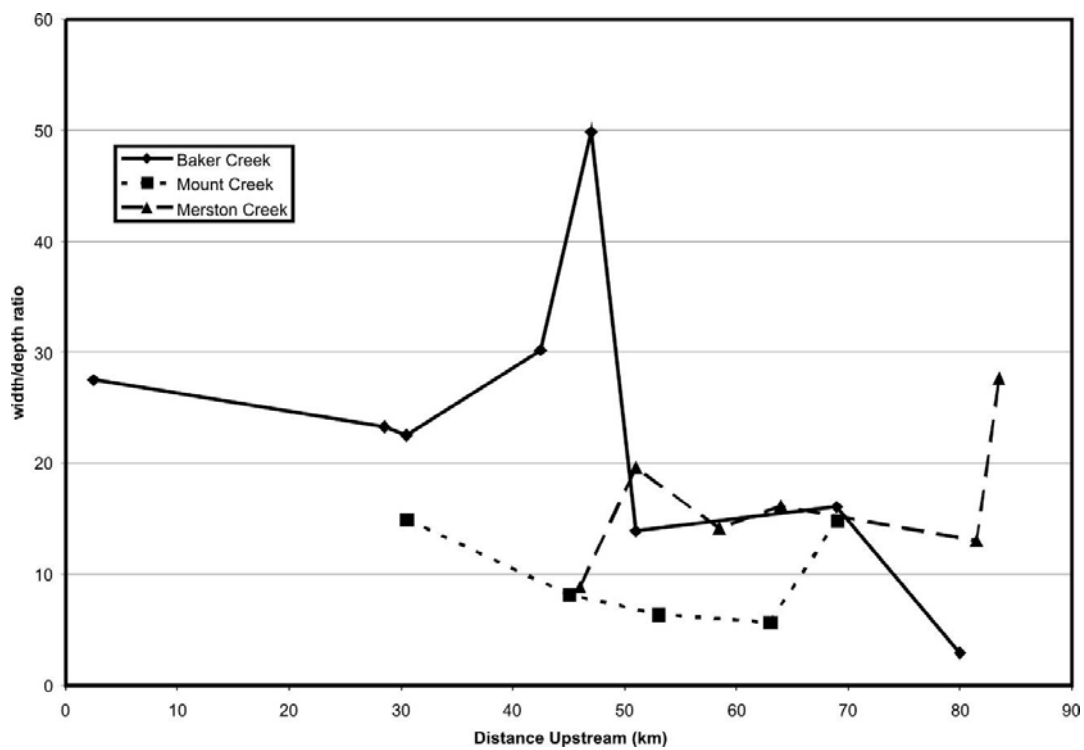


Figure 35. Changes in the width/depth ratio along Baker, Mount, and Merston Creeks.

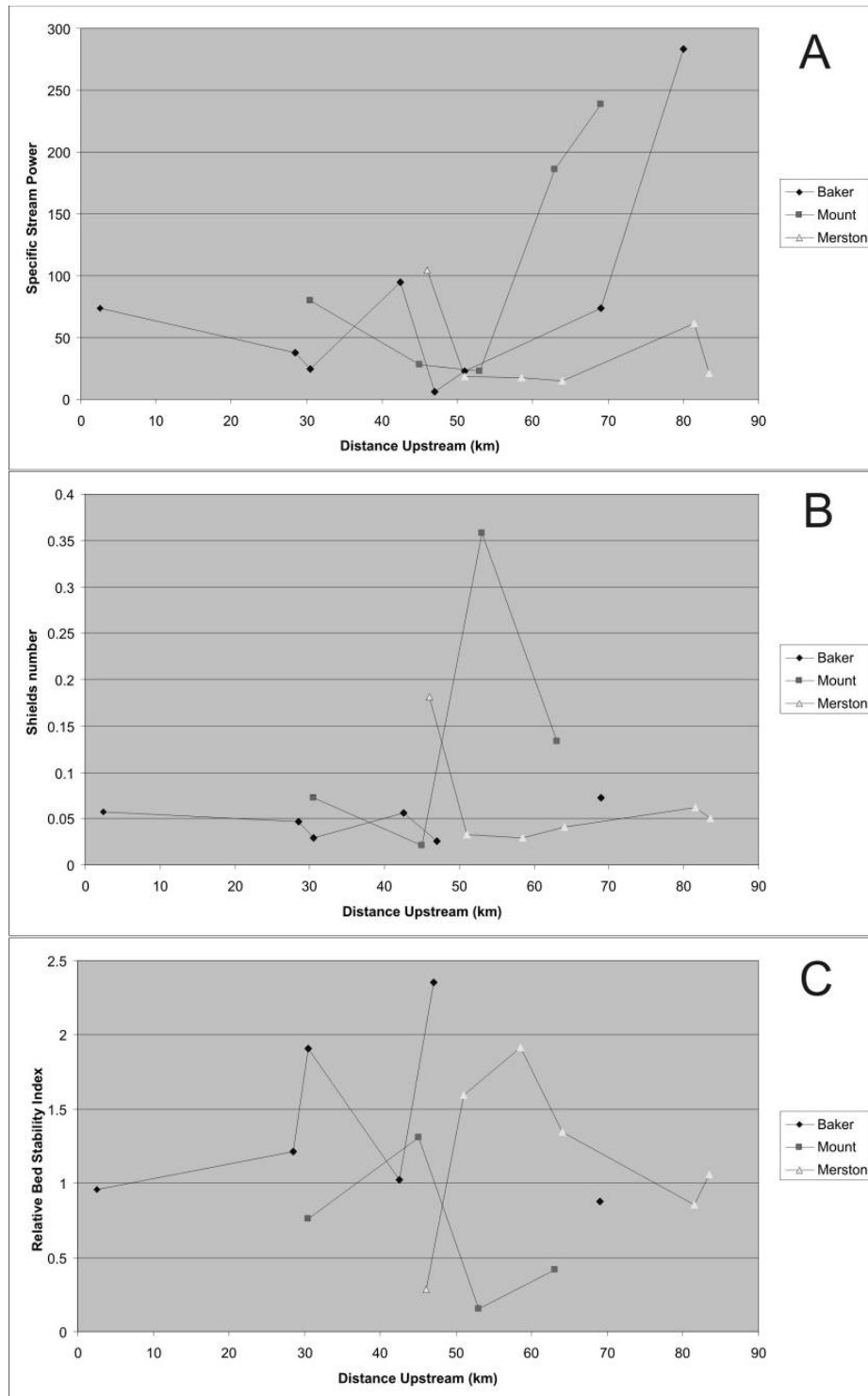


Figure 36. (A) Changes in specific stream power along Baker, Mount, and Merston Creeks. (B) Shields number changes along Baker, Mount, and Merston Creeks. (C) Changes in the relative bed stability index along Baker, Mount, and Merston Creeks. Values ≤ 1 are considered unstable, values from 1.0 to 2.0 are intermediate, and values > 2 are very stable (Olsen et al. 1997).

4.4.2 Channel classification using threshold methods

4.4.2.1 Stream power

Downstream changes in specific stream power are shown in Figure 36a. Specific stream power is maximized in the headwater reaches and decreases rapidly downstream, reaching minimum values in the low-gradient central plateau of the catchment. Values then increase slightly in the lowest reaches of all three creeks. Knighton (1999) suggests that for rivers with an exponential long profile, stream power values peak at an intermediate location between the headwaters and the lowermost reaches. This trend is not observed in the Baker Creek catchment. However, Knighton (1999) also suggests that where the rate of change of channel slope is greater than the rate of change of discharge, the long profile will dominate the trends in downstream stream power changes. Clearly, the distinctive long profile (Figure 33) is the dominant control on specific stream power trends and the exponential long profile has been highly modified by the varied geology and Quaternary evolution of the channel pattern at Baker Creek. Complex geological controls on long profile and stream power have been documented for numerous other catchments (e.g., Tooth et al. 2002; Marren et al. 2006).

Except for the headwater reaches of Baker and Mount Creeks, all specific stream power values are under 200 Wm^{-2} . High stream power values are to be expected in the steeper headwater reaches, and cannot be used to assess floodplain formation thresholds, since this channel style is not associated with floodplain development (Rosgen 1994; Montgomery and Buffington 1997). Downstream of the headwaters, all reaches of the Baker Creek catchment fall into Class B (medium-energy non-cohesive floodplains) of the Nanson and Croke (1992) classification (Table 9). Streams on the low-gradient central plateau of the catchment all fall into Class B3, meandering river, lateral migration floodplains. Minor anabranches in some reaches suggest that in some locations specific stream powers are currently at the low end of the $10\text{--}60 \text{ Wm}^{-2}$ range, but calculated values for the study sites fell in the range $14\text{--}27 \text{ Wm}^{-2}$. Higher-gradient reaches, both upstream and downstream of the central plateau, are classified as Class B2, wandering gravel-bed river floodplains. Specific stream powers range from 37 to 186 Wm^{-2} , with most sites between 61 and 100 Wm^{-2} . At Baker Creek, there is a clear distinction in terms of stream power between the two main types of floodplain present. The potential impact of increased discharges due to the MPB is discussed below.

4.4.2.2 Shields number

Downstream changes in the Shields number are shown in Figure 36b. The Church (2002) classification of alluvial channels based on Shields number is shown in Table 10. The widespread availability of coarse-grained sediment from Quaternary terraces and the volcanic bedrock means that relative to channel depth, channel bed material size is coarse, and Shields numbers are relatively low. This is particularly apparent in channels on the low-gradient central plateau, where relatively narrow and deep channels, combined with readily available coarse-grained Quaternary glaciofluvial outwash sediment in channel banks, leads to a Shields number of approximately 0.02, much lower than would normally be expected in this environment. The steeper, coarser-grained cobble-gravel channels that form upstream and downstream of the central plateau have Shields numbers in the range 0.05–0.07, and fall within the expected range in Table 10. Few sites are characterized by finer sediment, particularly site Mo3, and have Shields numbers greater than 0.1. The impact of changing discharge patterns on the Shields number is discussed below.

Table 9. Simplified version of the Nanson and Croke (1992) classification of floodplain types based on specific stream power.

Floodplain order	Type	Specific stream power, ω (Wm^{-2})
Class A: High-Energy Non-Cohesive Floodplains		
A1	Confined coarse-textured floodplains	>1000
A2	Confined vertical accretion floodplains	300–1000
A3	Unconfined vertical accretion sandy floodplains	300–600
A4	Cut-and-fill floodplains	~300
Class B: Medium-Energy Non-Cohesive Floodplains		
B1	Braided-river floodplains	50–300
B2	Wandering gravel-bed river floodplains	30–200(?)
B3	Meandering river, lateral-migration floodplains	10–60
Class C: Low-Energy Cohesive Floodplains		
C1	Laterally stable single-channel floodplains	<10
C2	Anastomosing river floodplains	<10

Table 10. Simplified version of the Church (2002) classification of alluvial river channels based on the Shields number.

Shields number	Sediment type	Channel characteristics
0.04+	Cobble–gravel	Cobble-gravel channel bed, single thread or wandering; relatively steep; low sinuosity; $w/d > 20$
0.1+	Sand to cobble–gravel	Gravel to sandy gravel, single thread to braided; complex bar development by lateral accretion; moderately steep; low sinuosity; w/d very high
1.0+	Sand to fine gravel	Mainly single-thread, irregularly sinuous to meandering; bar development by lateral and vertical accretion; moderate gradient; sinuosity < 2 ; $w/d < 40$
≤ 10	Sandy bed, fine sand to silt banks	Single thread, meandered, limited point bar development; vertical accretion on floodplains; low gradient; sinuosity > 1.5 ; $w/d < 20$.
> 10	Silt to fine sand bed, silt to clay–silt banks	Single-thread or anastomosed channels; vertical accretion on floodplain; very low gradient; sinuosity > 1.5 ; $w/d < 15$

4.4.2.3 *Relative bed stability*

The input data for the relative bed stability calculations and the results are in Table 8. The RBS index for each study site is plotted against distance upstream (Figure 36c). Olsen et al. (1997) state that values ≤ 1 are considered unstable while values in the range 1.0–2.0 are intermediate, and values > 2 are very stable. From Figure 35c, it can be seen that under the existing conditions, only one site has an RBS index > 2 , while eight sites fall into the 1.0–2.0 intermediate range, albeit in some cases very close to 1 (e.g., site B4 is 1.0267, and siteMe6 is 1.0567). Seven sites have RBS index values of < 1 and are thus considered unstable under existing conditions. Thus, assuming that the relative bed stability method is valid, almost all of the measurement sites within the Baker Creek catchment are, under present conditions, either unstable or at conditions close to the threshold for instability. Intermediate-stable sites tend to be on the low-gradient Interior Plateau of the catchment, particularly on Baker Creek and Merston Creek. Headwater reaches of all three creeks tend to be unstable or close to the stability threshold. The lowermost reach measured, which is immediately outside the city limits of Quesnel (where the banks have been reinforced), is also assessed as unstable. These results show that under present equilibrium conditions, as determined from field evidence for bankfull flow), rivers in the Baker Creek catchment are relatively active, and either tend towards instability, or are close to thresholds for instability. This assessment accords well with the geomorphological characteristics of the various reaches described previously. Future increases in discharge due to MPB-related hydrological changes may cause some reaches to cross relative bed stability thresholds. This possibility is explored further below.

4.4.3 **Sensitivity-based analysis of potential mountain pine beetle impacts**

The potential impacts of increased discharges can be expressed in terms of increased channel widths and depths using downstream hydraulic geometry (Leopold and Maddock 1953). The increased discharges can also be used to directly recalculate the available total stream power, and specific stream powers can be calculated using new channel widths estimated using downstream hydraulic geometry. The channel depths calculated using the hydraulic geometry approach can be used to recalculate the Shields number for each reach, given that the data in Table 8 indicate that channel depth is a good approximation of hydraulic radius in all reaches.

As the channel in the Baker Creek catchment is highly sinuous, it is difficult to determine the long-term impact of increased discharges on channel slope. Discharge increases may increase slope by inducing cutoffs. However, over longer periods, the increased channel widths may lead to an increase in meander wavelength, resulting in reduced or largely unchanged channel slopes. Channel slopes are therefore unchanged in the following analysis which also assumes that the bed material size distribution will remain unchanged. Since it has been shown above that in most reaches the relative roughness in Baker Creek is relatively high due to the readily available inputs of coarse sediment, this assumption seems reasonable. The major limitation of the downstream hydraulic geometry for this type of analysis is that it fails to take into account highly variable downstream changes in width/depth ratio. Because of the major slope and vegetation controls on width/depth ratio present in the Baker Creek catchment, channel widths are likely to be overestimated for the central plateau part of the catchment, and underestimated for the downstream end of the catchment.

The downstream hydraulic relationships for the Baker Creek catchment are shown in Figure 37. This analysis pools the data from all three subreaches of the catchment, which is reasonable since the variability within the dataset is primarily caused by changes in width/depth ratio that occur between the low-gradient reaches and the steeper reaches, rather than because of differences in the characteristics of the three subreaches. The downstream increase in gradient also means that velocity has a tendency to increase downstream, resulting in a negative exponent in the velocity equation. From Figure 37, the downstream hydraulic geometry equations for width, depth, and velocity are:

$$w = 2.3032Q^{0.688}$$

$$d = 0.2766Q^{0.398}$$

$$v = 1.5697Q^{-0.086}$$

Based on our simulated MPB and salvage logging effects using DHSVM possible increases to the mean annual flood at the outlet of Baker Creek could range from 20% to 100% of the existing flows. Notwithstanding that relative increases in peak flow on the upstream tributaries to Baker Creek are expected to be larger, discharge increases of 20%, 40%, 60%, 80%, and 100% will be used to test the sensitivity of geomorphic thresholds within the Baker Creek catchment.

The increases in discharge and channel width and depth for the five scenarios are shown in Table 11. Figure 38a shows plots of the calculated specific stream power based on these new discharges and widths. As width increases with discharge, specific stream power does not rise as rapidly as total stream power. Consequently, there are no changes in specific stream power sufficient to cause a reach to cross a threshold on the Nanson and Croke (1992) classification, even with a 100% increase in discharge. Except for the headwater reaches, all reaches are still classified as Calls B2 or B3. As both the genetic floodplain type definition, and the specific stream power definitions are so broad, it is difficult for a reach to cross thresholds based solely on the discharge increases associated with land-use changes.

For the plot of Shields number change with increasing discharge (Figure 38b), a slightly different picture emerges. Sites with very low Shields numbers (0.02–0.04) remain essentially unchanged, but sites with low to intermediate Shields numbers (0.04–0.1) increase and cross the 0.1 threshold. In all cases, the threshold is crossed with discharge increases of 60% more than the present discharge to 80% more than present conditions. These changes indicate that the narrow and deep low-gradient channels of the central plateau are resistant to change, while the wide and shallow channels of the higher-gradient reaches are more likely to undergo significant changes. These changes are likely to take the form of channel widening, increased sediment accumulation and bar development, and possible development of braiding.

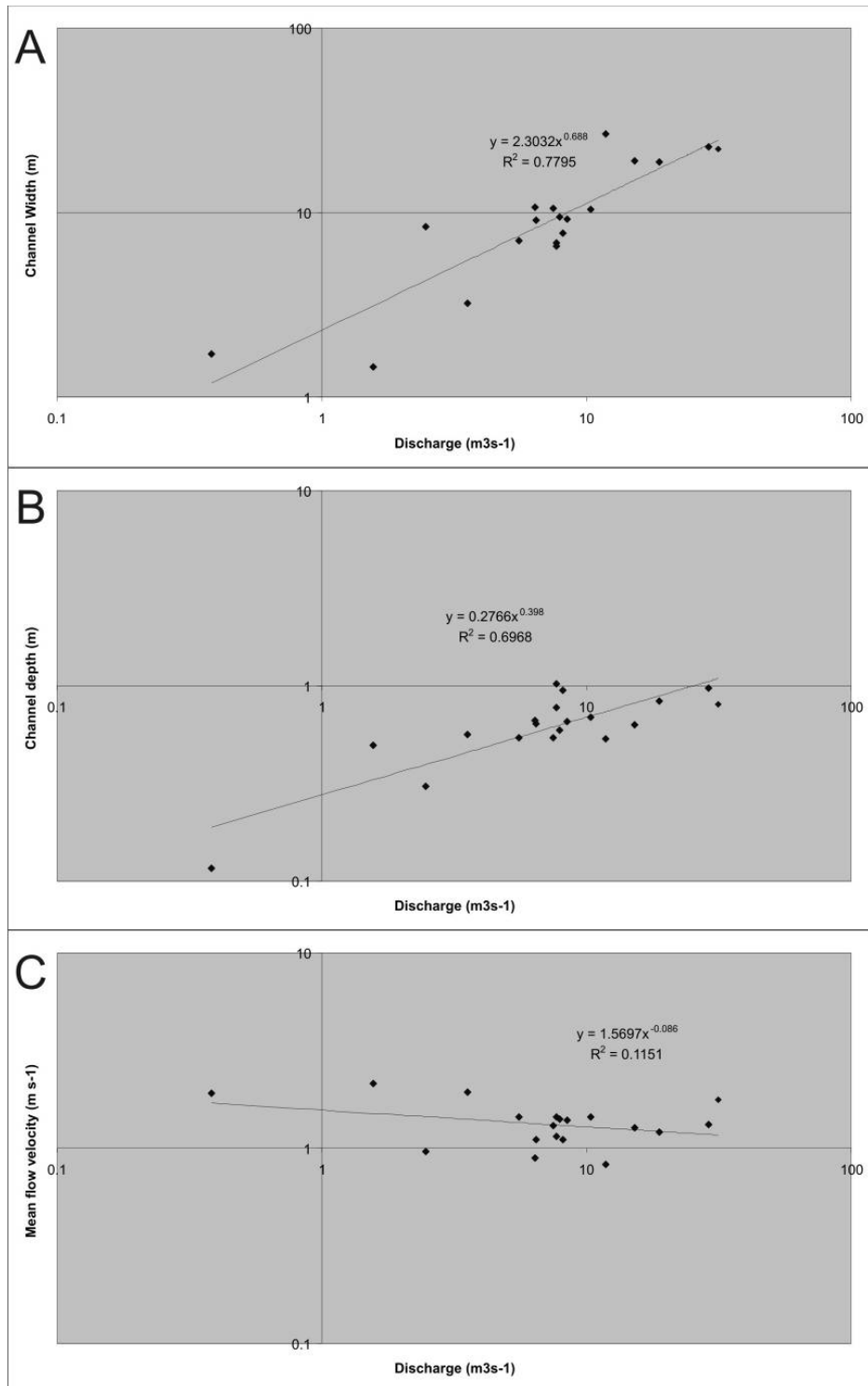


Figure 37. Downstream hydraulic geometry relationships for the Baker Creek catchment. (A) Width-discharge. (B) Depth-discharge. (C) Velocity-discharge relations.

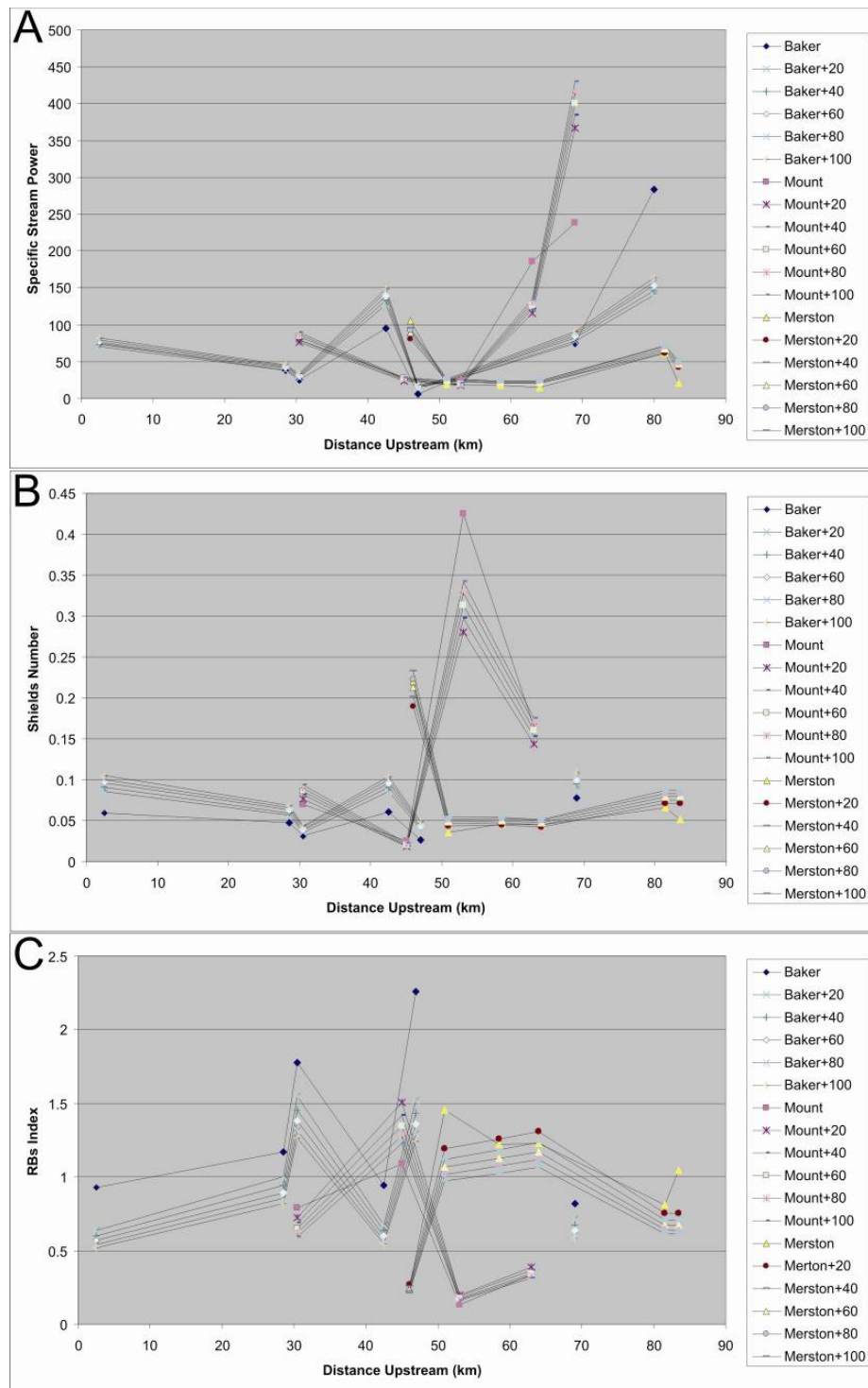


Figure 38. A sensitivity analysis of the potential impact of mountain pine beetle related hydrological changes on the Baker Creek catchment, based on possible discharge increases of 20%, 40%, 60%, 80%, and 100%. (A) Specific stream power changes in response to discharge increases. (B) Shields number index increases in response to discharge increases. (C) Change in the relative bed stability index in response to discharge increases.

As with the specific stream power and Shields number analysis, the relative bed stability index also indicates that the low-gradient reaches of the central part of the catchment are likely to remain stable, even under conditions where discharge increases by 100% (Figure 38c). Two sites cross the threshold from intermediate-stable to unstable as discharge increases. Site B2, which is at the upstream end of the steeper lower part of the catchment, crosses the threshold with only a 20% increase in discharge. Site Me2, which has a very slightly steeper channel than other reaches of the central plateau, just crosses the instability threshold when discharge increases by 100%. In general, the relative bed stability index indicates that steeper reaches of the catchment are liable to change under present conditions, and instability will increase as discharges rise. The low-gradient reaches are likely to remain stable under the hydrological conditions forecasted to occur due to the mountain pine beetle.

5 DISCUSSION

The analysis using specific stream power was able to successfully distinguish the different categories of floodplain type in the Baker Creek catchment: headwater channels, wandering gravel-bed river floodplains, and meandering river floodplains. However, classifications of this type are too broad to identify floodplain changes due to land use induced changes in runoff. At the reach scale, specific stream power can be highly variable and a single floodplain class can encompass as wide range of specific stream powers due to local changes in slope, discharge, and channel dimension. Given that valley slope is relatively fixed, and can only be changed to a limited degree by changes in channel length, large changes in discharge are required to cross the thresholds between floodplain classes. In the scenarios envisaged here as the likely response to MPB-related tree-kill and deforestation, discharge increases of up to 100% are insufficient to cross floodplain thresholds. However, stream power based analyses are useful for identifying the overall floodplain type, and the likely processes and stability associated with that type.

Because it is based on channel and sediment characteristics rather than the floodplain, the Church (2002) categorization of channels based on the Shields number is more appropriate for identifying channel changes due to relatively small, short-term increases in discharge such as those associated with the MPB. In the Baker Creek catchment, there was a distinction between channels that are likely to remain stable even with a 100% increase in discharges, and channels that are likely to cross stability thresholds and change character with increases in discharge of 60%–80%. This distinction was similar to the initial classification based on the Nanson and Croke (1992) classification, placing the floodplains into Classes B2 and B3. However, the analysis based on the Shields number showed that, given increases in discharge, the channel will change, even though the overall character of the floodplain will remain largely the same. The real benefit of this method is that the sensitivity analysis highlights a range of discharges that are critical for channel stability. These discharges can be used to inform hydrological and land use modeling, and produce harvesting scenarios that prevent these thresholds from being crossed.

Table 11. Scenarios for channel width and depth changes, based on downstream hydraulic geometry relationships based on the present channel, and possible increases in discharge of 20%, 40%, 60%, 80%, and 100%.

Loc.	Q	w	d	Q+20	w+20	d+20	Q+40	w+40	d+40	Q+60	w+60	d+60	Q+80	w+80	d+80	Q+100	w+100	d+100
B1	31.50	22.14	0.80	37.80	28.03	1.17	44.10	31.17	1.24	50.40	34.17	1.31	56.70	37.05	1.37	63.01	39.84	1.43
B2	28.94	22.65	0.97	34.73	26.44	1.13	40.51	29.40	1.20	46.30	32.23	1.27	52.09	34.95	1.33	57.88	37.58	1.39
B3	18.80	18.73	0.83	22.56	19.65	0.95	26.32	21.85	1.01	30.08	23.95	1.07	33.84	25.97	1.12	37.60	27.93	1.17
B4	15.20	19.02	0.62	18.24	16.98	0.87	21.28	18.88	0.93	24.32	20.69	0.98	27.36	22.44	1.03	30.40	24.13	1.07
B5	11.84	26.69	0.53	14.21	14.30	0.79	16.58	15.90	0.84	18.95	17.43	0.89	21.32	18.90	0.93	23.69	20.32	0.97
B6	8.47	9.18	0.66	10.17	11.36	0.69	11.86	12.63	0.74	13.56	13.84	0.78	15.25	15.01	0.81	16.95	16.14	0.85
B7	7.94	9.48	0.59	9.52	10.86	0.67	11.11	12.07	0.72	12.70	13.23	0.76	14.29	14.35	0.79	15.88	15.43	0.83
B8	1.56	1.46	0.49	1.87	3.54	0.35	2.18	3.94	0.37	2.49	4.32	0.39	2.81	4.69	0.41	3.12	5.043	0.43
Mo1	10.37	10.36	0.69	12.45	13.05	0.75	14.53	14.52	0.80	16.60	15.91	0.84	18.68	17.26	0.88	20.75	18.55	0.92
Mo2	8.17	7.76	0.94	9.81	11.08	0.68	11.45	12.32	0.72	13.08	13.51	0.76	14.72	14.65	0.80	16.35	15.75	0.84
Mo3	7.72	6.56	1.02	9.27	10.66	0.67	10.81	11.85	0.71	12.36	12.99	0.75	13.91	14.09	0.78	15.45	15.15	0.82
Mo4	3.54	3.21	0.56	4.25	6.23	0.49	4.96	6.93	0.52	5.67	7.60	0.55	6.38	8.24	0.57	7.09	8.86	0.60
Mo5	0.38	1.72	0.11	0.45	1.34	0.20	0.53	1.49	0.21	0.60	1.63	0.22	0.68	1.77	0.23	0.76	1.91	0.24
Me1	7.72	6.87	0.77	9.27	10.65	0.67	10.81	11.85	0.71	12.36	12.99	0.75	13.90	14.08	0.78	15.45	15.14	0.82
Me2	7.48	10.61	0.54	8.98	10.43	0.66	10.48	11.59	0.70	11.97	12.71	0.74	13.47	13.78	0.77	14.97	14.82	0.81
Me3	6.48	9.09	0.64	7.77	9.44	0.62	9.07	10.50	0.66	10.37	11.51	0.70	11.66	12.48	0.73	12.96	13.42	0.76
Me4	6.37	10.74	0.66	7.65	9.34	0.62	8.93	10.38	0.66	10.20	11.38	0.69	11.48	12.34	0.73	12.75	13.27	0.76
Me5	5.54	7.08	0.54	6.65	8.48	0.58	7.76	9.43	0.62	8.87	10.33	0.65	9.97	11.21	0.69	11.08	12.05	0.72
Me6	2.47	8.45	0.30	2.96	4.86	0.42	3.46	5.41	0.45	3.95	5.93	0.47	4.45	6.43	0.50	4.94	6.91	0.52

The relative bed stability approach produces similar results to the analysis based on the Shields number, which is unsurprising since both are based on channel shear stress. Both methods identify the same reaches as either stable or unstable. However, the results are less useful for identifying thresholds, since most unstable reaches are classified as unstable under current conditions, and only two reaches cross the threshold from stability to instability due to discharge increases. (One of those only just crosses the threshold, even with 100% discharge increases.) The relative bed stability approach is also weaker as it provides no information on the direction of the channel change, whereas the Shields number can be related more easily to channel characteristics.

Based on the stability analysis, the low-gradient reaches that occur in the centre of the catchment likely remain relatively stable, even as discharges increase. However, this assessment does not account for the increases in channel dimension that likely occur as discharges increase (Table 11). Further, the contrast in channel response between the low-gradient unforested reaches and the higher-gradient forested reaches cannot be incorporated into the analysis. The analysis in this study was based on changes to the channel-forming bankfull flow regime, but overbank flooding will likely become far more common, as the recurrence interval for higher magnitude floods decreases in response to the changes in the flood magnitude and frequency regime. Increased frequency of overbank flooding will be significant in putting large volumes of sediment into storage on the floodplain. Although sediment will likely be mobilized throughout the catchment, the significant sediment storage in the low-gradient floodplain reaches will manifest itself as a reduction in channel width/depth ratio. In the higher-gradient reaches, which are both most unstable and most likely to cross geomorphic thresholds, significant channel widening and an increase in width/depth ratios are likely. Sediment mobility will greatly increase, but will be offset by an increase in bar development, primarily as lateral accretion surfaces on enlarged meander bends, and through the development of braiding in wider, steeper reaches.

At present, no studies have documented the effects of MPB-related hydrological changes on fluvial geomorphology. Studies such as this one provide the only means of assessing the likely impact of the ongoing pine beetle epidemic and the consequent salvage logging. Baker Creek is typical of many rivers in Interior British Columbia in that much of its catchment consists of a low relief plateau. However, as a tributary of the Fraser River, lower Baker Creek is over-steepened where it enters the Fraser Basin physiographic region. This contrast between a low-gradient main catchment and a higher-gradient section above the Fraser River is common throughout the region. Thus, the results from this study have a wide applicability.

This study has implications for catchment management. First, higher-gradient reaches already have low relative bed stability indexes, and are likely to show increased rates of sediment mobility as discharges rise. Second, although sediment mobility is likely to remain low, and channel character will remain the same, low-gradient reaches will become significant sediment stores. Finally, based on the Shields number analysis, increases in the mean annual flood discharge in the 60%–80% range may significantly change channel character in the higher-gradient reaches. This final conclusion is particularly significant as it suggests that salvage harvesting strategies must be designed to minimize the risk of mean annual flood discharges rising beyond this level.

6 CONCLUSIONS

Chapter 4 of this project has identified thresholds for channel change in a 1570-km² catchment in the Central Interior region of British Columbia, Canada. This region is heavily impacted by the ongoing mountain pine beetle epidemic, with over 80% tree mortality in pine-leading stands across the catchment. Although the hydrological impact of the ongoing epidemic is unknown at present, preliminary hydrological modeling and the results of studies of earlier, smaller mountain pine beetle epidemics indicate that peak discharges could increase by 50%–100%, and that the return interval of all floods will decrease. This study tests the applicability of geomorphic threshold based techniques for assessing the impact of discharge changes on alluvial channels, and provides the first attempt to assess the likely impact of the mountain pine beetle on fluvial geomorphology in the Interior of British Columbia. Low-gradient channels typical of the Interior Plateau of British Columbia were

found to be relatively resistant to channel change, but are likely to become major sediment stores as large volumes of sediment are mobilized from elsewhere in the catchment and channels are widened. Higher-gradient reaches, typical of areas where channels cut down from the Interior Plateau to the Fraser River Basin, are already classified as unstable using the relative bed stability method, and are likely to be areas of significant sediment flux in the future. Using the Shields number based threshold method, a key threshold was identified when discharges increase by about 60%–80%. Channel character is likely to change, with channels widening, width/depth ratios increasing, sediment accumulation in bars and on the floodplain increasing, and braiding possibly developing. Future management decisions must be based around ensuring that discharges do not rise beyond this threshold.

The threshold-based techniques examined in this paper provided a useful means of assessing the potential for channel change in response to discharge increases. As it does not require grain-size information, the specific stream power approach has fewer data requirements, and an analysis can be relatively easily. However, the results are only useful for classifying floodplains into broad categories, which may correspond to a likelihood of change in a qualitative manner, but are largely insensitive to relatively small increases in discharge such as those induced by land-use change. In contrast, because they are based on channel sediment data, the Shields number based approaches are better at identifying thresholds for channel change, particularly when used as part of a sensitivity analysis. The relative bed stability approach gives a reasonable indication of which reaches are likely to be unstable, but it can provide no indication of the direction or likely result of the channel changes. Because the Shields number is closely related to channel characteristics, an analysis based on the Church (2002) channel classification is a simple, effective method for identifying critical thresholds in alluvial channels. If detailed studies relating channel type to Shields number are undertaken in a wider range of environments, it may become possible in the future to identify thresholds within the existing channel categories and produce more sophisticated analyses of channel change.

7 ACKNOWLEDGEMENTS

This project was funded in part by the Government of Canada through the Mountain Pine Beetle Initiative, a six-year, \$40 million program administered by Natural Resources Canada, Canadian Forest Service. Publication does not necessarily signify that the contents of this report reflect the views or policies of Natural Resources Canada, Canadian Forest Service. The authors also acknowledge the financial support from the Forest Practices Board of British Columbia and the British Columbia Ministry of the Environment.

8 CONTACT

Younes Alila, Watershed Hydrologist
Department of Forest Resources Management
Faculty of Forestry
The University of British Columbia
#2030 2424 Main Mall
Vancouver, BC V6T 1Z4
604 822-6058
Younes.Alila@ubc.ca

9 LITERATURE CITED

- Abbe, T.B.; Montgomery, D.R. 2003. Patterns and processes of wood debris accumulation in the Queets river basin, Washington. *Geomorphology* 51:81–107.
- Alila, Y.; Beckers, J. 2001. Using numerical modelling to address hydrologic forest management issues in BC. *Hydrological Processes* 15:3371–3387.
- Alila, Y., P. K. Kuras', M. Schnorbus, and R. Hudson (2009), Forests and floods: A new paradigm sheds light on age-old controversies, *Water Resour. Res.*, 45, W08416, doi:10.1029/2008WR007207.
- Andrews, E.D. 1983. Entrainment of gravel from naturally sorted riverbed material. *Geological Society of America Bulletin* 94:1225–1231.
- Beaudry, P. 2006. Snow surveys in Supply Block F, Prince George TSA. Report prepared for Canadian Forest Products Ltd., 5162 Northwood Pulp Mill Road, P.O. Box 9000, Prince George, BC.
- Beckers, J.; Alila, Y. 2004. A model of rapid preferential hillslope runoff contributions to peakflow generation in a temperate rainforest watershed. *Water Resources Research*, 40, W03501, DOI:10.1029/2003WR002582.
- Bernier, P.Y.; Swanson, R.H. 1993. The influence of opening size on snow evaporation in the forests of the Alberta Foothills. *Canadian Journal of Forestry Research* 23:239–244.
- Beschta, R.L.; Pyles, M.R.; Skaugset, A.E.; Surfleet, C.G. 2000. Peak flow responses to forest practices in the western cascades of Oregon, USA. *Journal of Hydrology* 233:102–120.
- Boon, S. 2007. Snow accumulation and ablation in a beetle-killed pine stand in Northern Interior British Columbia. *BC Journal of Ecosystems and Management* 8:1–13.
- Bowling, L.C.; Storck, P.; Lettenmaier, D.P. 2000. Hydrologic effects of logging in western Washington, United States. *Water Resources Research* 36(11):3223–3240.
- British Columbia Ministry of Environment. 2008. Historic snow survey data for British Columbia. URL: <http://a100.gov.bc.ca/pub/mss/stationdata.do?station=1C08>
- Butler, D.R.; Malanson, G.P. 1994. Canadian landform examples – 27: Beaver landforms. *The Canadian Geographer* 38:76–79.
- Butler, D.R.; Malanson, G.P. 2005. The geomorphic influences of beaver dams and failures of beaver dams. *Geomorphology* 71:48–60.
- Carling, P. 1988. The concept of dominant discharge applied to two gravel-bed streams in relation to channel stability thresholds. *Earth Surface Processes and Landforms* 13:355–367.
- Chow, V.T. 1959. Open channel hydraulics. McGraw-Hill Book Co., New York.
- Church, M. 2002. Geomorphic thresholds in riverine landscapes. *Freshwater Biology* 47:541–557.
- Church, M. 2006. Bed material transport and the morphology of alluvial river channels. *Annual Review of Earth and Planetary Sciences* 34:325–354.
- Dade, W.B. 2000. Grain size, sediment transport and alluvial channel pattern. *Geomorphology* 35:119–126.
- Dade, W.B.; Friend, P.F. 1998. Grain-size, sediment-transport regime and channel slope in alluvial rivers. *Journal of Geology* 106:661–675.

- Dalby, C.E. 1999. Discussion: "Assessing stream channel stability thresholds using flow competence estimates at bankfull stage" by D.S. Olsen, A.C. Whitaker, and D.F. Potts. *Journal of the American Water Resources Association* 35:185–186.
- Davis-Colley, R.J. 1997. Stream channels are narrower in pasture than in forest. *N.Z. Journal of Marine and Freshwater Research* 31:599–608.
- Eaton, B.; Church, M.; Ham, D. 2002. Scaling and regionalization of flood flows in British Columbia, Canada. *Hydrological Processes* 16:3245–3263.
- Elder, K.; Porth, L.; Troendle C.A. 2006. The effect of timber harvest on the Fool Creek watershed after five decades. *Eos Trans. AGU* 87(52), Fall Meet. Suppl., Abstract B21F-01.
- Emmett, W.W.; Wolman, M.G. 2001. Effective discharge and gravel-bed rivers. *Earth Surface Processes and Landforms* 26:1369–1380.
- Forest Practices Board. 2007. The effect of mountain pine beetle attack and salvage harvesting on streamflows. Forest Practices Board Publication FPB/SIR/16, March 2007. 29 p.
- Gomez, B.; Eden, D.N.; Peacock, D.H.; Pinkney, E.J. 1998. Floodplain construction by recent, rapid vertical accretion: Waipaoa River, New Zealand. *Earth Surfaces Processes and Landforms* 23:405–413.
- Gomez, B.; Rosser, B.J.; Peacock, D.H.; Hicks, D.M.; Palmer, J.A. 2001. Downstream fining in a rapidly aggrading gravel bed river. *Water Resources Research* 37:1813–1823.
- Gomi, T.; Moore, R.D.; Hassan, M.A. 2005. Suspended sediment dynamics in small forest streams of the Pacific Northwest. *Journal of the American Water Resources Association* 41:877–898.
- Gurnell, A. 1997. The hydrological and geomorphological significance of forested floodplains. *Global Ecology and Biogeography Letters* 6:219–229.
- Gurnell, A. 1998. The hydrogeomorphological effects of beaver dam-building activity. *Progress in Physical Geography* 22:167–189.
- Hartman, G.F.; Schrivener, J.C. 1990. Impacts of forestry practices on a coastal stream ecosystem. *Canadian Bulletin of Fisheries and Aquatic Sciences* No. 223. 148 p.
- Hartman GF, Schrivener JC, Miles MJ. 1996. Impacts of logging in Carnation Creek, a high energy coastal stream in British Columbia, and their implications for restoring fish habitat. *Canadian Journal of Fisheries and Aquatic Sciences* 53 (Supplement 1): 237-251.
- Hassan MA, Church M, Lisle TE, Brardinoni F, Benda L, Grant GE. 2005. Sediment transport and channel morphology of small, forested streams. *Journal of the American Water Resources Association* 41: 853-876.
- Hassan MA, Hogan DL, Bird SA, May CL, Gomi T, Campbell D. 2005. Spatial and temporal dynamics of wood in headwater streams of the Pacific Northwest. *Journal of the American Water Resources Association* 41: 899-919.
- Heede BR. 1991. Response of a stream in disequilibrium to timber harvest. *Environmental Management* 15: 251-255.
- Hélie, J.F.; Peters, D.L.; Tattree, K.R.; Gibson, J.J. 2005. Review and synthesis of potential hydrologic impacts of mountain pine beetle and related harvesting activities in BC. *Nat. Resour. Can., Can. For. Serv., Pac. For. Cent., Victoria, BC. Mountain Pine Beetle Initiative Working Paper 2005-23.* 26 p.
- Hendrick, R.L.; Filgate, B.D.; Adams, W.M. 1971. Application of environmental analysis to watershed snowmelt. *Journal of Applied Meteorology* 10:418–429.

- Jackson, C.R.; Sturm, C.A.; Ward, J.M. 2001. Timber harvest impacts on small headwater stream channels in the Coast Ranges of Washington. *Journal of the American Water Resources Association* 37:1533–1549.
- Jones, J.A. 2000. Hydrologic processes and peak discharge response to forest removal, regrowth and roads in 10 small experimental basins, western Cascades, Oregon. *Water Resources Research* 36:2621–2642.
- Jones, J.A.; Grant, G.E. 1996. Peak flow responses to clear-cutting and roads in small and large basins, western Cascade, Oregon. *Water Resources Research* 32:959–974.
- Jones, J.A.; Swanson, F.J.; Wemple, B.C.; Snyder, K.U. 2000. Effects of roads on hydrology, geomorphology, and disturbance patches in stream networks. *Conservation Biology* 14:76–85.
- Jost, G.; Weiler, M.; Gluns, D.R.; Alila, Y. 2007. The influence of forest and topography on snow accumulation and melt at the watershed-scale. *Journal of Hydrology* 347:101–115.
- Kean, J.; Smith, J.D. 2005. Generation and verification of theoretical rating curves in the Whitewater River basin, Kansa. *Journal of Geophysical Research* 110, F04012, doi:10.1029/2004JF000250.
- Knighton, A.D. 1999. Downstream variation in stream power. *Geomorphology* 29:293–306.
- Knox, J.C. 1977. Human impacts on Wisconsin stream channels. *Annals of the Association of American Geographers* 67:323–342.
- Komar, P.D. 1989. Flow-competence evaluations of the hydraulic parameters of floods: an assessment of the technique. Pages 297–311 *in* K. Bevan and P. Carling, eds. *Floods, hydrological, sedimentological and geomorphological implications*. John Wiley and Sons Ltd.
- La Marche, J.; Lettenmaier, D.P. 2001. Effects of forest roads on flood flows in the Deschutes River, Washington. *Earth Surfaces Processes and Landforms* 26:115–134.
- Lay, D. 1940. Fraser River tertiary drainage history in relation to placer-gold deposits. BC Department of Mines Bulletin 3.
- Lay, D. 1941. Fraser River tertiary drainage history in relation to placer-gold deposits (Part 2). BC Department of Mines and Petroleum Resources Bulletin 11.
- Leopold, L.B.; Maddock, T. Jr. 1953. The hydraulic geometry of stream channels and some physiographic implications. US Geological Survey Professional Paper 252. 57 p.
- Lewis, J.; Mori, S.R.; Keppeler, E.T.; Ziemer, R.R. 2001. Impacts of logging on storm peak flows, flow volumes and suspended sediment loads in Caspar Creek, California. Pages 85–125 *in* M.S. Wigmosta and S.J. Burges, eds. *Land use and watersheds: Human influence on hydrology and geomorphology in urban and forest areas*. AGU, Water Science and Application Ser. 2, Washington, D.C. 2001.
- Liébault, F.; Gomez, B.; Page, M.; Maerden, M.; Peacock, D.; Richard, D.; Trotter, C.M. 2005. Land-use change, sediment production and channel response in upland-regions. *River Research and Applications* 21:739–756.
- Lord, T.M.; Mackintosh, E.E. 1982. Soils of the Quesnel area, British Columbia. BC Soil Survey, Report No. 31. 93 p.
- MacDonald, L.H.; Stednick, J. 2003. Forests and water: A state of-the-art review for Colorado. Colorado Water Resources Research Institute. Completion Report No. 196. 65 p.
- Magilligan, F.J.; Stamp, M.L. 1997. Historical land-cover changes in hydromorphic adjustment in a small Georgia watershed. *Annals of the Association of American Geographers* 87:614–635.

- Marren, P.M.; McCarthy, T.S.; Tooth, S.; Brandt, D.; Stacey, G.C.; Leong, A.; Spottiswoode, B. 2006. A comparison of mud- and sand-dominated meanders in a downstream coarsening reach of the mixed bedrock-alluvial Klip River, eastern Free State, South Africa. *Sedimentary Geology* 190:213–226.
- Melloh, R.A.; Hardy, J.P.; Davis, R.E.; Robinson, P.E. 2001. Spectral albedo/reflectance of littered forest snow during the melt season. *Hydrological Processes* 15:3409–3422.
- Miall, A.D. 1996. *The geology of fluvial deposits: Sedimentary facies, basin analysis, and petroleum geology*. Springer-Verlag, New York. 582 p.
- Montgomery, D.R.; Buffington, J.M. 1997. Channel-reach morphology in mountain drainage basins. *Geological Society of America Bulletin* 109:596–611.
- Montgomery, D.R.; Schmidt, K.M.; Greenberg, H.M.; Dietrich, W.E. 2000. Forest clearing and regional landsliding. *Geology* 28:311–314.
- Moore, R.D.; Scott, D.F. 2005. Camp Creek revisited: Streamflow changes following salvage harvesting in a medium-sized, snowmelt-dominated catchment. *Canadian Water Resources Journal* 30:331–344.
- Moore, R.D.; Wondzell, S.M. 2005. Physical hydrology and the effects of forest harvesting in the Pacific Northwest: A review. *Journal of the American Water Resources Association* 41:763–784.
- Nanson, G.C.; Croke, J.C. 1992. A genetic classification of floodplains. *Geomorphology* 4:459–486.
- Nash, J.E.; Sutcliffe, J.V. 1970. River flow forecasting through conceptual models, 1. A discussion of principles. *Journal of Hydrology* 10:282–290.
- Northwest Hydraulic Consultants Ltd. 1992. Floodplain mapping investigation: Fraser and Quesnel Rivers at Quesnel design brief. Report prepared for B.C. Ministry of Environment, Lands and Parks. Report No. 1735/VJG.
- Olsen, D.S.; Whitaker, A.C.; Potts, D.F. 1997. Assessing stream channel stability thresholds using flow competence estimates at bankfull stage. *Journal of the American Water Resources Association* 33:1197–1207.
- Olsen, D.S.; Whitaker, A.C.; Potts, D.F. 1999. Reply to discussion by Charles E. Dalby: “Assessing stream channel stability thresholds using flow competence estimates at bankfull stage”. *Journal of the American Water Resources Association* 35:187–188.
- Petit, F. 1994. Dimensionless critical shear stress evaluations from flume experiments using different gravel beds. *Earth Surface Processes and Landforms* 19:565–576.
- Phillips, J.D.; Gomez, B. 2007. Controls on sediment export from the Waipaoa River basin. *New Zealand Basin Research* 19:241–252.
- Pomeroy, J.W.; Li, L. 1997. Development of the Prairie Blowing Snow Model for application in climatological and hydrological models. *In Proceedings Eastern Snow Conference* 54:186–197.
- Ralph, S.C.; Poole, G.C.; Conquest, L.L.; Naiman, R.J. 1994. Stream channel morphology and woody debris in logged and unlogged basins of western Washington. *Canadian Journal of Fisheries and Aquatic Sciences* 51:37–51.
- Rex, J.; Dubé, S. 2009. Hydrologic effects of mountain pine beetle infestation and salvage harvesting operations. Mountain pine beetle working paper 2009-05. Natural Resources Canada, Canadian Forest Service, Pacific Forestry Centre, Victoria, BC. 44p.

- Riddell, J.M., compiler. 2006. Geology of the Southern Nechako Basin NTS 92N, 92O, 93B, 93C, 93F, 93G. Petroleum Geology Map 2006-1. B.C. Min. Energy Mines and Petroleum Resource, Oil and Gas Division, Resource Development and Geoscience Branch, Victoria, BC.
- Rosgen, D.L. 1994. A classification of natural rivers. *Catena* 22:169–199.
- Schnorbus, M.; Alila, Y. 2004. Forest harvesting influences on the peak flow regime in the Columbia Mountains of southeastern BC: An investigation using long-term numerical modelling, *Water Resour. Res.* 40, W05205, doi:10.1029/2003WR002918.
- Shields, A. 1936. Application of the theory of similarity and turbulence research to the bedload movement. Saleh, Q.M. (Transl.) Mitt. Preuss. Vers. Wasserbau Schiffbau, vol. 26, Berlin.
- Slaymaker, O. 2000. Assessment of the geomorphic impacts of forestry in British Columbia. *Ambio* 27:381–387.
- Spittlehouse, D.L. 1998. Rainfall interception in young and mature conifer forests in British Columbia. Pages 171–174 in *Proc. 23rd Conference on Agricultural and Forest Meteorology*, American Meteorological Society, 1998.
- Spittlehouse, D.L.; Winkler, R.D. 2002. Modelling snowmelt in a forest and clearcut. Pages 121–122 in *Proc. 25th conference on Agricultural and Forest Meteorology*, Norfolk, VA. American Meteorological Society, Boston, MA.
- Storck, P.; Bowling, L.; Wetherbee, P.; Lettenmaier, D. 1998. Application of a GIS-based distributed hydrology model for prediction of forest harvest effects on peak stream flow in the Pacific Northwest. *Hydrological Processes*. 12: 889-904.
- Sweeney, B.W.; Bott, T.L.; Jackson, J.K.; Kaplan, L.A.; Newbold, J.D.; Standley, L.J.; Hession, W.C.; Horwitz, R.J. 2004. Riparian deforestation, stream narrowing, and loss of stream ecosystem services. *Proceedings of the National Academy of Sciences* 101:14132–14137.
- Tang, S.M.; Franklin, J.F.; Montgomery, D.R. 1997. Forest harvest patterns and landscape disturbance processes. *Landscape Ecology* 12:349–363.
- Teti, P. 2008. Effects of overstory mortality on snow accumulation and ablation. Mountain pine beetle working paper 2008-13. Natural Resources Canada, Canadian Forest Service, Pacific Forestry Centre, Victoria, BC. 21 p.
- Thomas, R.B.; Megahan, W.F. 1998. Peak flow responses to clear-cutting and roads in small and large basins, western Cascades, Oregon: A second opinion. *Water Resources Research* 34:3393–3403.
- Thyer, M.; Beckers, J.; Spittlehouse, D.; Alila, Y.; Winkler, R. 2004. Diagnosing a distributed hydrologic model for two high elevation forested catchments based on detailed stand- and basin-scale data. *Water Resources Research* 40(1), W01103, doi:10.1029/2003WR002414.
- Tipper, H.W. 1971. Glacial geomorphology and pleistocene history of central British Columbia. Dep. Energy, Mines and Resources, Ottawa, ON. Geological Survey of Canada Bulletin 196.
- Tooth, S.; McCarthy, T.S.; Brandt, D.; Hancox, P.J.; Morris R. 2002. Geological controls on the formation of alluvial meanders and floodplain wetlands: the example of the Klip River, eastern Free State, South Africa. *Earth Surface Processes and Landforms* 27:797–815.
- Trimble, S.W. 1997. Stream channel erosion and change resulting from riparian forests. *Geology* 25:467–469.
- Trimble, S.W.; Mendel, A.C. 1995. The cow as a geomorphic agent – a critical review. *Geomorphology* 13: 233–253.

- Troendle, C. A.; King, R.M. 1985. The effect of timber harvest on the Fool Creek watershed, 30 years later. *Water Resources Research* 21:1915–1922.
- Troendle C.A.; MacDonald, L.H.; Luce, C.H. 2006. Fuels management and water yield. In *Cumulative watershed effects of fuels management: A western synthesis*. US Department of Agriculture, Rocky Mountain Research Station General Technical Report RM-149. 32 p.
- Troendle, C.A.; Wilcox, M.S.; Bevenger, G.S.; Porth, L.S. 2001. The Coon Creek water yield augmentation project: Implementation of timber harvesting technology to increase streamflow. *Forest Ecology and Management* 143:179–187.
- van den Berg, J.H. 1995. Prediction of alluvial channel pattern of perennial rivers. *Geomorphology* 12:259–279.
- VanShaar, J.R.; Haddeland, I.; Lettenmaier, D.P. 2002. Effects of land-cover changes on the hydrological response of interior Columbia River basin forested catchments. *Hydrol. Process.* 16:2499–2520.
- Waichler, S.R., and M.S. Wigmosta, 2003: Simulation of Hourly Meteorology from Daily Data and Significance to Hydrology at H.J. Andrews Experimental Forest, *Journal of Hydrometeorology*, 4(2), 251–263.
- Watson, F.G.R.; Anderson, T.N.; Newman, W.B.; Alexander, S.E.; Garrott, R.A. 2006. Optimal sampling schemes for estimating mean snow water equivalents in stratified heterogeneous landscapes. *Journal of Hydrology* 328:432–452.
- Whitaker, A.; Alila, Y.; Beckers, J.; Toews, D.A.A. 2002. Evaluating peak flow sensitivity to clearcutting in different elevation bands of a snowmelt-dominated mountainous catchment. *Water Resources Research* 38: doi: 10.1029/2001514.
- Whitaker, A.; Alila, Y.; Beckers, J.; Toews, D. 2003. Application of the distributed hydrology soil vegetation model to Redfish Creek, BC: Model evaluation using internal catchment data. *Hydrological Processes* 17:199–224.
- Wigmosta, M.S.; Vail, L.W.; Lettenmaier, D.P. 1994. A distributed hydrology-vegetation model for complex terrain. *Water Resour. Res.* 30:1665–1679.
- Williams, G.P. 1978. Bank-full discharge of rivers. *Water Resources Research* 14:1141–1154.
- Winkler, R.D.; Roach, J. 2005. Snow accumulation in BC's southern interior forest. *Streamline* 9(1):1–5.
- Winkler, R.D.; Spittlehouse, D.L.; Golding D.L. 2005. Measured differences in snow accumulation and melt among clearcut, juvenile, and mature forests in southern British Columbia. *Hydrological Processes* 19:51–62.
- Wolman, M.G. 1954. A method of sampling coarse river-bed material. *Transactions of the American Geophysical Union* 35:951–956.
- Wolman, M.G.; Miller, J.P. 1960. Magnitude and frequency of forces in geomorphic processes. *Journal of Geology* 68:54–74.
- Wood, P.J.; Dykes, A.P. 2002. The use of salt dilution gauging techniques: Ecological considerations and insights. *Water Research* 36:3054–3062.
- Ziemer, R.; Lewis, J.; Rice, R.M.; Lisle, T.E. 1991. Modelling the cumulative watershed effects of forest management strategies. *Journal of Environmental Quality* 20:36–42.
- Zinke, P.J. 1967. Forest interception studies in the United States. Pages 137–161 *in* W.E. Sopper and H.W. Lull, eds. *International Symposium on Forest Hydrology*, Pergamon Press, New York.